QOS MANAGEMENT STRATEGIES FOR IOT APPLICATIONS

A Thesis Submitted

in Partial Fulfilment of the Requirements

for the Degree of

DOCTOR OF PHILOSOPHY

by

Lalit Kumar Baghel

(2019EEZ0026)

DEPARTMENT OF ELECTRICAL ENGINEERING

INDIAN INSTITUTE OF TECHNOLOGY ROPAR

March, 2025

Dedicated to

My Family *and* ***My Teachers***

Who are the inspiration and power behind the success of this work

Declaration of Originality

I hereby declare that the work which is being presented in the thesis entitled **QoS Management Strategies for IoT Applications** has been solely authored by me. It presents the result of my own independent investigation/research conducted during the time period from December 2019 to March 2025 under the supervision of Dr. Suman Kumar, Associate Professor, Department of Electrical Engineering, Indian Institute of Technology, Ropar, Punjab, India. To the best of my knowledge, it is an original work, both in terms of research content and narrative, and has not been submitted or accepted elsewhere, in part or in full, for the award of any degree, diploma, fellowship, associateship, or similar title of any university or institution. Further, due credit has been attributed to the relevant state-of-the-art and collaborations (if any) with appropriate citations and acknowledgments, in line with established ethical norms and practices. I also declare that any idea/data/fact/source stated in my thesis has not been fabricated/ falsified/ misrepresented. All the principles of academic honesty and integrity have been followed. I fully understand that if the thesis is found to be unoriginal, fabricated, or plagiarized, the Institute reserves the right to withdraw the thesis from its archive and revoke the associated Degree conferred. Additionally, the Institute also reserves the right to appraise all concerned sections of society of the matter for their information and necessary action (if any). If accepted, I hereby consent for my thesis to be available online in the Institute's Open Access repository, inter-library loan, and the title & abstract to be made available to outside organizations.

Signature

Name: Lalit Kumar Baghel
Entry Number: 2019EEZ0026
Program: PhD
Department: Electrical Engineering
Indian Institute of Technology Ropar
Rupnagar, Punjab 140001

Date: March 2025

Acknowledgement

Above all, it is God's grace that I had the opportunity to pursue a Ph.D. degree. It would not be possible to write this Ph.D. thesis without the help and support of the kind people around me, of whom only a few are specifically mentioned here. It is my pleasure to acknowledge the people, who associated directly and indirectly in completion of doctoral thesis work.

This thesis would not have been possible without the help, support and patience of my supervisor, Dr. Suman Kumar. It is matter of proud for anyone to learn from him about work and life. I want to present sincere gratitude to him for his constant encouragement, wherever I got stuck in my Ph.D. duration. His advice and support has been invaluable on both an academic and a personal level, for which I am extremely grateful. Working with him has been an amazing experience for many reasons. His help at every stage of my Ph.D., whether it was in formulating my initial research problems, or allowing me to walk on my path of research. Also, I learned to write and present ideas effectively from his comments and feedback. Moreover, I learned from his experience how to be a good mentor professionally and personally.

I am thankful to Prof. C. C. Reddy, Head, Electrical Engineering deppartment, IIT Ropar for the motivation and inspiration that triggered me for the thesis work. I would like to thank my doctoral committee members: Dr. Brijesh Kumbhani, Dr. Ashwani Sharma, and Dr. Sujata Pal for their valuable comments and suggestions to carry thesis work in right directions.

I would also want to thank my collaborators, Dr. Rohit Singh, Dr. Gaoyang Shan, Dr. Ajay Kumar, Dr. Chulsoon Hwang, Dr. Victor Khilkevich, Dr. Jingook Kim, Dr. Seyit Ahmet Sis and Dr. Luca Catarinucci for the countless discussions we have had on various topics. My stay at IIT Ropar would not have been so memorable without the friends that I have made along the way. I would like to thank Sameer, Dr. Vivek, Arnav, Mani Shankar, Prajjwal, Sagnik, Vikas, Dr. Nishant, Dhawal for being great friends and support. I take this opportunity to thank lab in-charge Mr. Kamaljeet Singh for taking care of various issues.

Finally, I would like to thank medical officers and staff members for taking care of all the researchers in such tough situations, and everybody who was important to the successful realization of dissertation, as well as expressing my apology that I could not mention personally one by one.

Certificate

This is to certify that the thesis entitled **QoS Management Strategies for IoT Applications**, submitted by **Lalit Kumar Baghel (2019EEZ0026)** for the award of the degree of **Doctor of Philosophy** of Indian Institute of Technology Ropar, is a record of bonafide research work carried out under my (our) guidance and supervision. To the best of my knowledge and belief, the work presented in this thesis is original and has not been submitted, either in part or full, for the award of any other degree, diploma, fellowship, associateship or similar title of any university or institution.

In my opinion, the thesis has reached the standard fulfilling the requirements of the regulations relating to the Degree.

Signature of the Supervisor(s)
Dr. Suman Kumar
Department of Electrical Engineering
Indian Institute of Technology Ropar
Rupnagar, Punjab 140001
Date: March 2025

Lay Summary

IoT has gained significant popularity due to its applications in various domains, including smart cities, healthcare, industrial automation, transportation, agriculture, supply chain, remote monitoring, etc. The applications from each domain have different quality of service requirements. For example, autonomous vehicles, industrial automation, real time surveillance, and emergency response systems require low latency to ensure timely data processing, decision making, and safety. Similarly, remote monitoring applications deployed at inaccessible locations, such as wildlife tracking, oil and gas field monitoring, smart meters in remote areas, and building and infrastructure monitoring, require higher energy efficiency for longer battery life and continuous operation. Given the importance of these applications and their requirements, this dissertation focuses on fulfilling these quality of service requirements. First, this dissertation proposes a performance model to analyze latency. Based on this performance, the model derives simplified analytical expressions to choose optimal transmission parameters that ensure minimal latency. Further, based on analytical expression, it proposes algorithms that autonomously optimize the network to achieve minimal latency. In addition to the above, this analysis provides valuable insights for service providers aiming to establish networks with such requirements. Thereafter, this dissertation proposes three different strategies for battery life enhancement, namely, battery life enhancement through effective hardware design and efficient utilization, battery life enhancement through hardware miniaturization, and battery life enhancement through aggregated data transmission. In addition to the above, this analysis provides a foundation for an Internet of Things engineer aiming to achieve higher energy efficiency and longer battery life.

Acronyms

5G: Fifth Generation
AoA: Angle of Arrival
BALUN: Balanced to Unbalanced Converter
BLE: Bluetooth Low Energy
CCTV: Closed Circuit Television
CPU: Central Processing Unit
CRC: Cyclic Redundancy Check
CRT: Chinese Remainder Theory
CSS: Chirp Spread Spectrum
DNN: Deep Neural Network
EC: Electrcal Conductivity
EEPROM: Electrically Erasable Programmable Read-only Memory
ESD: Electrostatic Discharge
FIFO: First in First Out
FSSAI: Food Safety and Standards Authority of India
GMSK: Gaussian Minimum Shift Keying
GPIO: General Purpose Input Output Pins
GPS: Global Positioning System
GSM: Global System for Mobile Communication
I2C: Inter-Integrated Circuit
IC: Integrated Circuit
IIoT: Industrial Internet of Things
IoT: Internet of Things
ISM: Industrial, Scientific, and Medical
LAN: Local Area Network
LDO: Low Drop Out
LED: Light Emitting Diode
LoRa: Long Range
LoS: Line of Sight
LPWAN: Low Power Wide Area Network
LTE: Long Term Evolution
MCU: Microcontroller Unit
ML: Machine Learning
MOSFET: Metal Oxide Semiconductor Field Effect Transistor
MSK: Minimum Shift Keying
NBIoT: Narrow Band Internet of Things
NFC: Near Field communication
OOK: On Off Keying
OTG: On the Go
OVRN: Overrun

PDU: Protocol Data Unit
pH: Potential of Hydrogen
QoS: Quality of Service
RFID: Radio Frequency Identification
RSSI: Received Signal Strength Indicator
RTC: Real Time Clock
SIG: Bluetooth Special Interest Group
SoC: System on Chip
SPI: Serial Peripheral Interface
TDoA: Time Difference of Arrival
TDS: Total Dissolved Solids
ToA: Time of Arrival
UART: Universal Asynchronous Receiver Transmitter
USART: Universal Synchronous and Asynchronous Receiver Transmitter
USB: Universal Serial Bus
WiFi: Wireless Fidelity
WTM: Watermark
ZigBee: Zonal Intercommunication Global Standard

Abstract

This dissertation aims at managing and fulfilling two crucial Quality of Service (QoS) requirements of Internet of Things (IoT) applications, namely, latency and energy efficiency. Indeed, significant research efforts have been made toward achieving low latency and higher energy efficiency for latency sensitive and energy constrained IoT applications. However, the existing solutions possess various limitations. For instance, the literature on latency sensitive applications primarily emphasized on selecting low latency protocol to achieve minimal latency; certainly selecting low latency protocol is important, however merely selecting low latency protocol does not guarantee minimal latency. For example, in Bluetooth Low Energy (BLE) (a low latency protocol chosen for latency analysis and minimization in this dissertation) transmission, when the advertising interval is set too large, the BLE gateway receiving the packets must wait for advertising packets to arrive, which increases the overall latency. Conversely, with a small advertising interval, the advertising packets become overpopulated, resulting in extensive collisions. This, in turn, raises the overall latency. This shows the importance of selecting transmission parameters (advertising interval in BLE). However, in this context, none of the existing works have provided simplified expressions to choose optimal parameters for minimizing latency. Moreover, the current solutions often assume homogeneous network scenarios; however, the majority of IoT applications, including the smart manufacturing industry, have a variety of sensors having different data sizes, likely to form a heterogeneous network. Likewise, the solutions for energy constrained applications have the following shortcomings; Firstly, the sensors are powered directly from the power supply which makes the sensor to consumes few µA's of current even in the sleep mode. Secondly, utilizes global positioning system (GPS) for real time location estimation even when higher accuracies are not desired or high errors in real time locations can be tolerated. Since it is a known fact that GPS requires a significant energy budget for its operation, hence affects overall battery life significantly. Thirdly, the existing solutions transmit raw data, usually generated frequently, consequently increasing total transmission and causing high energy consumption. Besides, it transmits a fixed number of copies to overcome data loss issues. However, transmitting a fixed number of copies may not completely overcome packet loss and may also lead to redundant transmissions. Hence, to address the aforementioned issues, this dissertation first proposes a performance model to analyze latency considering the heterogeneous scenario. Based on the performance model, derives simplified analytical expressions for optimal parameter selection that ensures minimal latency. Moreover, based on these analytical expressions, this dissertation proposes algorithms that autonomously optimize the network and ensure minimal latency. The work considers two different scenarios, namely, sensor nodes-gateway communication and sensor nodes-gateway-user communication. In addition to the above, this analysis provides valuable insights for service providers aiming to establish networks with such requirements. Thereafter, this dissertation proposes three different strategies for increasing energy efficiency and battery life enhancement, namely: (i) battery life enhancement through effective hardware design

and efficient utilization, (ii) battery life enhancement through hardware miniaturization, and (iii) battery life enhancement through aggregated data transmission. Battery life enhancement through effective hardware design and efficient utilization involves: (a) utilizing general purpose input output pins (GPIOs) to power sensors and (b) optimizing controller clock configuration. Further, battery life enhancement through hardware miniaturization involves replacing expensive and energy intensive GPS with a energy efficient received signal strength indicator (RSSI) based real time localization algorithm which estimates real time locations without incorporating additional positioning hardware, thus saving significant energy. Furthermore, battery life enhancement strategy aggregated data transmission involves: (a) thresholding method that reduces the total number of transmissions and saves a significant amount of energy by only transmitting parametric data over raw data, which is usually sensed and transmitted very frequently, and (b) analytical expression for selecting number of copies required to overcome the packet loss and redundant transmissions, thus saving significant energy. In addition to the above, this analysis provides a foundation for an IoT engineer to achieve higher energy efficiency and longer battery life.

Keywords: Latency; Energy Efficiency; Quality of Service (QoS); Bluetooth Low Energy (BLE); Long Range (LoRa); Remote Monitoring; Internet of Things (IoT); Industrial Internet of Things (IIoT).

List of Publications

Publications From This Dissertation

Journal

- L. K. Baghel, G. Shan and S. Kumar, "Analytical Framework for Data Reception Latency Modelling in BLE 5.x Based Clustered Architecture," in IEEE Communications Letters, vol. 28, no. 6, pp. 1447-1451, June 2024. [Objective 1]
- L. K. Baghel, G. Shan, R. Singh, S. Kumar, B-H. Roh and J. Ali, "BLE 5.x-Based Enhanced Service Architecture for Delay-Sensitive IoT Applications," in IEEE Transactions on Mobile Computing, (Major revision Submitted). [Objective 1]
- L. K. Baghel, V. K. Malav and S. Kumar, "THERMOD: Development of a Cost Effective Solution for Integrated Sensing and Logging," in IEEE Sensors Journal, vol. 22, no. 6, pp. 6136-6144, 15 March15, 2022. [Objective 2]
- L. K. Baghel, S. Gautam, V. K. Malav and S. Kumar, "TEMPSENSE: LoRa Enabled Integrated Sensing and Localization Solution for Water Quality Monitoring," in IEEE Transactions on Instrumentation and Measurement, vol. 71, pp. 1-11, 2022. [Objective 3]
- L. K. Baghel, R. Raina, S. Kumar, L. Catarinucci and R. Colella "BLE-Driven Power-Efficient Integrated Sensing and Communication Framework for Livestock Monitoring," in IEEE Journal of Radio Frequency Identification, (Major revision Submitted). [Objective 4]

Other Publications

Journal

- L. K. Baghel, G. Shan, R. Singh, S. Kumar and B-H. Roh, "Clustering to Enhance Throughput in Bluetooth Low Energy Based Heterogeneous Networks," in IEEE Transactions on Green communication and Networking, [Major Revision Submitted].
- L. K. Baghel, R. Raina, S. Kumar, and L. Catarinucci, "IoT Based Integrated Sensing and Logging Solution for Cold Chain Monitoring Applications," in IEEE Journal of Radio Frequency Identification, vol. 8, pp. 837-846, 2024.
- D. Saluja, R. Singh, L. K. Baghel and S. Kumar, "Scalability Analysis of LoRa Network for SNR-Based SF Allocation Scheme," in IEEE Transactions on Industrial Informatics, vol. 17, no. 10, pp. 6709-6719, Oct. 2021.

Conference Proceeding

- L. K. Baghel, S. Ahmet Sis, F. Ustuner and S. Kumar, "EMI Reduction in Multilayer PCBs Using Planar Interdigital Slot Structures on the Reference Planes," 2022 IEEE 9th International Symposium on Microwave, Antenna, Propagation and EMC Technologies for Wireless Communications (MAPE), Chengdu, China, 2022, pp. 352-356.

- L. K. Baghel, S. Kumar, S. A. Sis and J. Kim, "Crosstalk Reduction in Coupled Microstrip Lines using TT-shaped DMS Approach," 2023 Joint Asia-Pacific International Symposium on Electromagnetic Compatibility and International Conference on ElectroMagnetic Interference & Compatibility (APEMC/INCEMIC), Bengaluru, India, 2023, pp. 1-4.

- L. K. Baghel, R. Raina and S. Kumar, "Low Profile Curved Shape Bluetooth Antenna for IoT Applications," 2023 IEEE 17th International Conference on Industrial and Information Systems (ICIIS), Peradeniya, Sri Lanka, 2023, pp. 158-162.

- L. K. Baghel, R. Raina and S. Kumar, "Evolution of Bluetooth Classic Audio towards Bluetooth LE Audio: Challenges and Road Ahead," 2023 IEEE 17th International Conference on Industrial and Information Systems (ICIIS), Peradeniya, Sri Lanka, 2023, pp. 459-464.

- L. K. Baghel, S. Kumar and S. A. Sis, "Crosstalk Reduction in Coupled Microstrip Lines using Interdigital Split on Reference Plane," 2023 7th International Electromagnetic Compatibility Conference (EMC Turkiye), Istanbul, Turkiye, 2023, pp 1-2.

- R. Raina, L. K. Baghel and S. Kumar, "Design and Analyses of Planar Antenna for Bluetooth based IoT Applications," 2023 First International Conference on Microwave, Antenna and Communication (MAC), Prayagraj, India, 2023, pp. 1-5.

- L. K. Baghel, R. Singh, S. Kumar and S. A. Sis, "EMI Reducing Inverted F Slot on Reference Plane of Mixed Signal Design," 2024 IEEE Asia-Pacific Microwave Conference (APMC), Bali, Indonesia, 2024, pp. 465-467.

Contents

List of Figures

List of Tables

Chapter 1

Introduction

The Internet of Things (IoT) represents a major shift in how devices interact and communicate, moving beyond traditional computing to integrate a broad range of physical objects into the digital world [1]. By connecting everyday items such as home appliances [2, 3], wearable health monitors [4], industrial machinery [5, 6], and city infrastructure [7] IoT allows these objects to collect, share, and act on data independently. This connectivity enhances automation, enables real time monitoring, and supports data driven decision making, leading to innovations across various fields [8].

As IoT technology evolves, it promises to revolutionize various domains, from homes and healthcare to industrial processes and urban management, shaping a future where interconnected devices work harmoniously to address complex challenges and enhance human well being [9]. At its core, IoT aspires to optimize efficiency, improve quality of life, and drive sustainability through intelligent automation and real time insights. This vision includes advancing low latency communication to support time sensitive applications such as autonomous vehicles and smart manufacturing, as well as achieving high energy efficiency to extend the operational life of battery powered devices [10].

Hence, this dissertation focuses on minimizing latency and achieving higher energy efficiency to accomplish the above highlighted visions of IoT. The rest of the introductory chapter is structured as follows. Section 1.1 discusses the key application domains of IoT. Section 1.2 discusses crucial IoT applications and their Quality of Service (QoS) requirements. Section 1.3 discusses the architecture of IoT. Section 1.4 provides an overview of different IoT technologies used for wireless data transmission. This section also discusses how to select these technologies. Section 1.5 provides insights into various issues related to latency sensitive and energy constrained IoT applications. Section 1.6 discusses the objectives formulated to address the issues highlighted in Section 1.5. Finally, Section 1.7 provides the dissertation outline and summarizes the key contributions of each chapter.

1.1 Key Application Domains of IoT

The IoT has diverse applications across multiple industries, demonstrating its broad utility and significant impact [11]. Below are key areas where IoT technologies are making a difference (summarized in Figure 1.1).

- **Home:** IoT applications in the home include smart thermostats that autonomously regulate temperature, smart lighting systems that provide automated illumination,

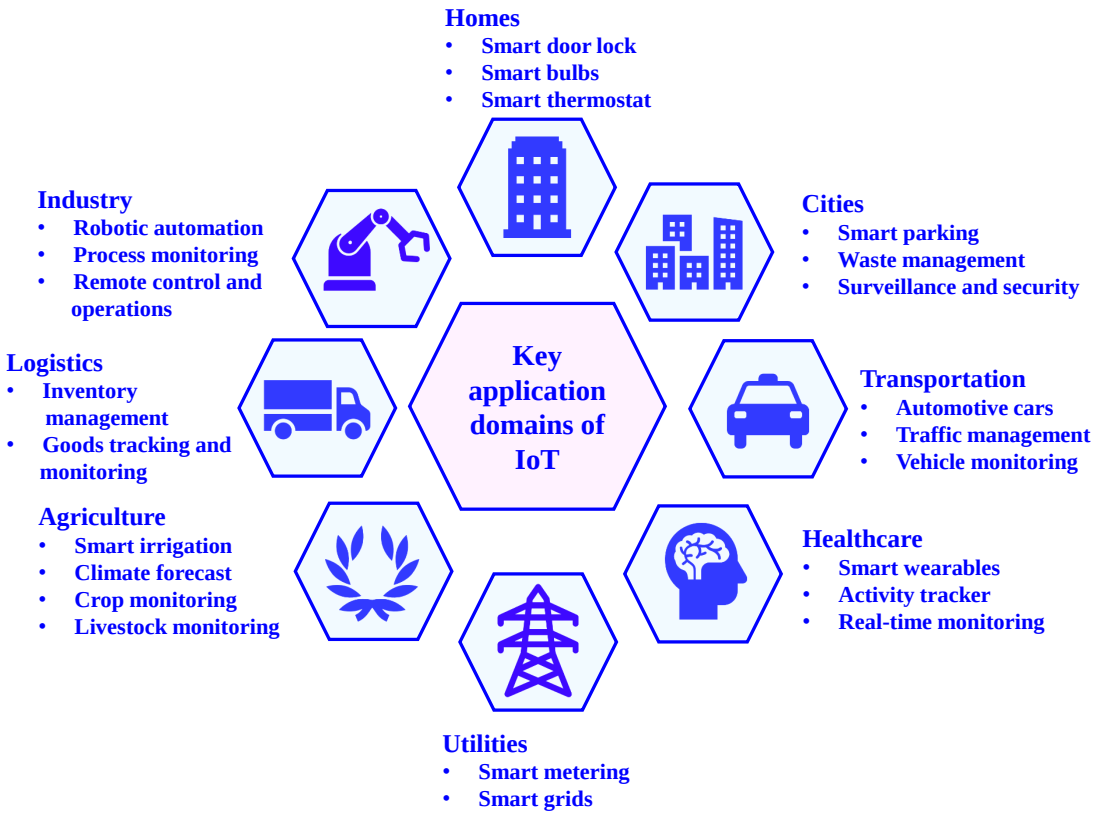

Figure 1.1: Key application domains of IoT.

advanced security systems that deliver real-time alerts, occupancy sensors that adjust settings based on room usage, and smart wearable devices for immersive experiences like virtual and augmented reality [12, 3]. IoT applications in home offers increased comfort, security, and efficiency.

- **Cities:** IoT applications in urban environments include real time traffic management that optimizes traffic flow and reduces congestion, public safety enhancements through closed circuit television (CCTV) surveillance, air quality monitoring that tracks pollution levels, smart waste management systems that streamline collection processes, and intelligent street lighting and parking solutions that improve urban efficiency [13, 14, 15, 16, 17]. IoT applications in cities improve safety, environmental conditions, and operational efficiency and, as a result, enhance the overall quality of life for residents.

- **Transportation:** IoT applications in transportation include connected vehicles that enable communication between vehicles and infrastructure, fleet management systems that monitor and optimize the performance of vehicle fleets, and traffic monitoring tools that provide real-time data on road conditions and traffic flow [18, 19]. IoT applications in transportation streamline operations, enhance safety, and improve overall efficiency.

- **Healthcare:** IoT applications in healthcare includes real time and remote patient

monitoring that track vital signs and health metrics, activity trackers that monitor physical activity and health data, smart warbles that provide continuous health insights, advanced medical devices such as insulin pumps and heart monitors that support personalized treatment plans. IoT applications in healthcare support better health management and timely medical interventions [20, 21, 22].

- **Utilities:** IoT applications in utilities includes; smart grid technologies that optimize energy distribution, energy consumption monitoring systems that track and manage usage, and the integration of renewable energy sources such as solar and wind power [23, 24, 25]. IoT applications in utilities contribute to more efficient and sustainable utility management, reducing energy waste and supporting environmental sustainability [23, 24, 25].

- **Agriculture:** IoT applications in agriculture include precision farming technologies that utilize soil sensors to monitor and manage soil conditions, automated irrigation systems that optimize water usage, and livestock tracking solutions that monitor animal health and productivity. IoT applications in agriculture improve agricultural practices, improve resource management and increase productivity [26, 27, 28].

- **Logistics & Retail:** IoT applications in logistics and retail includes; real time inventory management systems that track stock levels and optimize supply chain operations, personalized marketing tools that target consumers based on their behavior, and asset tracking solutions that monitor the location and status of goods and equipment. IoT applications in logistic and retail, improves operational efficiency, reduces overall time and operational costs, and enhance customer experiences by streamlining inventory and supply chain processes [29, 30].

- **Industries:** IoT applications in industries includes; robotic automation that enhance production processes, real time process monitoring tools that provide insights into manufacturing operations, and remote control solutions that allow for the management of industrial equipment from remote place. IoT applications in industries contribute to improved efficiency, reduced downtime and operation costs, driving overall productivity in industrial environments. [31, 32, 33, 34, 35].

These applications highlight how IoT technologies are transforming various aspects of our lives, improving efficiency, safety, and sustainability across different domains.

1.2 Crucial IoT Applications and their QoS Requirements

The QoS requirements for IoT applications can differ significantly based on their specific use cases and industry contexts. As illustrated in Figure 1.2, different IoT applications have different QoS requirements [36, 37, 38]. For instance, smart industry applications such as robotic automation, predictive maintenance, and industrial process control require low latency, high reliability, etc. Low latency ensures real time response and

efficient automation, whereas reliability ensures consistent data flow and operational stability. Similarly, smart agriculture applications require higher energy efficiency, data integrity, etc. Higher energy efficiency ensures longer battery life, whereas accurate data from sensors ensures reliable and precise monitoring, enabling effective decision making. Likewise, smart city applications require higher scalability, where infrastructure must accommodate an expanding number of connected devices and growing data volumes for applications like traffic management and public safety. Also, smart homes require energy efficiency, low latency, etc. Again, higher energy efficiency ensures longer battery life, which is crucial, whereas low latency here ensures seamless interaction with devices such as smart thermostats and lighting systems.

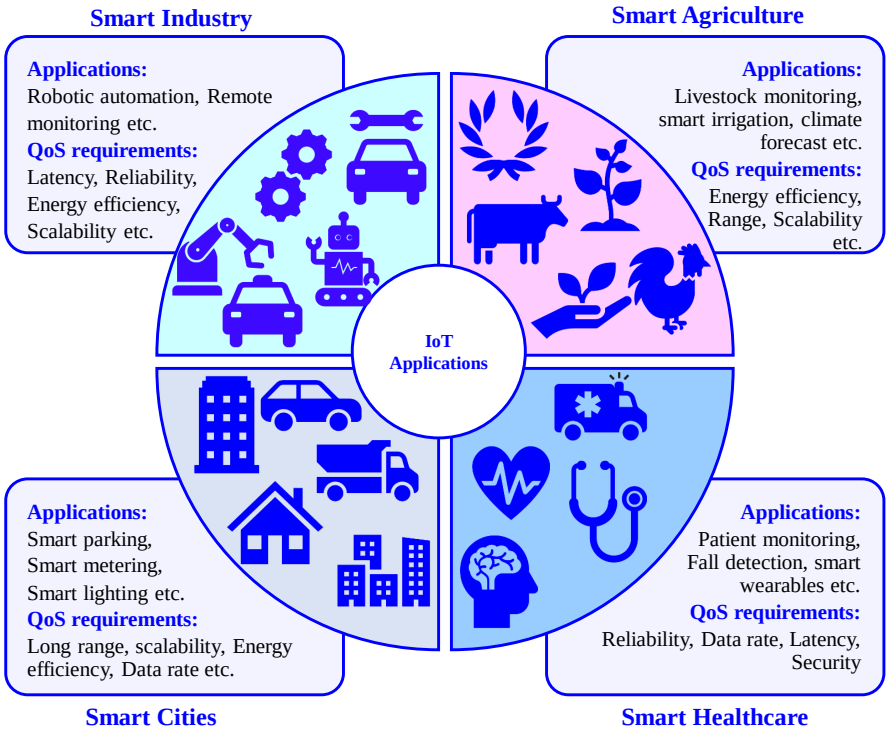

Figure 1.2: IoT applications and QoS requirements.

Across these diverse applications, the common QoS themes—low latency, energy efficiency, reliability, scalability, data integrity, and security—are adapted to meet the specific challenges and requirements of each sector, ensuring effective and reliable IoT solutions [36].

- **Low Latency:** Critical for applications requiring real time responses, such as autonomous vehicles and industrial automation. Example: Autonomous vehicles need minimal data transmission delays to support rapid decision making for safe navigation.
- **Energy Efficiency:** Essential for extending battery life and reducing operational costs, particularly in remote inaccessible or sensor intensive deployments. Example: Environmental monitoring sensors must be energy efficient to minimize maintenance and prolong operational life in remote areas.

- **Reliability:** Ensures consistent and accurate data transmission, crucial for applications in healthcare and industrial settings. Example: Healthcare monitoring systems rely on reliable data transmission to enable timely medical responses.

- **Scalability:** Supports the ability to handle growing numbers of devices and data volumes, which is important for smart city implementations. Example: Smart city infrastructure must accommodate an increasing number of devices and data as urban IoT deployments expand.

- **Data Integrity:** Guarantees that data remains accurate and consistent throughout its lifecycle, vital for applications like asset tracking and environmental monitoring. Example: Agricultural IoT systems need reliable data from soil sensors to support precision farming and enhance crop yield.

- **Security:** Protects data confidentiality, integrity, and authenticity to safeguard against unauthorized access and cyber threats. Example: Industrial IoT systems must implement strong security measures to prevent cyber attacks and protect sensitive operational data [39, 40, 41].

The aforementioned IoT applications highlight diverse QoS requirements ranging from low latency, longer battery life, and high reliability to scalability and security, depending on the specific use case and industry. Hence, meeting these requirements is crucial for ensuring the effectiveness and reliability of IoT deployments across various sectors. From the above discussion, it can be observed that achieving minimal latency and longer battery life is crucial for many applications. Hence, this dissertation primarily focuses on achieving minimal latency and higher energy efficiency in order to fulfill the vision of IoT. The IoT architecture is discussed in the subsequent section.

1.3 IoT Architecture

Most IoT applications use a four layer architecture, as shown in Figure 1.3 [42].

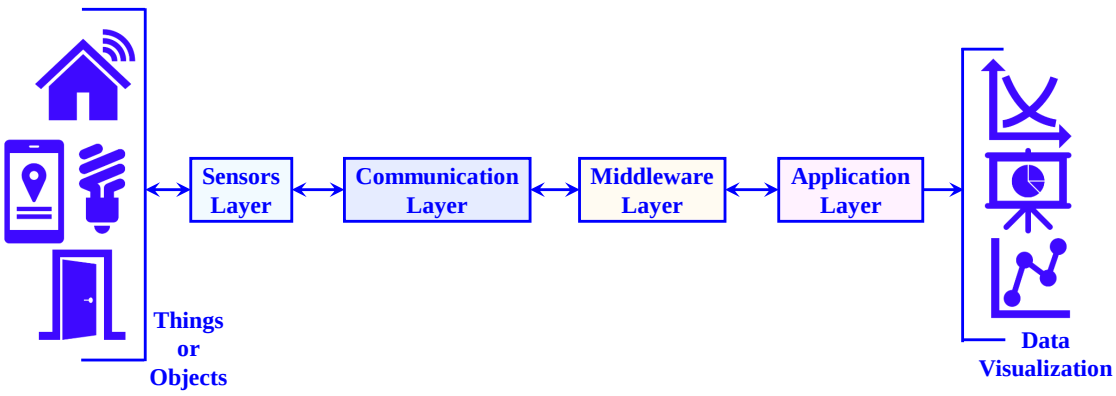

Figure 1.3: A four layer IoT architecture.

Perception Layer: The Perception Layer, also referred to as the sensor layer, plays a crucial role in identifying physical objects and gathering data from them using various sensors. These sensors capture various information, such as temperature, humidity, location, and environmental conditions. Depending on specific applications, different types of sensors are utilized; for example, SHT40 sensors are employed for monitoring temperature and humidity levels.

Communication layer: The Communication Layer, also known as the transmission or network layer, facilitates the transfer of data collected by sensors to a central gateway or base station, and vice versa, using diverse networking technologies like Bluetooth Low Energy (BLE), Sigfox, Long Range (LoRa), or Narrow Band Internet of Things (NBIoT). This layer ensures seamless connectivity and efficient data transmission across the IoT network.

Middle layer: Sitting between the communication and application layers, the Middle Layer, or data processing layer, undertakes the storage, analysis, and processing of data received from the communication layer. It leverages advanced data analytics methodologies and technologies such as databases, cloud computing, and big data processing modules. For instance, in smart transportation applications, this layer can analyze real time traffic data to predict future traffic conditions and optimize traffic management strategies.

Application Layer: The Application layer is where end users interact with the IoT system, accessing application specific services. For example, users may utilize mobile apps to remotely monitor and control devices like air conditioners or coffee makers. This layer ensures seamless integration of IoT functionalities into everyday applications, enhancing user convenience and operational efficiency in diverse contexts..
The technologies used by different IoT applications are discussed in the subsequent section.

1.4 IoT Technologies

Different IoT applications have different requirements in terms of latency, energy efficiency, data rate, coverage range, mobility, cost, etc. A single technology cannot meet these requirements of different IoT applications [43, 44]. For instance, BLE can provide low latency and high energy efficiency, but at the cost of short-medium coverage range [45]. Accordingly, different wireless technologies are usually adopted depending on the needs of the applications. For instance, BLE can be adopted for applications consisting of a large number of devices, requiring low latency, short to medium coverage range, high energy efficiency, and lower cost [45, 46]. Likewise, LoRa can be adopted for applications consisting of a large number of devices requiring longer range, high energy efficiency, and lower cost [46, 47]. The available IoT technologies are shown in Figure 1.4 [38].

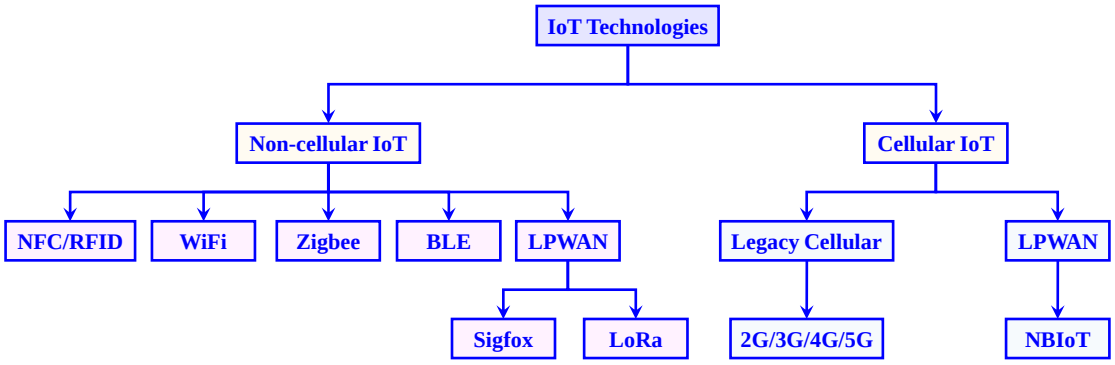

Figure 1.4: IoT technologies.

Most of the IoT applications, for instance, smart manufacturing and autonomous vehicles, require low latency, short-medium coverage range, higher energy efficiency, and higher scalability. Likewise, numerous IoT applications involve remote monitoring, for instance, crop monitoring and smart metering, which require a network that covers a large geographic area, possesses higher energy efficiency, is low cost, and is scalable with an increasing number of connected devices. To meet these requirements, Low Power Wide Area Networks (LPWAN) have recently emerged as the most promising wireless technology [46]. LPWANs offer attractive features such as long range, higher energy efficiency, and low cost communications. However, they are mainly suitable for applications that can tolerate delays and do not require high data rates. The comparison of LPWAN technologies with cellular communication technologies and short range technologies in terms of energy efficiency, latency, and coverage range is shown in Figure 1.5 [38]. The popular LPWAN technologies are LoRa [48], sigfox [49], and NBIoT [50]. An introduction and comparison of these LPWAN technologies are presented in [51, 52]. Among all these LPWAN technologies, LoRa has attracted more attraction due to its open standards that allow an individual to build an autonomous network at a lower cost [46]. Since this dissertation focuses on BLE for latency sensitive applications and LoRa for remote monitoring applications hence, a brief overview of each technology is provided in the subsequent section.

1.4.1 Overview of BLE

BLE is a wireless communication technology designed to provide low power, short range connectivity. Introduced as part of the Bluetooth 4.0 specification by the Bluetooth Special Interest Group (SIG), BLE is optimized for applications requiring minimal energy consumption while maintaining moderate data transfer rates [53]. It is widely used in various applications, including wearable devices, health monitors, and smart home technologies.

Key Features

- **Low Energy:** BLE is engineered for energy efficiency, making it ideal for battery

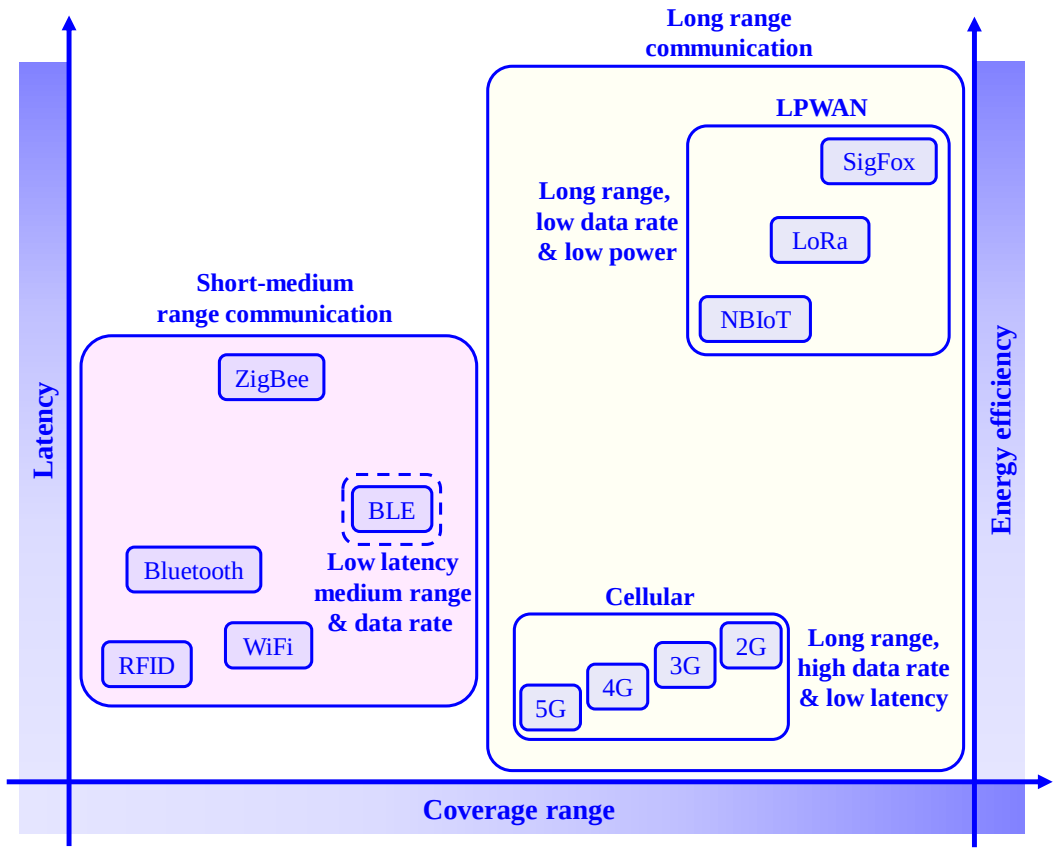

Figure 1.5: Different wireless communication technologies.

operated devices. It achieves this through its efficient use of communication intervals, allowing devices to remain in a low power sleep mode between data transmissions. This design enables BLE devices to operate for months or even years on small coin cell batteries.

- **Range:** BLE typically supports communication ranges of up to 200 meters in open space [45]. This medium range capability is suitable for applications where devices are within close proximity, such as machine automation in the smart industry.

- **Scalability:** BLE advertisement can support thousands of devices within a single network, making it suitable for large scale deployments such as smart cities and smart industries.

- **Data Rate:** BLE operates with data rates up to 2 Mbps. This data rate is adequate for the majority of applications that require periodic data transmission rather than high bandwidth communication.

1.4.1.1 BLE Communication

This section discusses BLE communication in detail, in particular it discusses different modes of communication, different advertising modes, packets structures etc.

Link Layer Modes: A BLE device resides in either of the following modes: standby, initiating, advertising, connection, and scanning. The data transfer occurs either in advertising or connection mode. The advertising mode can be entered directly from the standby mode (lowest power mode, no transmission, and reception), whereas the connection mode requires one intermediate mode, i.e., either the advertising or initiating mode, as shown in Figure 1.6. In advertising mode, data transfer occurs directly without

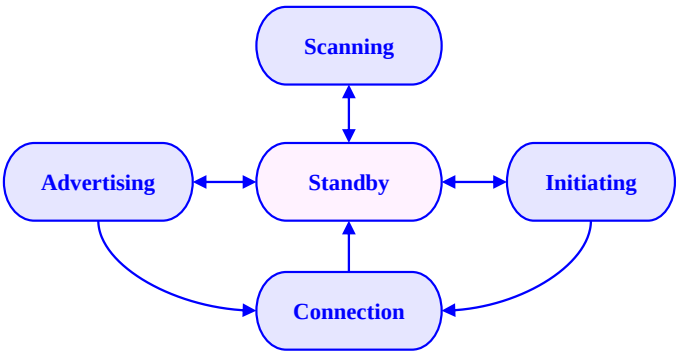

Figure 1.6: Link layer modes in BLE.

establishing a connection. This is also known as BLE advertising mode. Meanwhile, in connection mode, data transfers occur only when the connection is established. This is also known as BLE connection mode. Within the connection mode, two roles are defined,

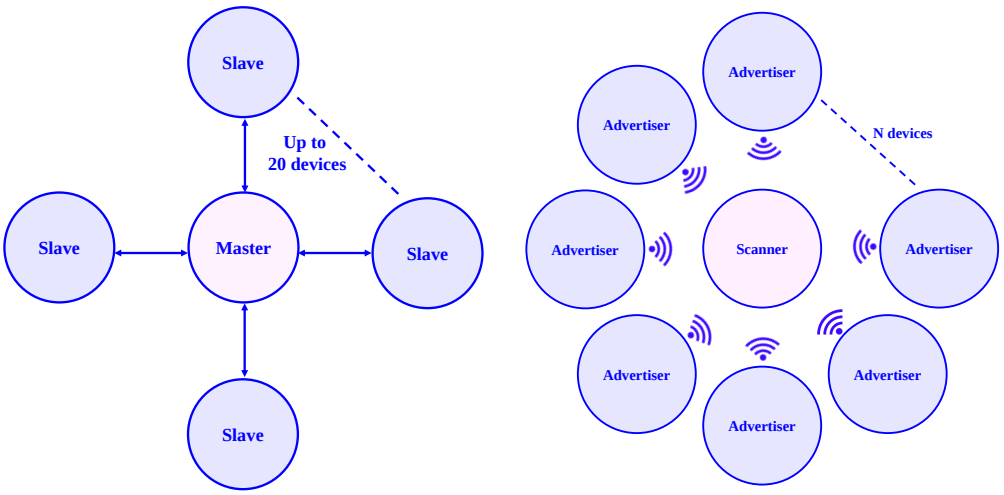

(a) BLE connection mode (connection oriented communication)

(b) BLE advertising mode (connectionless communication)

Figure 1.7: Communication modes in BLE

i.e., master (when entered from the initiating mode) and slave (when entered from the advertising mode). The data transfer in BLE connection mode comes at the cost of high energy consumption. Also, if the connection drops, re-connection occurs at the cost of increased energy consumption. Further, BLE connection mode supports a limited number of devices, whereas BLE advertising mode supports a large number of devices as shown in Figure 1.7. Hence, BLE advertising mode is preferred for energy constrained IoT applications [54, 55].

BLE Advertising Channels BLE advertising mode uses 40 RF channels in the 2.4 GHz band. The center frequencies for these channels are distributed according to the equation, i.e., 2402 + n*2MHz, where n ranges from 0 to 39. The channels are divided into two groups, i.e., primary channels and secondary channels. The three channels with channel index 37 (2402MHz), 38 (2426MHz), and 39 (2480MHz) are known as primary channels, whereas the remaining 37 channels with channel indexes 0-10 and 11-36, are known as secondary channels, as shown in Figure 1.8. The primary channels are used in BLE legacy advertising, whereas secondary channels are used in BLE extended and periodic advertising. The primary advertising channels are selected so that the BLE transmissions may not interfere with the WiFi transmissions occurring on the co-existing channels (shown in blue shade).

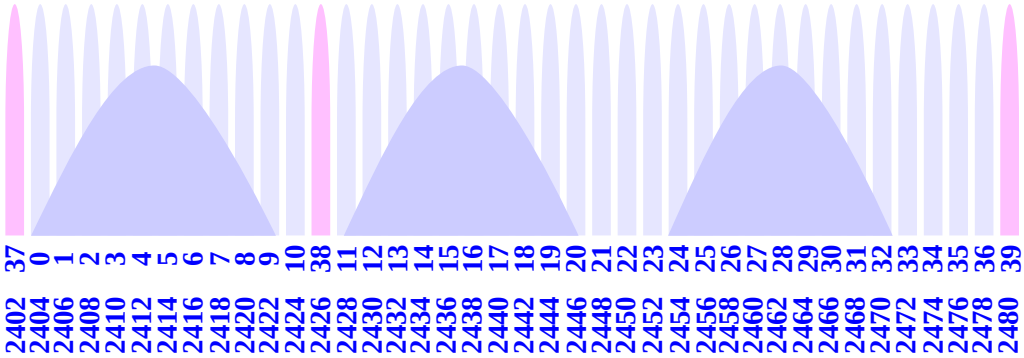

Figure 1.8: BLE advertising channels.

BLE Advertising Types: BLE advertising is of three types, namely, BLE legacy advertising, BLE extended advertising, and BLE periodic advertising. BLE legacy advertising is used for small data transfer applications, whereas BLE extended and periodic advertising is used for large data transfer applications. In particular, BLE legacy advertising supports 31 bytes, and BLE extended and periodic advertising supports 254 bytes of host data in one packet. BLE legacy advertising uses primary channels for data transmission, whereas BLE extended and periodic advertising uses primary channels to indicate advertising on secondary channels and secondary channels for data transmission. The total time taken by one BLE advertisement is known as an advertising period. For BLE legacy and extended advertising, the adverting period consists of a fixed value known as advertising interval (20ms-10,485.75s) and a pseudo random value (0-10ms). The random value randomizes the BLE legacy and extended advertisement transmissions in time from different BLE devices, hence avoiding repetitive collisions. However, the random delay in BLE legacy and extended advertisements makes it harder for the gateway to follow the BLE advertiser in the long run; hence, to address this issue, BLE periodic advertisement was launched, which consists of only a fixed advertising period starting from 7.5ms to 81.91875s.

Establishing BLE legacy advertising requires transmission of ADV_IND packet on primary

channels. However, establishing BLE extended advertising requires (i) transmitting ADV_EXT_IND on primary channels containing information such as timing offset and channel index of AUX_ADV_IND packet to inform a gateway that an advertisement will be sent on secondary channels, (ii) then transmitting AUX_ADV_IND packet on secondary channels containing the advertisers data. Similarly, establishing BLE periodic advertising requires (i) transmitting ADV_EXT_IND on primary channels containing information such as timing offset and channel index of AUX_ADV_IND packet to inform gateway that an advertisement will be sent on secondary channels, (ii) AUX_ADV_IND packet on secondary channels containing timing offset of AUX_SYNC_IND packet, periodic advertising period value, and channel map for AUX_SYNC_IND packets, and (iii) AUX_SYNC_IND packet on secondary channels containing host data. The detailed process for BLE legacy, extended, and periodic advertising is shown in Figure 1.9.

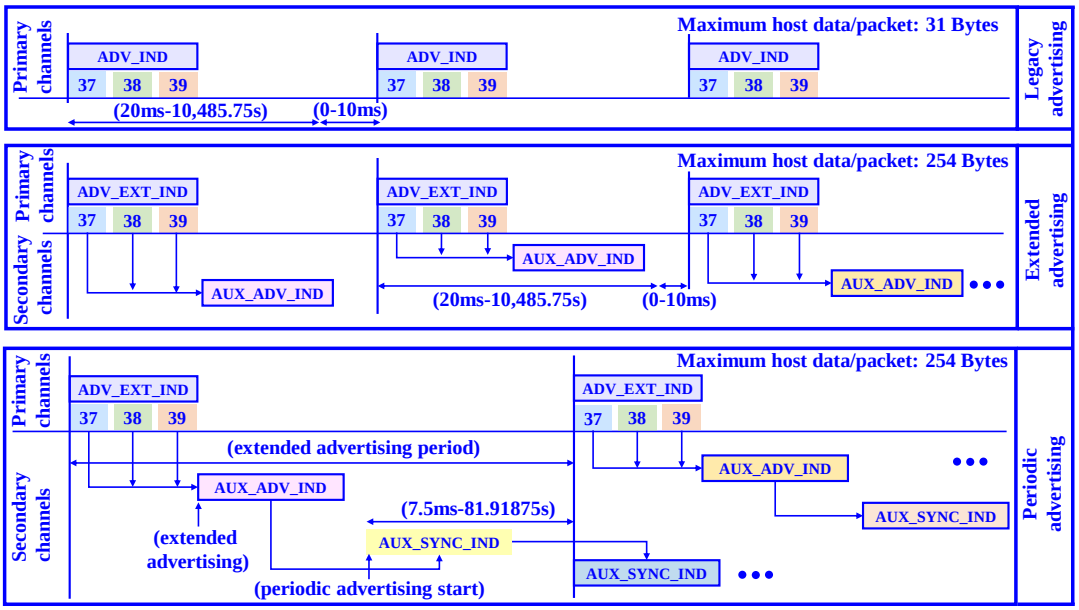

Figure 1.9: Advertising modes in BLE

BLE Advertising Packet Structure BLE packet structure for different advertising modes is shown in Figure 1.10. The packets have four main fields, i.e., preamble, access address, protocol data unit (PDU), and CRC. The preamble field is used for frequency synchronization, automatic gain control, and symbol time estimation. All the advertising channel packets have the same access address, i.e., 0x8E89BE06. The cyclic redundancy check (CRC) field is used for error correction and detection. The PDU field consists of host data. In particular, BLE legacy advertising supports 31 bytes, and BLE extended and periodic advertising supports 254 bytes of host data in one packet.

BLE Architecture: Figure 1.11 shows the architecture of BLE based IoT solutions. It consists of BLE sensor nodes, each equipped with sensors that collect data. These sensor nodes transmit the collected data to a central gateway via a BLE link. Once received by

BLE Legacy Advertising

Preamble (1 Byte)	Access address (4 Bytes)	PDU (2-39 Bytes)	CRC (3 Bytes)

BLE Extended and Periodic Advertising

Preamble (1 or 2 Bytes)	Access address (4 Bytes)	PDU (2-257 Bytes)	CRC (3 Bytes)

Figure 1.10: Packet structure for different advertising modes of BLE

the gateway, the data is forwarded to a server over an internet connection. Users can then access and analyze the data from the server.

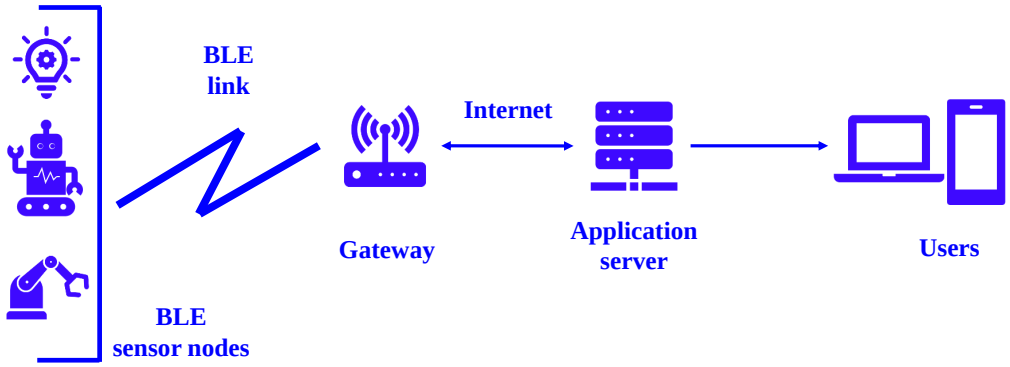

Figure 1.11: BLE architecture.

1.4.2 Overview of LoRa

LoRa is a LPWAN technology designed for long range wireless communication [56]. LoRa, developed by Semtech Corporation, is a key enabler of the IoT by facilitating connectivity in applications requiring long range data transmission with minimal energy consumption. LoRa operates in the sub-GHz radio frequency bands, typically around 868 MHz in Europe, 915 MHz in North America, and 433 MHz in Asia. It employs a modulation scheme known as Chirp Spread Spectrum (CSS), which enables it to achieve significant range and penetration capabilities. The CSS technique spreads the signal over a wide bandwidth, enhancing its robustness against interference and enabling reliable communication over distances that can reach up to 15-20 kilometers in rural areas and several kilometers in urban environments [57].

Key Features

- **Long Range:** LoRa primary advantage is its extended communication range, which is substantially greater than that of traditional cellular networks and other short range technologies like Bluetooth. This long range capability makes it ideal for applications where devices are dispersed over large areas.

- **Low Energy:** LoRa devices are designed to operate on low energy, allowing them to function for years on small batteries. This energy efficiency is crucial for IoT applications where devices are often deployed in remote or hard to access locations.
- **Scalability:** LoRa networks can support thousands of devices within a single network, making it suitable for large scale deployments such as smart cities and agricultural monitoring systems.
- **Low Data Rate:** While LoRa excels in range and energy efficiency, it is optimized for low data rate transmissions. This characteristic is well suited for applications that require infrequent updates or small data payloads, such as sensor readings and status updates.

Network Architecture: LoRa networks are typically structured in a star topology and primarily consist of LoRa sensor nodes, gateway, network server, and application server as shown in Figure 1.12.

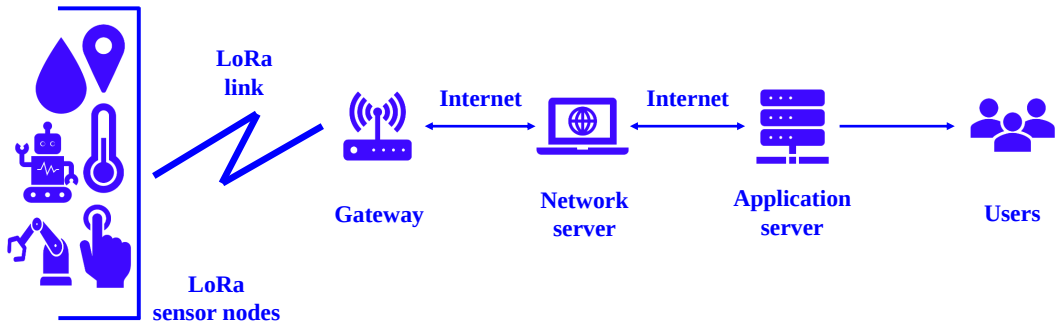

Figure 1.12: LoRa architecture.

- **Sensor Nodes:** These are the devices equipped with sensors or actuators that communicate with the network.
- **Gateways:** Gateways receive signals from multiple end devices and relay the data to a central network server. They also send downlink messages from the server to the end devices.
- **Network Server:** The network server manages data traffic, performs duplication, and handles network specific tasks such as security and routing.
- **Application Server:** This server processes the data received from the network server and interfaces with end user applications.

1.5 Issues in Current IoT Solutions

As introduced at the beginning of the chapter, achieving the vision of IoT requires both minimal latency and higher energy efficiency. Certainly, choosing a technology with low

latency and higher energy efficiency can solve the problem. However, merely selecting such technologies does not guarantee minimal latency and higher energy efficiency. This realization motivated us to investigate the existing solutions that address latency and energy efficiency. The literature survey revealed several shortcomings in the current solutions, whose details are given below:

1.5.1 Issues in Solutions for Latency Sensitive Applications

Besides the transmission technology, latency is significantly influenced by the configuration of transmission parameters. This underscores the importance of selecting the right parameters to achieve minimal latency. In this context, the following shortcomings were found in the literature:

- Lack of analytical model to analyze latency [58, 59, 60].
- No emphasis on transmission parameter selection to get minimal latency.
- No simplified expression to choose the transmission parameters.

1.5.2 Issues in Solutions for Energy Constrained Applications

An IoT solution is based on three main pillars, i.e., sensor node (sensing device), sensing (the process of obtaining data from sensors), and communication (the process of transmitting data to the central server).

- **Sensor Node:** It is found that the existing nodes for energy constrained applications are based on general purpose microcontroller boards and sensor breakout boards, which affect accuracy, increase size and increases energy consumption, thereby reducing overall battery life [61, 62]. Besides, the sensors are powered directly from the power supply. Due to the continuous power supply, sensors consume few µA's of current even in the sleep mode.
- **Sensing:** Further, it is observed that the existing solutions utilize a global positioning system (GPS) for real time location estimation even when higher accuracies are not desired or high errors in real time locations can be tolerated; however, it is a known fact that GPS requires significant energy budget for its operation, hence effects overall battery life significantly [63].
- **Communication:** The existing solutions sense and transmit the data, causing inefficient resource utilization as a packet space may not be fully utilized for a single sense event [54, 64]. Further, the existing solutions transmit raw data obtained from sensors, consequently increasing total number of transmissions, hence reducing overall battery life significantly [65, 66]. Furthermore, existing solutions transmit a fixed number of copies to overcome packet loss. However, transmitting a fixed number of copies may not necessarily overcome packet loss and may also lead to unnecessary transmissions, hence further degrading overall battery life.

1.6 Formulated Objectives

In the previous section, we have discussed issues in existing works. Now in this section, we have formulated objectives to address each of these issues.

1.6.1 Latency Minimization Through Optimal Parameter Selection

The first challenge that we identified in the previous section is to achieve minimal latency. To address this challenge, this dissertation first proposes a performance model that can be used to analyze the latency, then provides close form expressions to choose the optimal parameters that give the minimal latency. A summary of the identified challenge-1, issues with existing work, and the objectives formulated to address this challenge is given in Figure 1.13.

1.6.2 Battery Life Enhancement Through Effective Hardware Design and Efficient Utilization.

The second challenge that we identified in the previous section is to integrate sensors, controller, and communication circuitry on a single platform. To address this challenge, this dissertation develops an integrated sensing and communication platform that utilizes the general purpose of input output pins (GPIOs) for powering sensors. A summary of the identified challenge-2, issues with existing work, and the objectives formulated to address this challenge is given in Figure 1.13.

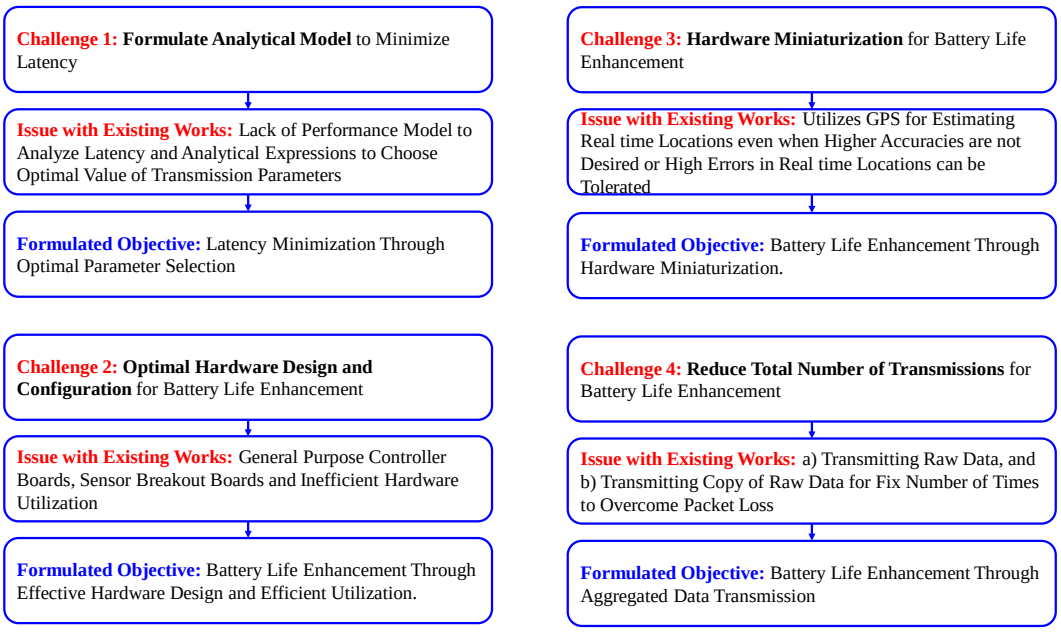

Figure 1.13: Summary of identified challenges and objectives formulated.

1.6.3 Battery Life Enhancement Through Hardware Miniaturization

The third challenge that we identified in the previous section is to identify an energy efficient alternative to GPS for real time location estimation. To address this challenge, this dissertation proposes a received signal strength indicator (RSSI) based localization solution for real time location estimation. A summary of the identified challenge-3, issues with existing work, and the objectives formulated to address this challenge is given in Figure 1.13.

1.6.4 Battery Life Enhancement Through Aggregated Data Transmission

The fourth challenge that we identified in the previous section is to reduce the total number of raw data transmissions. To address this challenge, this dissertation proposes an aggregated data transmission approach based on statistical parameters. A summary of the identified challenge-4, issues with existing work, and the objectives formulated to address this challenge is given in Figure 1.13.

1.7 Thesis Outline

This dissertation aims to manage and fulfill two crucial QoS requirements, namely, a) latency and b) energy efficiency. Based on these QoS requirements, this dissertation is divided into two parts: Part A and Part B. Part A deals with issues in latency sensitive applications and their solutions. Part B deals with issues in energy constrained applications and their solutions. From Part A, Chapter 2, and Chapter 3, and Part B, Chapters 4, 5, and 6 are formulated. The brief overview of chapters (chapter 1 onward) constituting this dissertation is summarized below (also shown in Figure 1.14):

1.7.1 Chapter 2: Latency Minimization for Sensor Nodes-Gateway Communication

This chapter discusses latency minimization through optimal parameter selection for sensor nodes-gateway communication scenario. In particular, this chapter first discusses the performance model to analyze the latency, followed by latency minimization. Based on the minimal latency close form expressions for transmission parameter selection are derived that ensure minimal latency. Lastly, it discusses how selecting proper transmission parameters can also improve battery life.

1.7.2 Chapter 3: Latency Minimization for Sensor Nodes-Gateway-User Communication

This chapter discusses latency minimization through optimal parameter selection for applications requiring sensor nodes-gateway-user communication scenarios. In particular, this chapter first discusses the performance model to analyze latency for sensor

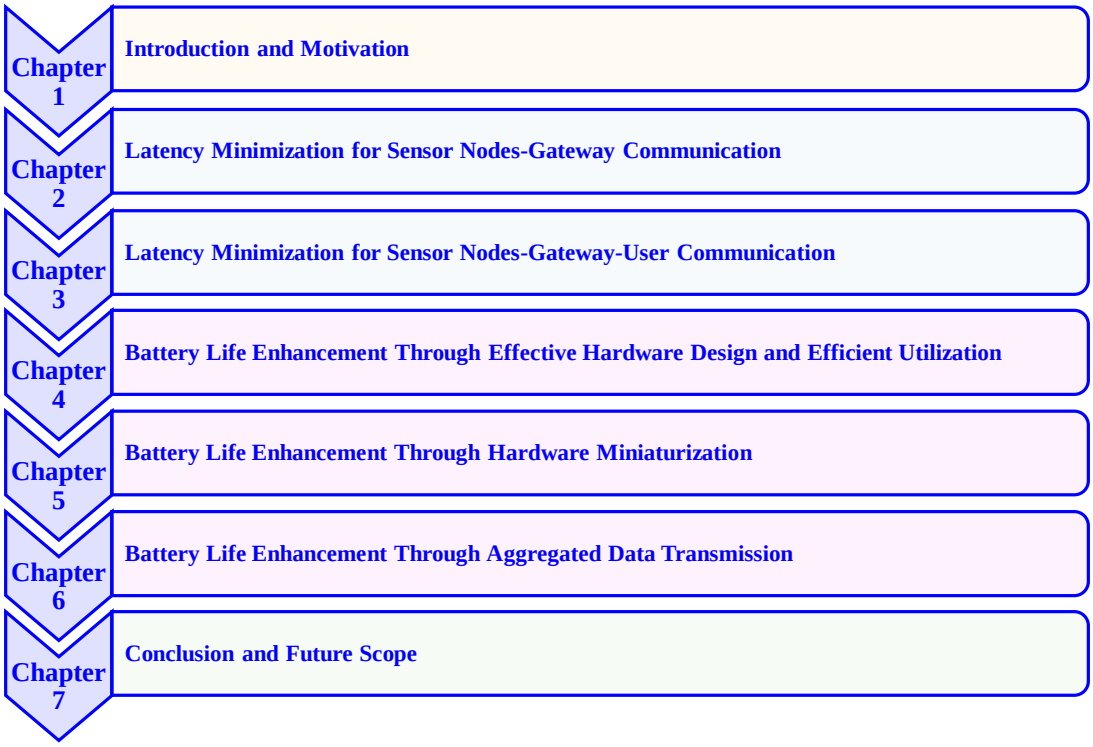

Figure 1.14: Thesis layout.

nodes-gateway and gateway-users. Based on the performance model, optimization is performed. Based on the optimization model, analytical expressions are derived, which can directly be used for transmission parameter selection assuring minimal latency.

1.7.3 Chapter 4: Battery Life Enhancement Through Effective Hardware Design and Efficient Utilization

This chapter discusses battery life enhancement through optimal hardware design and efficient utilization. In particular, it discusses how powering sensors directly from the power supply and through GPIO impacts the overall battery life. Further, it discusses how clock configuration impact overall battery life. Furthermore, the current consumption results for battery life evaluation are analyzed and discussed.

1.7.4 Chapter 5: Battery Life Enhancement Through Hardware Miniaturization

This chapter discusses battery life enhancement through hardware miniaturization. In particular, this chapter discusses how replacing GPS (a power hungry device) with RSSI based localization algorithm can increase energy efficiency and overall battery life. Further, it discusses the experiments conducted in indoor and outdoor environments to verify algorithms, followed by a discussion and comparison of experimental data with the GPS data, which confirms that the GPS can be replaced with the proposed RSSI based localization algorithm in dense scenario where GPS may not work and or where accuracy in few meters can be tolerated.

1.7.5 Chapter 6: Battery Life Enhancement Through Aggregated Data Transmission

This chapter discusses battery life enhancement through aggregated data transmission. In particular, this chapter first discusses how raw data can be converted to aggregated data, i.e., the identification of statistical parameters. Then, it discusses an analytical framework for selecting the number of copies required to overcome packet loss and redundant transmissions. Lastly, the battery life results are discussed and compared with the existing solutions.

1.7.6 Chapter 7: Conclusion and Future Scope

This chapter concludes the dissertation by summarizing the key findings. This chapter also discusses several future research directions.

Chapter 2

Latency Minimization for Sensor Nodes-Gateway Communication

As discussed in the introductory chapter, latency is critical for latency sensitive applications; for example, in autonomous vehicles, even a minor delay in processing sensor data can impact real time decision making and safety on the road [67]. Hence, we focus on minimizing latency for key latency sensitive IoT applications such as robotic automation in industries, smart parking solutions [68], [69]. Typically, such applications involve one of the two scenarios: sensor nodes-gateway communication and sensor nodes-gateway-user communication. Hence, this chapter focuses on minimizing latency for sensor nodes-gateway communication scenario, while the subsequent chapter focuses on minimizing latency for sensor nodes-gateway-user communication scenario.

To begin with, we have considered a smart manufacturing industry use case requiring sensor nodes-gateway communication. In smart manufacturing industries, numerous robot arms operate simultaneously along the production line. Each robot arm is equipped with sensors that continuously transmit sensor data or control signals to the gateway, as shown in Figure 2.1. The sensor node requirements for such applications can go up

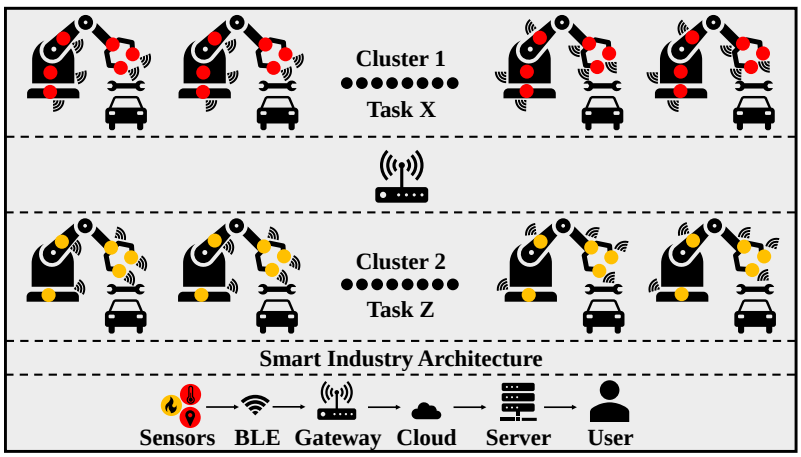

Figure 2.1: Illustration of clustered architecture use case.

to 10^6-10^7 devices per square kilometer [70]; this consequently puts several challenges and limits the utilization of conventional cellular technologies. However, the recent advancements in low latency, low energy protocols, especially BLE, have emerged as the most promising candidates for implementing such types of Industrial Internet of Things (IIoT) applications [29]. However, merely selecting a low latency communication protocol

does not guarantee minimal latency. Hence, selecting optimal transmission parameters is crucial. For example, in BLE advertising, when the advertising interval is set too large, the BLE gateway receiving the packets must wait for advertising packets to arrive, which increases the overall data reception latency. Conversely, with a small advertising interval, the advertising packets become overpopulated, resulting in extensive collisions. This, in turn, raises the overall data collection latency [71], [72]. Therefore, selecting an optimal value of transmission parameters (optimal advertising interval) is important. However, none of the existing works have provided simplified expressions to choose optimal parameters for minimizing latency. Moreover, the current solutions often assume homogeneous network scenarios; however, the majority of IoT applications, including the smart manufacturing industry, have a variety of sensors with different data sizes, hence likely to form a heterogeneous network. To address the aforementioned issues, first, we have developed a performance model considering a heterogeneous scenario to analyze latency, and based on the performance model, we have derived an analytical expression for selecting optimal transmission parameters (optimal advertising interval). Based on these analytical expressions, we proposed algorithms that autonomously optimize the network and ensure minimal latency. A brief review of existing works and their shortcomings, as well as how our proposed work differs from the existing works, is introduced below.

2.1 Related Work and Motivation

Indeed, significant research efforts have been made towards determining the optimal advertising interval [58], [59], [60]; however, they have certain shortcomings. For instance, the authors in [58] have shown that there exists an optimal value that gives minimal data reception latency. However, the authors have not provided any analytical expression to choose the optimal interval value. Besides, the authors in [59] have formed a mathematical model to select the advertising interval based on Chinese remainder theory (CRT). However, the algorithm's complexity grows significantly when the number of BLE sensor nodes in the network increases; additionally, it does not assure the optimality of the selected interval. Likewise, the authors in [60] have put forth a numerical algorithm to determine the optimal solution; however, the proposed algorithm has high computational complexity and may pose challenges in practical hardware implementations.

Apart from the aforementioned shortcomings, the existing solutions are solely based on BLE legacy advertisement, which has limited data transmission capability, i.e., 31 bytes in one packet [68]. Also, the transmissions in BLE legacy advertisement are limited to three advertising channels (37, 38, 39), which significantly populates the network and causes collisions, consequently increasing the overall latency. Furthermore, the existing solutions have considered only networks with the same set of BLE parameters; however, a BLE based IIoT network may have BLE sensor nodes that operate on different sets of BLE parameters, which is a critical bottleneck in the existing solutions. The shortcomings of the existing works are summarized in Table 2.1.

Table 2.1: State of the art solutions and their shortcomings.

References	**BLE Mode**	**Optimal expression**	**Clustered Architecture**
[58]	Legacy	✗	✗
[59]	Legacy	Algorithm	✗
[60]	Legacy	Algorithm	✗
[68]	Legacy	✓	✗
Proposed	Extended	✓	✓

Hence, to address the aforementioned issues, this chapter proposes a BLE based extended advertisement methodology (shown in Figure 2.2) for IIoT BLE sensor nodes with larger data (can accommodate up to 255 bytes in one packet) and a heterogeneous scenario where the BLE sensor nodes in the network may have a different set of BLE parameters. In particular, we have derived the optimal advertising interval simplified close form expression for a heterogeneous network consisting of n clusters.

2.2 Contributions

Specifically, the contributions of this chapter are summarized as follows:

- Analytically derived close form expression for optimal transmission parameter selection (optimal advertising interval).
- A low complexity algorithm based on an analytical framework has been developed that autonomously optimizes the advertising interval based on the network parameters.
- An energy consumption model has also been proposed, which will help the service providers to choose the parameters efficiently and will also help in determining the estimated battery life of the BLE sensor nodes in the networks.
- Further analytical results are also compared with simulation results, which are in good agreement with simulation results that validate the proposed solution.

2.3 System Model

This section describes the system model for a densely deployed BLE based heterogeneous network considering a smart manufacturing industry use case. The proposed model is based on BLE extended advertising consisting of ADV_EXT_IND packets of duration T_{adv} and AUX_ADV_IND packets of duration $T_{aux,n}$, advertised at $T_{ap,n}$ period which consists of $T_{ai,n}$ and random delay (T_{rd}) as shown in Figure 2.2. In a BLE based heterogeneous network, BLE sensor nodes operate on different sets of BLE parameters, and based on the set of BLE parameters used, they are grouped together, and the groups are called clusters. In particular, we have considered the n cluster scenario. The BLE sensor nodes

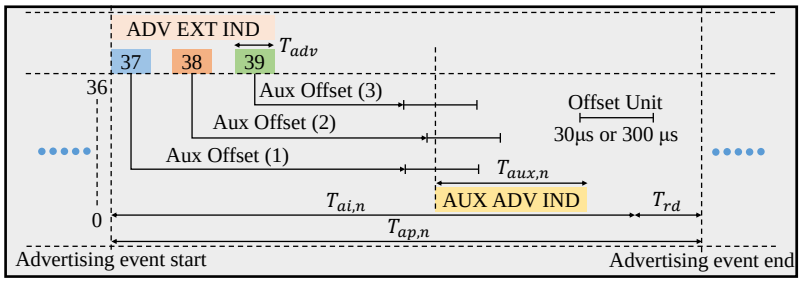

Figure 2.2: Parametric nomenclature in BLE extended advertising.

in 1^{st} cluster of the heterogeneous network have N_1, $T_{aux,1}$, $T_{ap,1}$ set of BLE parameters, whereas, 2^{nd} cluster have N_2, $T_{aux,2}$, $T_{ap,2}$, similarly n^{th} cluster have N_n, $T_{aux,n}$, $T_{ap,n}$ set of BLE parameters respectively. The BLE sensor nodes in such networks transmit the data packets randomly, which may cause the overlapping of data packets in time; this phenomenon is called collision [73]. Based on overlapping time (vulnerable time, which is T_{adv}, and $T_{aux,n}$ long for an extended advertising data packet), the probability of packet success is derived, followed by the average number of packet required for successful transmission calculations, which when multiplied by advertising period gives latency [68]. In addition to the above, an average energy consumption model is also proposed which will help the service provider to choose parameters efficiently and will also help in estimating the battery life of the BLE sensor nodes in the network. The BLE gateway is configured in continuous scanning mode with scan interval (T_{si}) greater than the advertising period ($T_{ap,n}$) for better performance [74]. Hence, it is assumed that the BLE gateway successfully decodes the received (non collided) packet [74].

2.3.1 Latency Modeling in Heterogeneous IIoT Environment

In this analysis, n clusters are considered, having N_i ($i = 1$ to n), the number of BLE sensor nodes in each cluster. Each BLE sensor node in a cluster is transmitting two packets; *i)* a control packet (ADV_EXT_IND) of size T_{adv} on primary channels $(37, 38, 39)$ and *ii)* an actual data packet (AUX_ADV_IND) of size $T_{aux,n}$ on secondary channels $(0 - 36)$, with advertising period of $T_{ap,n}$ duration [75] as shown in Fig. Figure 2.2. Transmission of a reference BLE sensor node in a cluster, for instance, n^{th} cluster, is said to be successful when it does not collide with the transmissions from $(N_n - 1)$ BLE sensor nodes within n^{th} cluster and the transmissions of $\sum_{i=1}^{n-1} N_i$ BLE sensor nodes from remaining $(n - 1)$ clusters. The collisions caused by transmissions within the cluster are referred to as intracluster collisions, whereas the collisions caused by transmissions from BLE sensor nodes in other clusters are called intercluster collisions. For example, in n^{th} cluster, the control (ADV_EXT_IND) and data (AUX_ADV_IND) packets of a reference BLE sensor node may collide with the transmissions from other $(N_n - 1)$ BLE sensor nodes within the cluster. Similarly, control (ADV_EXT_IND) and data (AUX_ADV_IND) packets of a reference BLE sensor node in the cluster may collide with the control (ADV_EXT_IND) and data (AUX_ADV_IND) packets transmissions of $\sum_{i=1,}^{n-1} N_i$ BLE sensor nodes from $(n-$

1) clusters. So, within n^{th} cluster, there can be a total of $2(N_n-1)+\sum_{i=1}^{n-1}2N_i$ collisions, i.e., $2(N_n-1)$ intracluster (each BLE sensor node at max can contribute two collisions and there are (N_n-1) BLE sensor nodes within the cluster, hence $2(N_n-1)$ collisions), similarly $\sum_{i=i}^{n-1}2N_i$ intercluster collisions (each BLE sensor node at max can contribute two collisions and there are $\sum_{i=1}^{n-1}N_i$ total BLE sensor nodes hence $\sum_{i=1}^{n-1}2N_i$ collisions). Hence, the probability that the control (ADV_EXT_IND) and data (AUX_ADV_IND) packet transmissions of reference BLE sensor node in n^{th} cluster are not colliding with the transmissions of other (N_n-1) BLE sensor nodes within n^{th} cluster and the transmissions of $\sum_{i=1}^{n-1}N_i$ BLE sensor nodes from other $(n-1)$ clusters:

$$P_{succ,n}=\overbrace{\left(1-\frac{2T_{adv}}{T_{ap,n}}\right)^{N_n-1}\left(1-\frac{1}{Y}\frac{2T_{aux,n}}{T_{ap,n}}\right)^{N_n-1}}^{\text{due to transmissions from } N_n \text{ BLE sensor nodes from } n^{th} \text{ cluster (I)}}\times\underbrace{\prod_{i=1}^{n-1}\left(1-\frac{2T_{adv}}{T_{ap,i}}\right)^{N_i}\left(1-\frac{1}{Y}\frac{T_{aux,n}+T_{aux,i}}{T_{ap,i}}\right)^{N_i}}_{\text{due to transmissions from } \sum_{i=1}^{n-1}N_i \text{ BLE sensor nodes from } (n-1) \text{ clusters (II)}} \tag{2.1}$$

where, $P_{succ,n}$, is the probability of success for a transmission from a reference BLE sensor node in n^{th} cluster. T_{adv}, $T_{aux,n}$ are control and data packet size, $T_{ap,n}$ is the advertising period, N_n is the number of BLE sensor nodes in n^{th} cluster respectively. $T_{aux,i}$, $T_{ap,i}$, N_i is the data packet size, advertising period, and number of BLE sensor nodes in i^{th} cluster, where i can take value from 1 to $(n-1)$ in case of calculations for n^{th} cluster. $1/Y$ is the probability of secondary channel (0-36) selection $(=1/37)$.

The first term (I) in (2.1) represents the probability of packet success for a reference BLE sensor node in n^{th} cluster when N_n BLE sensor nodes are advertising. In particular, $(1-(2T_{adv}/T_{ap,n}))^{N_n-1}$ represents probability of control packets success and $(1-(2T_{aux,n}/YT_{ap,n}))^{N_n-1}$ represents probability of data packets success. The second term (II) in (2.1) represents the probability of packet success for a reference BLE sensor node in n^{th} cluster when $\sum_{i=1}^{n-1}N_i$ BLE sensor nodes from other $(n-1)$ clusters are transmitting. In particular, the first sub term (of II), $(1-(2T_{adv}/T_{ap,i}))^{N_i}$ represents the probability of control packet success for a BLE sensor node in n^{th} cluster when i^{th} cluster BLE sensor nodes are transmitting, similarly the second sub term (of II), $(1-((T_{aux,n}+T_{aux,i})/YT_{ap,i}))^{N_i}$ represents the probability of data packet success for a BLE sensor nodes in n^{th} cluster, when i^{th} cluster BLE sensor nodes are transmitting. Since there are total n clusters, and for a reference BLE sensor node in n^{th} cluster, i takes values from 1 to $(n-1)$, consequently the product term.

Now, the expression for the average number of transmissions required for successful reception of a reference BLE sensor node in n^{th} cluster ($N_{avg,n}$) can be derived as (mean of geometric distribution):

$$N_{avg,n}=\frac{1}{P_{succ,n}} \tag{2.2}$$

The data reception latency $L_{dr,n}$ for a reference BLE sensor node in n^{th} cluster can be calculated by multiplying the average number of transmissions required for successful reception $N_{avg,n}$ with the advertising period ($T_{ap,n}$). The data reception latency for reference BLE sensor node in n^{th} cluster can be calculated as:

$$\begin{aligned} L_{dr,n} &= N_{avg,n} T_{ap,n} \\ &= \frac{T_{ap,n}}{\left(1-\frac{2T_{adv}}{T_{ap,n}}\right)^{N_n-1}\left(1-\frac{1}{Y}\frac{2T_{aux,n}}{T_{ap,n}}\right)^{N_n-1} \times \\ \prod_{i=1}^{n-1}\left(1-\frac{2T_{adv}}{T_{ap,i}}\right)^{N_i}\left(1-\frac{1}{Y}\frac{T_{aux,n}+T_{aux,i}}{T_{ap,i}}\right)^{N_i}} \end{aligned} \tag{2.3}$$

If the network has only one cluster then (2.3) is reduced to:

$$\begin{aligned} L_{dr,1} &= T_{ap,1} N_{avg,1} \\ &= \frac{T_{ap,1}}{\left(1-\frac{2T_{adv}}{T_{ap,1}}\right)^{N_1-1}\left(1-\frac{1}{Y}\frac{2T_{aux,1}}{T_{ap,1}}\right)^{N_1-1}} \end{aligned} \tag{2.4}$$

The above equation gives the latency of the network having only one cluster, making it a homogeneous network (a special case of the proposed model), transmitting T_{adv}, $T_{aux,1}$ packets at $T_{ap,1}$ advertising period. Hence, the proposed model can efficiently be used for homogeneous networks. All the notations used in this chapter are summarized in Table 2.2.

Table 2.2: Summary of notations.

Notation	Description
n	Number of clusters
N_n	Number of BLE sensor nodes in cluster $'n'$
T_{adv}	Control packet size
$T_{aux,n}$	Data packet size for cluster $'n'$
$T_{ap,n}$	Advertising period for cluster $'n'$
$T_{ap,n}^{opt}$	Optimal advertising period for cluster $'n'$
$N_{avg,n}$	Average number of packets for cluster $'n'$
$L_{dr,n}$	Latency for BLE sensor node in cluster $'n'$

2.3.2 Energy Modeling in Heterogeneous IIoT Environment

One BLE transmission comprises of two advertising events in one advertising period, i.e., *i)* control (*adv*) *ii)* data packet (*aux*) [75], each event has three subevents defined as preadv, adv, postadv, and preaux, aux, and postaux respectively [74, 76]. Hence, the total energy consumption (E_{tot}) during one period (T_{ap}) can be calculated by adding all sub events corresponding to control (*adv*) and data packet events (*aux*).

$$\begin{aligned} E_{adv,n} &= E_{adv,pre} + E_{adv} + E_{adv,post} \\ E_{aux,n} &= E_{aux,pre} + E_{aux} + E_{aux,post} \\ E_{tot,n} &= E_{adv,n} + E_{aux,n} \end{aligned} \tag{2.5}$$

Since the BLE transmission suffers collisions, consequently requiring retransmissions, thus the average energy consumption for a successful transmission ($E_{succ,n}$) can be obtained as follows:

$$E_{succ,n} = \frac{E_{tot,n}}{P_{succ,n}} \tag{2.6}$$

2.4 Optimization Algorithm

In this section, the expressions for optimal advertising interval are derived first, followed by algorithms that autonomously optimize the BLE based heterogeneous IIoT networks. The optimal expression of the advertising interval for a reference BLE sensor node in n^{th} cluster is derived in this section. With (2.7), we can determine the value of $T_{ap,n}^{opt}$, which minimizes the $L_{dr,n}$ as follows:

$$L_{dr,n} = \frac{T_{ap,n}}{\left(1 - \frac{2T_{adv}}{T_{ap,n}}\right)^{N_n - 1} \left(1 - \frac{1}{Y}\frac{2T_{aux,n}}{T_{ap,n}}\right)^{N_n - 1} \times \underbrace{\prod_{i=1}^{n-1} \left(1 - \frac{2T_{adv}}{T_{ap,i}}\right)^{N_i} \left(1 - \frac{1}{Y}\frac{T_{aux,n} + T_{aux,i}}{T_{ap,i}}\right)^{N_i}}_{\text{No terms of } T_{ap,n}\text{, hence, constant, assume K}}} \tag{2.7}$$

The derivative of (2.7) with respect to $T_{ap,n}$ can be written as:

$$\frac{\partial L_{dr,n}}{\partial T_{ap,n}} = D\left(A\left(T_{ap,n}\right)^2 + BT_{ap,n} + C\right) \tag{2.8}$$

where,

$$\begin{aligned} &A = Y, B = -2N_nYT_{adv} - 2N_nT_{aux,n} \\ &C = (8N_n - 4)\, T_{adv}T_{aux,n} \\ &D = \left(Y(T_{AP,n})^2\right)^{N_n - 1} (T_{ap,n} - 2T_{adv})^{-N_n} \\ &\quad (YT_{ap,n} - 2T_{aux,n})^{-N_n} K^{-1} \end{aligned} \tag{2.9}$$

Since, $T_{ap,n}, T_{ap,i}, > 2T_{adv}$, $T_{ap,n}, T_{ap,i}, > (T_{aux,n} + T_{aux,i})$, and $Y > 0$, hence $D > 0, K > 0$. Let $T_{ap,n}^{opt}$ be the value of $T_{ap,n}$ which satisfies $\partial L_{dr,n}/\partial T_{ap,n} = 0$, then

$$A(T_{ap,n}^{opt})^2 + BT_{ap,n}^{opt} + C = 0 \tag{2.10}$$

The roots of (2.10), can be obtained using the following formula:

$$T_{ap,n}^{opt} = \frac{-B \pm \sqrt{B^2 - 4AC}}{2A} \tag{2.11}$$

By putting parameter values described in [75], in (2.11), we have $B^2 - 4AC \gg 0$ for all possible values. Since the range of $T_{ap,n}$ varies from 20 ms to 10485.759375 s[75], $T_{ap,n}^{opt}$ can be obtained as:.

$$T_{ap,n}^{opt} \approx \frac{-B}{A} = 2N_n \left(T_{adv} + \frac{T_{aux,n}}{Y} \right) \tag{2.12}$$

The shape of $L_{dr,n}$ depends on the sign of $\partial L_{dr,n}/\partial T_{ap,n}$, i.e., the region where $\partial L_{dr,n}/\partial T_{ap,n}$ has a negative value, $L_{dr,n}$ decreases as $T_{ap,n}$ increases and vice versa. From (2.12), we can obtain the following relationship: $(\partial L_{dr,n}/\partial T_{ap,n} < 0)$ for $T_{ap,n} < T_{ap,n}^{opt}$ and $(\partial L_{dr,n}/\partial T_{ap,n} > 0)$ for $T_{ap,n} > T_{ap,n}^{opt}$. This means that the $L_{dr,n}^{n}$ has minima at $T_{ap,n}^{opt}$. Hence, the expression for optimum advertising interval can be given as:

$$T_{ai,n}^{opt} = 2N_n \left(T_{adv} + \frac{T_{aux,n}}{Y} \right) - T_{rd} \tag{2.13}$$

where, $T_{ai,n}^{opt}$ is the optimal advertising interval for n^{th} cluster BLE sensor nodes.
The BLE gateway broadcasts the computed optimal advertising interval value. All the BLE sensor nodes in the respective cluster update the advertising interval to the optimal advertising interval. The detailed update procedure is described in Algorithm 1. The

Algorithm 1 Broadcasting optimal advertising period for reference BLE sensor node in n^{th} cluster.

1: Get: n, N_i $T_{aux,i}$ for $i = 1$ to n, T_{adv}.
2: BLE gateway computes $T_{ap,n}^{opt}$, $T_{ai,n}^{opt}$ for n^{th} cluster based on (2.12), (2.13).
3: BLE gateway broadcasts $T_{ap,n}^{opt}$, $T_{ai,n}^{opt}$ for n^{th} cluster BLE sensor nodes.
4: n^{th} cluster BLE sensor nodes receive $T_{ai,n}^{opt}$.
5: n^{th} cluster BLE sensor nodes starts transmission at $T_{ai,n}^{opt}$.
6: **If** (n, N_i $T_{aux,i}$ changes), **go to Step 1**.
7: **Else** keep on transmitting at $T_{ap,n}^{opt}$, $T_{ai,n}^{opt}$.

proposed model is also valid for the legacy based homogeneous model as confirmed by the results obtained in Figure 2.3.

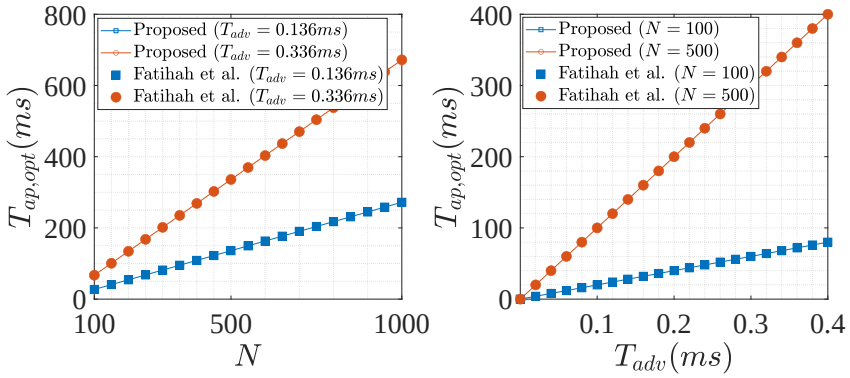

Figure 2.3: Illustration of the backward compatibility of the proposed model and comparison with existing works.

2.5 Results and Discussion

In this section, the analytical results of the proposed model are discussed. In particular, we have investigated the impact of the number of BLE sensor nodes, advertising interval, and

data size on latency in a heterogeneous network. In this context, we have considered two cluster scenario having N_1 and N_2 number of BLE sensor nodes transmitting T_{adv}, $T_{aux,1}$ packets at $T_{ap,1}$ and T_{adv}, $T_{aux,2}$ packets at $T_{ap,2}$ respectively. The detailed simulation parameters are listed in Table 2.3.

Table 2.3: Simulation parameters.

Parameter	**Value**
n	2
N_1	150 to 500
N_2	150 to 500
T_{adv}	0.144 ms [75]
$T_{aux,1}$	0.16, 0.64, 1.28, 2.12 ms [75]
$T_{aux,2}$	0.16, 0.64, 1.28, 2.12 ms [75]
$T_{ap,1}$	20 ms to 1000 ms [75]
$T_{ap,2}$	20 ms to 1000 ms [75]

Further, analytical results are also compared with simulation results, which are in good agreement with simulation results that validate the proposed solution. The analytical results are verified using the simulator developed in [60].

2.5.1 Analytical Results for Heterogeneous IIoT Networks

The analytical results for the latency of the two cluster heterogeneous network is shown in Figure 2.4. 1^{st} and 2^{nd} cluster has N_1 and N_2 number of BLE sensor nodes transmitting T_{adv}, $T_{aux,1}$ packets at $T_{ap,1}$ and T_{adv}, $T_{aux,2}$ packets at $T_{ap,2}$ respectively. BLE sensor nodes in both clusters are operating simultaneously. For the reference BLE sensor node in 1^{st} cluster, the parameters of 2^{nd} cluster are varied. Figure 2.4a shows the variation of the

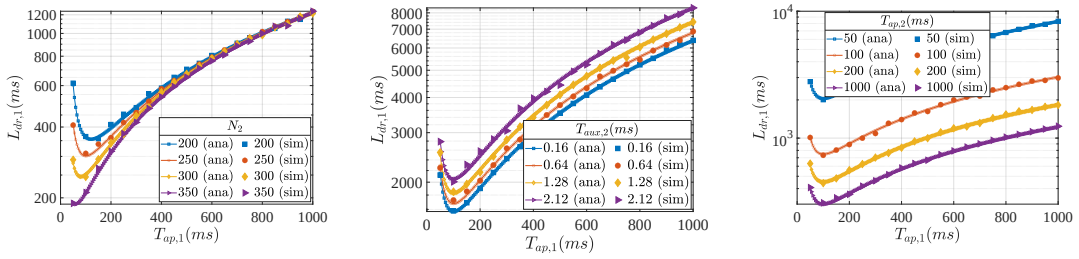

(a) (b) (c)

Figure 2.4: Impact of advertising period ($T_{ap,1}$) on data reception latency ($L_{dr,1}$) for heterogeneous scenario: (a) impact of N_2, (b) impact of $T_{aux,2}$, (c) impact of $T_{ap,2}$.

latency of the reference BLE sensor nodes in 1^{st} cluster with the number of BLE sensor nodes in 2^{nd} cluster with $T_{ap,2} = 1000ms$, $T_{aux,1} = T_{aux,2} = 2.120ms$, $N_1 = N - N_2$, $N = 500$. As the number of BLE sensor nodes in 2^{nd} cluster increases, the latency of the reference BLE sensor node in 1^{st} cluster increases. Similarly, Figure 2.4b shows the variation of the latency of reference BLE sensor node in 1^{st} cluster with the packet duration

of BLE sensor nodes in 2^{nd} cluster with $T_{ap,2} = 50ms$, $T_{aux,1} = 2.120ms$, $N_1 = N_2 = 250$. It can be observed that the increase in packet duration of BLE sensor nodes in 2^{nd} cluster increases the latency of reference BLE sensor node in 1^{st} cluster. Likewise, the advertising period of BLE sensor nodes in 2^{nd} cluster significantly increases the latency of reference BLE sensor node in 1^{st} cluster as shown in Figure 2.4c with $T_{aux,1} = T_{aux,2} = 2.120ms$, $N_1 = N_2 = 250$. Hence, there exists an optimal value of advertising period for the reference BLE sensor node in 1^{st} cluster, which gives minimal latency for a given packet duration, advertising period, and number of BLE sensor nodes in 2^{nd} cluster. It can easily be computed by the analytical close form expression obtained in (2.12), (2.13) implemented in the Algorithm 1 running in the BLE gateway.

2.5.2 Analytical Results for Average Energy Consumption

The analytical results for the average energy consumption of a reference BLE sensor node in 1^{st} cluster ($E_{succ,1}$) considering a two cluster heterogeneous scenario are discussed in this section. As in [74, 76], we have used the following parameters to obtain $E_{succ,1}$: 8.84, 7.56, 7.03, 8.84, 37.1 and 7.03 in $ms * mA$ for $E_{adv,pre}, E_{adv}, E_{adv,post}, E_{aux,pre}, E_{aux}, E_{aux,post}$. From Figure 2.5 for $N_1 = 200$, $T_{aux,1} = 2.120ms$, with $N_2 = 300$, $T_{aux,2} = 1.28ms$, $T_{ap,2} =$

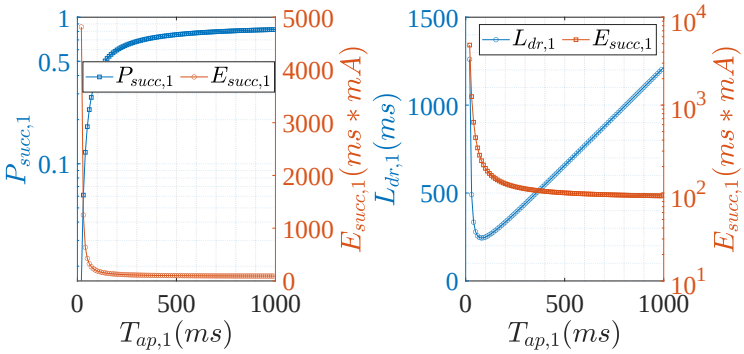

Figure 2.5: Impact of advertising period ($T_{ap,1}$) on average energy consumption ($E_{succ,1}$).

$1000ms$, it can be observed that low values of $T_{ap,1}$ have higher $E_{succ,1}$, while after a certain value, it becomes almost constant. It is because lower $T_{ap,1}$ increases total transmissions, consequently increasing collisions, requiring more retransmissions, thus increasing $E_{succ,1}$. Whereas, the longer $T_{ap,1}$, leads to less transmissions, resulting in fewer collisions, requiring less retransmissions, thus $E_{succ,1}$ is almost constant. This analysis is useful in determining the approximate lifetime of battery operated BLE sensor nodes in the network in addition to selecting the suitable $T_{ap,1}$ for longer battery life if required.

2.6 Conclusion

This chapter minimizes the latency for sensor nodes-gateway communication scenario considering an industrial automation use case. At first, a performance model considering a heterogeneous scenario is developed to analyze latency. Using this model, analytical

expression for selecting optimal advertising interval are derived. Based on these analytical expressions, algorithms are proposed that autonomously optimize the network and ensure minimal latency. In addition to the above, an energy consumption model that helps estimate the battery lifetime of the sensing nodes, along with suitable parameter selection, is developed and discussed. Further, this chapter presents the simulations to verify the proposed model and analysis.

Chapter 3

Latency Minimization for Sensor Nodes-Gateway-User Communication

In the previous chapter, we have derived simplified analytical expressions for selecting optimal transmission parameters to ensure minimal latency for sensor nodes-gateway communication. In this chapter, we will focus on minimizing latency for sensor nodes-gateway-user communication scenario. In this scenario, the BLE sensor nodes transmit the data to the BLE gateway. BLE gateway collects information from all the BLE sensor nodes and transmits it to users. The users then send the request to get additional information. Hence, to get minimal latency, the transmission from BLE sensor nodes to BLE gateway and BLE gateway to users must have minimal latency. The latency in transmissions from BLE sensor nodes to users primarily depends on the choice of transmission parameters, i.e., advertising interval [60, 77]. For example, when the advertising interval is too large, the BLE gateway receiving the packets must wait for advertising packets to arrive, increasing the latency. Conversely, with a small advertising interval, the advertising packets become overpopulated, resulting in extensive collisions. This, in turn, raises the overall latency [71]. Hence, a comprehensive service architecture for selecting optimal transmission parameters to ensure minimal latency for sensor nodes-gateway-user communication is required. However, to our knowledge, no such analytical framework exists to date. To address this, we have proposed a new service architecture that ensures minimal latency for BLE sensor nodes-gateway-user communication. In particular, we first developed a comprehensive analytical framework to analyze and minimize latency for transmission from BLE sensor nodes to users. Further, based on the analytical framework, we derived simplified close form expressions for selecting optimal advertising interval. Moreover, based on these close form analytical expressions, we proposed algorithms that autonomously optimize the network and ensure minimal latency for the data transmitted by the BLE sensor node and the latency experienced by users. From here onward, we have used the term delay over latency. However, both of them have the same meaning here. A brief review of existing works and their shortcomings, as well as how our proposed work differs from the existing works, is introduced below.

3.1 Related Work and Motivation

The existing works primarily have two service architectures to provide service to users: a) BLE sensor nodes-users [78, 79, 80] and b) BLE sensor nodes-BLE gateway-server-users [81]. These service architectures have certain shortcomings. For instance, in the BLE sensor nodes-user model, it is difficult for a user to receive data from all BLE sensor nodes in minimal time; also, requesting additional data directly from BLE sensor nodes comes at a higher energy cost, significantly impacting battery life [58, 60]. Similarly, the users in BLE sensor nodes-BLE gateway-server-users service architecture must have good internet connectivity to access data. However, the internet connectivity might be poor in some scenarios, i.e., underground smart parking applications, or redundant in some scenarios, i.e., distributed applications like announcements in underground airports, advertising in supermarkets, etc. More importantly, neither of these service architectures provides analytical expressions to analyze and minimize delay and analyze and maximize battery life, which is very important to achieve minimal delay and maximal battery life. In addition, these service architectures are based on BLE legacy advertisement mode, which utilizes three primary channels, causing severe collisions when overall BLE sensor nodes increase significantly, hence more retransmissions for successful data transmission, consequently causing additional delays [68, 71]; this highlights the importance of selecting suitable advertising mode. Furthermore, these works are limited to homogeneous networks that utilize the same set of BLE parameters for transmissions from BLE sensor nodes, BLE gateway, and BLE users, respectively. However, the transmissions from BLE sensor nodes to BLE gateway and BLE gateway to BLE users have different data sizes and perhaps occur at different intervals; hence, they are likely to form a heterogeneous network. Therefore, the homogeneous network assumption does not fit well, and thus, the homogeneous network assumption fails to provide minimal delay.

Apart from the aforementioned service architectures, there also exists BLE sensor nodes-BLE gateway service architecture [58, 59, 60]; however, similar to above, this architecture also doesn't provide simplified expressions to choose transmissions parameters, ensuring minimal delays. For instance, the authors in [58] have shown that there exists an optimal value that gives minimal delay. However, the authors hardly provided any analytical expression to choose the optimal interval value. Besides, the authors in [59] have formed a mathematical model to select the advertising interval based on Chinese remainder theory (CRT). However, the algorithm's complexity grows significantly when the number of BLE sensor nodes in the network increases; additionally, it does not assure the optimality of the selected interval. Likewise, the authors in [60] have put forth a numerical algorithm to determine the optimal solution; however, the proposed algorithm has high computational complexity and may pose challenges in practical hardware implementations. In addition to the above, none of these works have discussed how to analyze and maximize the battery life of BLE sensor nodes.

From the above discussion, it can be inferred that the existing service architecture either

fails at providing minimal delay or has redundancy in the architecture; hence, they do not seem to fulfill the stringent requirements of the aforementioned applications efficiently. In summary, the aforementioned works have the following shortcomings: *i)* based on either BLE sensor nodes-user or BLE sensor nodes-BLE gateway-server-user service architecture, *ii)* limited to homogeneous networks, *iii)* utilizes BLE legacy advertising, and *iv)* lack of a well developed analytical model to analyze the delay experienced by BLE users and lack of simplified analytical expression for setting optimal advertising intervals for BLE sensor nodes, BLE gateway, and BLE users.

To address the aforementioned challenges, in this chapter, we first developed a new service architecture in which BLE sensor nodes transmit the data to the BLE gateway, and the BLE gateway collects information from all BLE sensor nodes and then transmits it to all BLE users, considering a two cluster heterogeneous framework as shown in Figure 3.1.

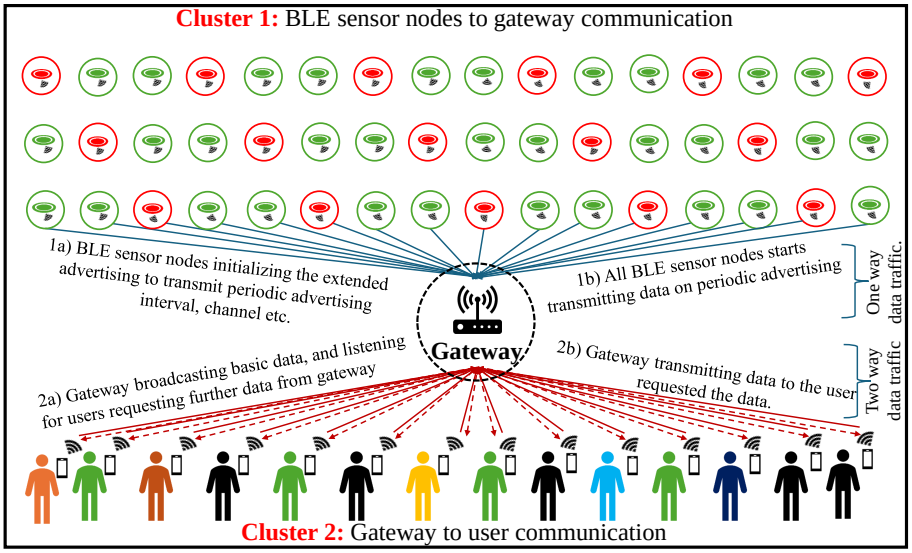

Figure 3.1: Illustration of proposed service architecture.

In particular, BLE sensor nodes and BLE gateway make one cluster. Similarly, BLE gateway and BLE users together make a second cluster. The proposed service architecture uses BLE 5.x extended and periodic advertising mode, which utilizes 37 secondary channels and 3 primary channels, hence offering much lower delay and energy consumption. Further, based on the new service architecture, an analytical model has been developed to analyze delay experienced by transmissions from BLE sensor nodes and BLE users. Furthermore, simplified closed form analytical expressions are derived based on the analytical model, ensuring minimal delay for users and maximal battery life for BLE sensor nodes.

In addition to the above, to further improve the efficiency of the proposed service architecture, this chapter also proposes a new scheme for handling multiple concurrent requests from BLE users, where more than one user simultaneously requests data from the BLE gateway, unlike existing schemes, which either use random backoff scheme [82] causing unnecessary delays or use the time gap between the transmission of ADV_EXT_IND packets on primary channels, which can have a maximum value of 9.824ms and hence

can handle a small number of users only [83]. However, the proposed service architecture can handle many users while ensuring minimal delays. In particular, we introduced a random window discretized into slots; users chose a random slot from these slots to request information from the BLE gateway. As a result, this reduces collisions coming from simultaneous requests transmitted by users and hence reduces the delays. The proposed service architecture has numerous applications in various domains, including manufacturing industries, cities, retail, etc. These prominent applications and the step wise implementation procedure are discussed in detail later in the chapter.

3.2 Contributions

Specifically, the contribution of this chapter can be summarized as follows;

- Proposed a novel service architecture in which BLE sensor nodes transmit the data to the BLE gateway. BLE gateway collects information from all BLE sensor nodes and then transmits it to all BLE users, considering a two cluster heterogeneous framework. The proposed service architecture uses BLE extended and periodic advertising mode for data transmission, considering a two cluster heterogeneous network proposed in this chapter.
- Based on the service architecture, a comprehensive analytical framework has been developed to analyze and minimize the delay from BLE sensor nodes to BLE users.
- Further, based on the analytical framework, simplified closed form expressions are derived to choose the optimal advertising interval. Moreover, based on these close form analytical expressions, algorithms are proposed to optimize the delay in such applications autonomously.
- An energy consumption model has also been developed, which helps to achieve longer battery life while assuring minimal delay. This model can also help service providers estimate BLE sensor nodes lifespan.
- Prominent applications where the proposed service architecture fits best are discussed in detail with a stepwise procedure to efficiently develop such applications while fulfilling the desired delay and energy requirements.

3.3 System Model

This section describes the system model of the proposed service architecture. The proposed service architecture consists of BLE sensor nodes, gateway, and users. Communication between BLE sensor nodes, gateway, and users is a three step process. *Step 1:* The BLE sensor nodes send the data to the BLE gateway. *Step 2:* The BLE gateway switches to scanning mode and receives the data from BLE sensor nodes. On successful reception, the BLE gateway switches to advertising mode and broadcasts the basic data to the users.

Step 3: The users send the request to the BLE gateway to get additional information. BLE gateway switches to scanning mode, receives the user request, switches back to advertising mode, and transmits the requested data to the user. In step 3, it can be noted that the BLE gateway and users follow the following mode pairs: *i)* advertising-scanning, *ii)* scanning-advertising and *iii)* advertising-scanning mode respectively for the two way communication between BLE gateway and user. Once the user request is successfully served, the process executes again from *Step 1* and so on. This procedure is also shown in Figure 3.1.

Now, for a good user experience, the delay from the BLE sensor node to the BLE gateway and the total delay in serving the user request should be minimized, which depends primarily on the set of BLE parameters chosen. The number of users, the number of BLE sensor nodes, the size of BLE sensor node data, and the size of the user request and response data are not the same. Hence, using the same set of BLE parameters for all BLE sensor nodes, BLE gateway, and users will not give minimal delay and may degrade the network performance significantly. Therefore, we assigned different BLE parameters for BLE sensor nodes, BLE gateway, and users in the proposed service architecture. Further, based on the set of BLE parameters used, all the elements in the proposed service architecture are divided into two groups, and the elements within a group use the same set of BLE parameters for data exchange. In particular, we have divided into two groups, namely Cluster 1 and Cluster 2, as shown in Figure 3.1. All the BLE sensor nodes transmitting data to the BLE gateway together forms Cluster 1, similarly, the users communicating and requesting data to the gateway forms Cluster 2. The cluster 1 utilizes BLE extended advertising, with $\zeta_{ei,b}$ (extended advertising interval), and periodic advertising with $\zeta_{pi,b}$ (periodic advertising interval), ζ_{adv} (size of extended advertising packet), $\zeta_{aux,b}$ (size of auxiliary packet), $\zeta_{syc,b}$ (size of periodic advertising data packet), $\kappa_{e,b}$, $\kappa_{p,b}$ (number of secondary advertising channels for extended and periodic advertising) BLE parameters respectively. Similarly, cluster 2 utilizes BLE extended advertising (nonconnectable scannable), with $\zeta_{ei,g}$ (extended advertising interval), ζ_{adv} (size of extended advertising packet), $\zeta_{aux,g}$ (size of auxiliary packet) respectively as BLE parameters. Cluster 1 has λ_b number of BLE sensor nodes, and cluster 2 has λ_u number of users at any time instant.

All the BLE sensor nodes transmitting data to the BLE gateway together forms Cluster 1, similarly, the users communicating and requesting data to the gateway forms Cluster 2. The cluster 1 utilizes BLE extended advertising, with $\zeta_{ei,b}$ (extended advertising interval), and periodic advertising with $\zeta_{pi,b}$ (periodic advertising interval), ζ_{adv} (size of extended advertising packet), $\zeta_{aux,b}$ (size of auxiliary packet), $\zeta_{syc,b}$ (size of periodic advertising data packet), $\kappa_{e,b}$, $\kappa_{p,b}$ (number of secondary advertising channels for extended and periodic advertising) BLE parameters respectively. Similarly, cluster 2 utilizes BLE extended advertising (nonconnectable scannable), with $\zeta_{ei,g}$ (extended advertising interval), ζ_{adv} (size of extended advertising packet), $\zeta_{aux,g}$ (size of auxiliary packet), $\kappa_{e,g}$, (number of secondary advertising channels for extended advertising) respectively as BLE parameters.

Cluster 1 has λ_b number of BLE sensor nodes, and cluster 2 has λ_u number of users at any time instant.

An example of such a clustered network having one BLE sensor node in Cluster 1 and one user in Cluster 2 exchanging data successfully is shown in Figure 3.2. In particular, in

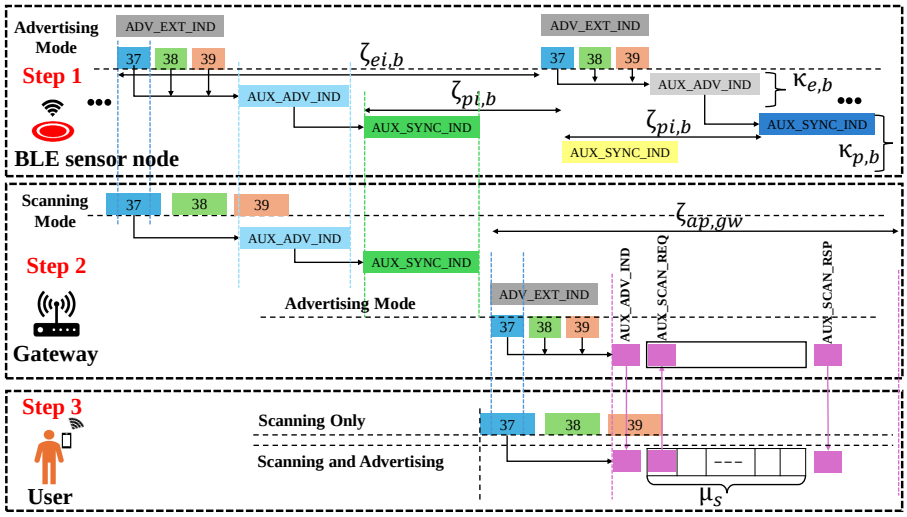

Figure 3.2: Illustration of successful data exchange between BLE sensor node-gateway and gateway-user.

step 1, the BLE sensor node configured in advertising mode transmits the ADV_EXT_IND and AUX_ADV_IND packets to initiate periodic advertising followed by AUX_SYNC_IND periodic advertising packet. In step 2 the BLE gateway configured in scanning mode starts scanning the ADV_EXT_IND, AUX_ADV_IND and AUX_SYNC_IND packets and on successful reception of these packets BLE gateway switches to advertising mode and transmits AUX_ADV_IND packet containing basic information to users. In step 3, users configured in scanning mode receive these packets. On successful reception, the users switch the mode to advertising and send the AUX_SCAN_REQ packet to the BLE gateway to request further data. On receiving the AUX_SCAN_REQ request packet, the BLE gateway sends the requested data in the AUX_SCAN_RSP packet. This completes the data exchange process between the BLE sensor node to the BLE gateway and the BLE gateway to the user, respectively. The objectives of the proposed work can be summarized as follows;

1. The first and foremost objective is to develop the analytical model (considering a two cluster heterogeneous network) to analyze the delay experienced by the transmissions from BLE sensor nodes and the user requests.

2. The Second objective is to optimize the analytical model to get optimal close form expressions, which minimize the delay experienced by the transmissions from the BLE sensor node to reach the BLE gateway and the delay experienced by the user to get its request served by the BLE gateway. In particular, optimal close form expressions for advertising interval, number of slots, and random interval are

derived. Later, develop algorithms that opt for optimal close form expressions and can autonomously optimize the network.

3. The Third objective is to derive the optimal closed form expression for BLE gateway scan duration to receive each transmission, i.e., extended and periodic advertising transmissions from BLE sensor nodes and data request transmissions from users. Later, formulate a scheduling algorithm for all these transmissions.

3.3.1 Packet Success Probability Analysis for Cluster 1 and Cluster 2

The proposed work utilizes nonconnectable, nonscannable extended, and periodic advertising for BLE sensor nodes to BLE gateway communication (cluster 1) and nonconnectable scannable advertising for BLE gateway to user communication (cluster 2). The packets, namely ADV_EXT_IND, AUX_ADV_IND AUX_SYNC_IND are used for nonconnectable nonscannable extended and periodic advertising with duration ζ_{adv}, $\zeta_{aux,b}$, $\zeta_{syc,b}$ and the packets namely ADV_EXT_IND, AUX_SCAN_REQ, AUX_SCAN_RSP are used for nonconnectable scannable advertising with duration ζ_{adv}, $\zeta_{req,u}$ and $\zeta_{res,u}$. All the ADV_EXT_IND packets are transmitted on primary channels (37, 38, 39), whereas all the other packets AUX_ADV_IND, AUX_SYNC_IND, AUX_SCAN_REQ, AUX_SCAN_RSP are transmitted on secondary channels (0-36).

3.3.1.1 Overview of Packet Collision and Packet Collision Probability

The transmissions from the BLE sensor nodes to the BLE gateway (cluster 1) and users to the BLE gateway (cluster 2) are random in nature; hence, they may collide, resulting in two types of collisions, i.e., intra cluster (collisions due to transmissions on the same channel within cluster) and inter cluster (collisions due to transmissions on the same channel from the other cluster) as shown in Figure 3.3a. To avoid inter cluster collisions, we have assigned separate channels for each cluster, i.e., $\kappa_{e,b}$, $\kappa_{p,b}$ for extended and periodic advertisement for cluster 1, on the other hand, intra cluster collisions are difficult to avoid due to randomness in transmission timings.
The time window in which a collision can happen is known as vulnerable time, which is twice the size of the BLE advertising packet. Hence, the probability of collision for nonconnectable, nonscannable extended, and periodic advertising events with ADV_EXT_IND, AUX_ADV_IND AUX_SYNC_IND packets when only two BLE sensor nodes are present and transmitting can be obtained as $2\zeta_{adv}/\zeta_{ei,b}$, $2\zeta_{aux,b}/\kappa_{e,b}\zeta_{ei,b}$ and $2\zeta_{syc,b}/\kappa_{p,b}\zeta_{pi,b}$ respectively; where, ζ_{adv} is the duration of ADV_EXT_IND packet, $\zeta_{ei,b}$ is the extended advertising interval, $\zeta_{aux,b}$ is the duration of AUX_ADV_IND packet, $\kappa_{e,b}$ is the number of secondary channels assigned for AUX_ADV_IND packets of BLE sensor nodes, $\zeta_{syc,b}$ is the duration of AUX_SYNC_IND packet, $\kappa_{p,b}$ is the number of secondary channels assigned for AUX_SYNC_IND packets of BLE sensor nodes and $\zeta_{pi,b}$ is the periodic advertising interval. Similarly, the users receiving the AUX_ADV_IND packet may send the AUX_SCAN_REQ packet at the same time to the BLE gateway, which will

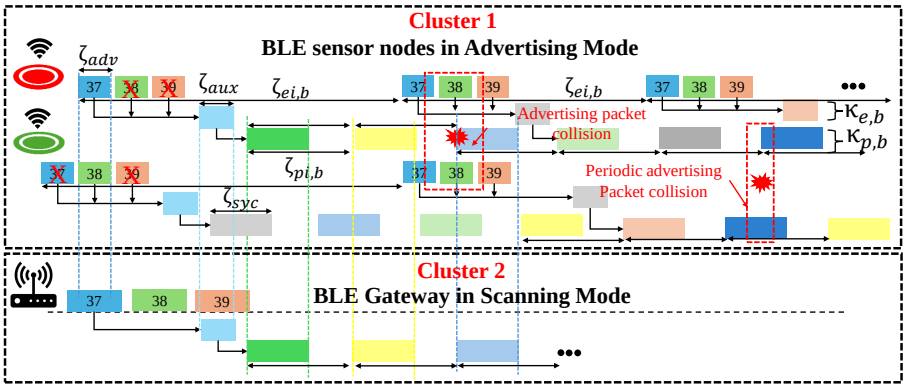

(a) collision of extended, periodic advertising packet of reference BLE sensor node with random BLE sensor node within cluster 1 (intracluster collision)

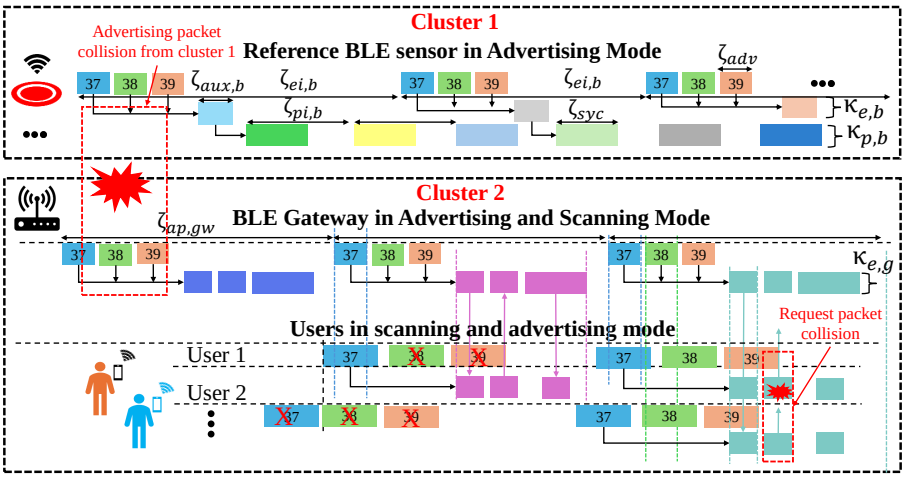

(b) collision of extended advertising packet of reference BLE sensor node and BLE gateway (inter cluster collision) (collision on primary channels) and collision between request packet of two users (user 1 and user 2)

Figure 3.3: Illustration of inter and intracluster collision in BLE sensor nodes-gateway-user communication scenario.

collide as shown in Figure 3.3b. Hence the probability of AUX_SCAN_REQ packet collision can be obtained as $2\zeta_{req,u}/\zeta_{ei,g}$; where, $\zeta_{req,u}$ is the request packet AUX_SCAN_REQ duration, $\zeta_{ei,g}$ is the gateway extended advertising interval. These expressions are used in the subsequent subsection to obtain the probability of success expressions.

3.3.1.2 Packet Success Probability Derivation for Cluster 1

The BLE sensor node to BLE gateway communication is a two step process, i.e., *a)* the BLE sensor nodes first transmit the extended advertising packets, *b)* then transmit the periodic advertisement packets which have the actual information. Hence, both packets should be received without collision for successful communication from the BLE sensor node to the BLE gateway. Extended advertising requires two sub transmissions, i.e., first ADV_EXT_IND packet of ζ_{adv} duration is transmitted on primary channels (37, 38, 39); this is also known as legacy advertisement, then the AUX_ADV_IND packet of $\zeta_{aux,b}$ duration is transmitted on secondary channels. Hence, the probability of successful

transmission, i.e., no collision ($\rho_{st,eb}$) of a BLE sensor node extended advertisement packet, can be given as;

$$\rho_{st,eb} = \underbrace{\left(1 - \frac{2\zeta_{adv}}{\zeta_{ei,b}}\right)^{\lambda_b - 1}}_{\rho_{st,lb}} \left(1 - \frac{1}{\kappa_{e,b}} \frac{2\zeta_{aux,b}}{\zeta_{ei,b}}\right)^{\lambda_b - 1} \tag{3.1}$$

where $\rho_{st,lb}$ represents the probability of successful transmission of BLE sensor node legacy advertisement packet, ζ_{adv} is the size of extended advertising indication packet (ADV_EXT_IND), $\zeta_{aux,b}$ is the size of the auxiliary packet (AUX_ADV_IND), $\kappa_{e,b}$ is the number of secondary channels assigned to the BLE sensor node for the extended advertisement to the BLE gateway, $\zeta_{ei,b}$ is the extended advertising interval, λ_b is the number of BLE sensor nodes. Similarly, the probability of successful transmission, i.e., no collision ($\rho_{st,pb}$) of the BLE sensor node periodic advertisement packet, can be given as;

$$\rho_{st,pb} = \left(1 - \frac{1}{\kappa_{p,b}} \frac{2\zeta_{syc,b}}{\zeta_{pi,b}}\right)^{\lambda_b - 1} \tag{3.2}$$

where $\rho_{st,pb}$ represents the probability of successful transmission of BLE sensor node periodic advertisement packet, $\zeta_{syc,b}$ is the size of the periodic advertisement packet (AUX_ADV_IND), $\kappa_{p,b}$ is the number of secondary channels assigned to the BLE sensor node for the periodic advertisement to the BLE gateway, $\zeta_{pi,b}$ is the periodic advertising interval, λ_b is the number of BLE sensor nodes.

3.3.1.3 Packet Success Probability Derivation for Cluster 2

The interaction between the BLE user and the BLE gateway is a two step process, *a)* The BLE gateway transmits an extended advertising packet (AUX_ADV_IND), *b)* which, upon successful reception by the BLE user, the users immediately sends the AUX_SCAN_REQ packet to the BLE gateway to request further information. Hence, it's highly likely that these request packets will definitely collide with other user request packets. To solve this problem, we have proposed a random window discretized into slots. The user randomly selects the slots to transmit request packets. Now, for this two way communication with the slotted approach to be successful, either of the packets should not collide with other packets. The transmission from a BLE gateway to the user is successful when the transmissions from BLE sensor nodes and the BLE gateway on the primary channel do not collide with each other, and the user should not transmit the request packets in the same slot. Hence, the probability of successful transmission of the user request packet ($\rho_{st,rq}$) can be given as;

$$\rho_{st,rq} = \left(1 - \frac{1}{\mu_s}\right)^{\lambda_u - 1} \left(1 - \frac{2\zeta_{adv}}{\zeta_{ei,b}}\right)^{\lambda_b} \tag{3.3}$$

where μ_s represents the number of slots, which can be calculated as;

$$\mu_s = \frac{\zeta_{ri}}{\zeta_{req,u}} \tag{3.4}$$

where, ζ_{ri} is the size of the introduced random window and $\zeta_{req,u}$ is the size of user request packet (AUX_SCAN_REQ).

3.3.2 Delay Evaluation Model for Cluster 1 and Cluster 2

3.3.2.1 Delay for BLE sensor nodes to BLE Gateway Transmission (Cluster 1)

Since extended advertisement broadcast requires $1/\rho_{st,eb}$ attempts for successful transmission, and each packet is transmitted at $\zeta_{ei,b}$ interval, hence the delay experienced by BLE sensor node extended advertisement packet ($\tau_{e,b}$) can be given as;

$$\tau_{e,b} = \frac{\zeta_{ei,b}}{\left(1 - \frac{2\zeta_{adv}}{\zeta_{ei,b}}\right)^{\lambda_b - 1} \left(1 - \frac{1}{\kappa_{e,b}} \frac{2\zeta_{aux,b}}{\zeta_{ei,b}}\right)^{\lambda_b - 1}} \tag{3.5}$$

Similarly, the delay experienced by the BLE sensor node periodic advertisement packet ($\tau_{p,b}$) can be given as;

$$\tau_{p,b} = \frac{\zeta_{pi,b}}{\left(1 - \frac{1}{\kappa_{p,b}} \frac{2\zeta_{syc,b}}{\zeta_{pi,b}}\right)^{\lambda_b - 1}} \tag{3.6}$$

(3.5) and (3.6) can be used directly to calculate the delay experienced by the BLE sensor node extended and periodic advertisement packet in the network consisting of λ_b BLE sensor nodes.

3.3.2.2 Delay for User to BLE Gateway Communication (cluster 2)

The user starts scanning at a random point in time. Therefore, the average time to receive the first ADV_EXT_IND is $\zeta_{ei,g}/2$. Once successful, the transmission of AUX_SCAN_REQ requires $1/\rho_{st,rq}$ attempts before successful transmission. Hence, the total delay experienced by the user to get its request packet served ($\tau_{u,r}$) is given by the following equation;

$$\tau_{u,r} = \begin{array}{l} \frac{\zeta_{ei,g}}{2} + \Delta_{37} + \left(\frac{1}{\rho_{st,rq}} - 1\right) \zeta_{ei,g} + \\ \zeta_{aux,g} + 2\Delta_{ifs} + \zeta_{ri} + \zeta_{req,u} + \zeta_{res,g} \end{array} \tag{3.7}$$

where, $\zeta_{ei,g}$ is the BLE gateway advertising interval, $\zeta_{aux,g}$ is the auxiliary packet size, Δ_{ifs} is the inter frame space, ζ_{ri} is the random window size, $\zeta_{req,u}$ is the request packet size and $\zeta_{res,g}$ is the response packet size.

3.3.3 Optimal Expressions for $\zeta_{ei,b}$, $\zeta_{pi,b}$ and ζ_{ri}

In this section, first, the optimal expressions for $\zeta_{ei,b}$, $\zeta_{pi,b}$ and ζ_{ri} are derived, and then based on the optimal expressions the algorithms are proposed which autonomously optimizes the network based on proposed service architecture.

The optimal value of $\zeta_{ei,b}$ can be obtained directly from [84];

$$\zeta_{ei,b}^{opt} = 2\lambda_b \left(\zeta_{adv} + \frac{\zeta_{aux,b}}{\kappa_{e,b}} \right) \tag{3.8}$$

where, $\zeta_{ei,b}^{opt}$ gives minimal $\tau_{e,b}$.

Similarly, to get minimal $\tau_{p,b}$, we need to select optimal $\zeta_{pi,b}$. Hence to get optimal $\zeta_{pi,b}$, we first need to take the partial derivative of $\tau_{p,b}$ with respect to $\zeta_{pi,b}$ and equate it 0;

$$\frac{\partial \tau_{p,b}}{\partial \zeta_{pi,b}} = \frac{\kappa_{p,b}\zeta_{pi,b} - 2\lambda_b \zeta_{syc,b}}{\kappa_{p,b}\left(1 - \frac{2\zeta_{syc,b}}{\kappa_{p,b}\zeta_{pi,b}}\right)^{\lambda_b} \zeta_{pi,b}} = 0 \tag{3.9}$$

Let $\zeta_{pi,b}^{'}$ be the value of $\zeta_{pi,b}$ which satisfies the above condition, then

$$\zeta_{pi,b}^{'} = \frac{2\lambda_b \zeta_{syc,b}}{\kappa_{p,b}} \tag{3.10}$$

For $\zeta_{pi,b}^{'}$ to be optimal, $\partial^2 \tau_{p,b}/\partial \zeta_{pi,b}^2$ should be positive at $\zeta_{pi,b}^{'}$.

$$\frac{\partial^2 \tau_{p,b}}{\partial \zeta_{pi,b}^2} = \frac{4\lambda_b \left(\lambda_b - 1\right) \zeta_{syc,b}^2}{\kappa_{p,b}\left(1 - \frac{2\zeta_{syc,b}}{\kappa_{p,b}\zeta_{pi,b}}\right)^{\lambda_b} \zeta_{pi,b}^2 \left(\kappa_{p,b}\zeta_{pi,b} - 2\zeta_{syc,b}\right)} > 0 \tag{3.11}$$

Since, $\kappa_{p,b}\zeta_{pi,b} > 2\zeta_{syc,b}$ and $\lambda_b - 1 > 0$ hence the $\partial^2 \tau_{p,b}/\partial \zeta_{pi,b}^2 > 0$, which confirms $\tau_{p,b}$ attains minima at $\zeta_{pi,b}^{'}$, hence the optimal value of $\zeta_{pi,b}$ that minimizes $\tau_{p,b}$ can be given as;

$$\zeta_{pi,b}^{opt} = \frac{2\lambda_b \zeta_{syc,b}}{\kappa_{p,b}} \tag{3.12}$$

Likewise, to get minimal $\tau_{u,r}$ we need to select optimal μ_s and ζ_{ri}. Hence to get optimal μ_s, we first need to take the partial derivative of $\tau_{u,r}$ with respect to μ_s and equate it 0. Rearranging (3.7), by putting the value of $\rho_{st,rq}$, ζ_{ri} from (3.3) and (3.4) in (3.7), we will get,

$$\begin{aligned} \tau_{u,r} = & \left(\frac{1}{\left(1 - \frac{1}{\mu_s}\right)^{\lambda_u - 1} \left(1 - \frac{2\zeta_{adv}}{\zeta_{ei,b}}\right)^{\lambda_b}} - 1 \right) \zeta_{ei,g} \\ & + \frac{\zeta_{ei,g}}{2} + \Delta_{37} + \zeta_{aux,g} + 2\Delta_{ifs} \\ & + \left(\mu_s + 1\right) \zeta_{req,u} + \zeta_{res,g} \end{aligned} \tag{3.13}$$

Taking partial derivative of (3.13) with respect to μ_s, we will get,

$$\frac{\partial \tau_{u,r}}{\partial \mu_s} = -\left(\lambda_u - 1\right)\left(1 - \frac{1}{\mu_s}\right)^{-\lambda_u} \frac{1}{\left(\mu_s^2 \rho_{st,lb}\right)} \zeta_{ei,g} + \zeta_{req,u} \tag{3.14}$$

Rearranging (3.14), we will get the following equation:

$$\frac{\partial \tau_{u,r}}{\partial \mu_s} = -\left(\lambda_u - 1\right) \frac{\left(\mu_s - 1\right)^{-\lambda_u}}{\left(\mu_s\right)^{-\lambda_u}} \frac{1}{\left(\mu_s^2 \rho_{st,lb}\right)} \zeta_{ei,g} + \zeta_{req,u} \tag{3.15}$$

Since λ_u and $\mu_s \gg 1$, so $(\mu_s - 1)^{-\lambda_u}/(\mu_s)^{-\lambda_u}$ in (3.15) can be approximated to 1, then we get the following;

$$\frac{\partial \tau_{u,r}}{\partial \mu_s} = -\left(\lambda_u - 1\right) \frac{1}{\left(\mu_s^2 \rho_{st,lb}\right)} \zeta_{ei,g} + \zeta_{req,u} \tag{3.16}$$

Let, $\mu_s^{'}$ be the value of μ_s, which satisfies $\partial \tau_{u,r}/\partial \mu_s = 0$, then,

$$\mu_s^{'} = \sqrt{\frac{\left(\lambda_u - 1\right) \zeta_{ei,g}}{\rho_{st,lb} \zeta_{req,u}}} \tag{3.17}$$

For $\mu_s^{'}$ to be optimal, $\partial^2 \tau_{u,r}/\partial \mu_s^2$ should be positive at $\mu_s^{'}$ i.e.,

$$\frac{\partial^2 \tau_{u,r}}{\partial \mu_s^2} = \left(\lambda_u - 1\right)\left(1 - \frac{1}{\mu_s}\right)^{-\lambda_u}\left(\frac{2\zeta_{ei,g}}{\mu_s^3 \rho_{st,lb}}\right) + \lambda_u \left(\lambda_u - 1\right)\left(1 - \frac{1}{\mu_s}\right)^{-\lambda_u - 1}\left(\frac{2\zeta_{ei,g}}{\mu_s^3 \rho_{st,lb}}\right) > 0 \tag{3.18}$$

Since, λ_u and μ_s is > 1, hence, the $(\partial^2 \tau_{u,r}/\partial \mu_s^2 > 0)$, which confirms $\tau_{u,r}$ attains minima at $\mu_s^{'}$, hence the optimal value of μ_s that minimizes $\tau_{u,r}$ can be given as;

$$\mu_s^{opt} = \sqrt{\frac{\left(\lambda_u - 1\right) \zeta_{ei,g}}{\rho_{st,lb} \zeta_{req,u}}} \tag{3.19}$$

Further, putting μ_s^{opt} in (3.4), we can get ζ_{ri}^{opt} as;

$$\zeta_{ri}^{opt} = \mu_s^{opt} \zeta_{req,u} \tag{3.20}$$

Hence, the close form expressions obtained in (3.8), (3.12), and (3.20) can be used to get minimal delays for BLE sensor node ($\tau_{e,b}$, $\tau_{p,b}$) and user ($\tau_{u,r}$) respectively. Based on these expressions, the algorithms (Algorithm 2 and Algorithm 3) autonomously minimize the delay for BLE sensor nodes in cluster 1 and users in cluster 2.

Algorithm 2 Cluster 1 Optimization.

Input:ζ_{adv}, $\zeta_{aux,b}$, $\zeta_{syc,b}$, $\kappa_{e,b}$, $\kappa_{p,b}$, λ_b.
Output: $\zeta_{ei,b}^{opt}$, $\zeta_{pi,b}^{opt}$
1: BLE gateway computes $\zeta_{ei,b}^{opt}$, $\zeta_{pi,b}^{opt}$ from (3.8) and (3.12).
2: BLE gateway broadcasts $\zeta_{ei,b}^{opt}$, $\zeta_{pi,b}^{opt}$ to all BLE sensor nodes.
4: BLE sensor nodes receives $\zeta_{ei,b}^{opt}$, $\zeta_{pi,b}^{opt}$.
5: BLE sensor nodes starts transmission at $\zeta_{ei,b}^{opt}$, $\zeta_{pi,b}^{opt}$.
6: **If** ($\zeta_{aux,b}$, $\zeta_{syc,b}$, $\kappa_{e,b}$, $\kappa_{p,b}$, λ_b changes), **go to Step 1**.
7: **Else** keep on transmitting at $\zeta_{ei,b}^{opt}$, $\zeta_{pi,b}^{opt}$.

Algorithm 3 Cluster 2 Optimization.

Input: ζ_{adv}, $\zeta_{aux,g}$, $\zeta_{req,g}$, $\zeta_{rsp,g}$, $\zeta_{ei,b}$, $\zeta_{ei,g}$, λ_u.
Output: μ_s^{opt} and ζ_{ri}^{opt}
1: BLE gateway computes μ_s^{opt}, ζ_{ri}^{opt} from (3.19) and (3.20).
2: BLE gateway broadcasts μ_s^{opt}, ζ_{ri}^{opt} to all users.
4: All users gets μ_s^{opt}, ζ_{ri}^{opt}.
5: All users starts transmission at μ_s^{opt}, ζ_{ri}^{opt}.
6: **If** ($\zeta_{aux,g}$, $\zeta_{req,u}$, $\zeta_{rsp,g}$, $\zeta_{ei,b}$, $\zeta_{ei,g}$, λ_u changes), **go to Step 1**.
7: **Else** keep on transmitting at μ_s^{opt}, ζ_{ri}^{opt}.

3.3.4 BLE Gateway Optimal Scan Duration and Scheduling

3.3.4.1 Determining BLE Gateway Scan Duration to Receive BLE Sensor Node Extended Advertisement Packet

The probability of successfully receiving an extended advertisement packet from a BLE sensor node by the BLE gateway can be given as:

$$\rho_{sr,eb} = 1 - (1 - \rho_{st,eb})^{\gamma_1} \tag{3.21}$$

Where, $\gamma_1 = \zeta_{sd,eb}/\zeta_{ei,b}$, $\zeta_{sd,eb}$ is the scan duration of BLE gateway to receive extended advertisement packet of BLE sensor node, $\rho_{st,eb}$ is the probability of successful transmission (without collision) of the extended advertising packet of the BLE sensor node.

Rearranging the above equation, we can get the expression for the scan duration of the BLE gateway ($\zeta_{sd,eb}$) to receive the BLE sensor node extended advertisement packet as:

$$\zeta_{sd,eb} = \frac{ln\,(1 - \rho_{st,eb})}{ln\,(1 - \rho_{sr,eb})}\zeta_{ei,b} \tag{3.22}$$

The above equation can directly be used to find the scan duration of the BLE gateway for successfully receiving the extended advertisement packet from the BLE beacon as per the QoS requirement defined by $\rho_{sr,eb}$.

3.3.4.2 Determining BLE Gateway Scan Duration to Receive BLE sensor node Periodic Advertisement Packet

The probability of successfully receiving a periodic advertisement packet from a BLE sensor node by the BLE gateway can be given as:

$$\rho_{sr,pb} = 1 - (1 - \rho_{st,pb})^{\gamma_2} \tag{3.23}$$

Where, $\gamma_2 = \zeta_{sd,pb}/\zeta_{pi,b}$, $\zeta_{sd,pb}$ is the scan duration of BLE gateway to receive periodic advertisement packet of BLE sensor node, $\rho_{st,pb}$ is the probability of successful transmission (without collision) of the periodic advertising packet of the BLE sensor node.
Rearranging the above equation, we can get the expression for the scan duration of the BLE gateway ($\zeta_{sd,pb}$) to receive the BLE sensor node periodic advertisement packet as:

$$\zeta_{sd,pb} = \frac{ln\,(1 - \rho_{st,pb})}{ln\,(1 - \rho_{sr,pb})}\zeta_{pi,b} \tag{3.24}$$

The above equation can directly be used to find the scan duration of the BLE gateway for successfully receiving the periodic advertisement packet from the BLE sensor node as per the QoS requirement defined by $\rho_{sr,pb}$.

3.3.4.3 Determining BLE Gateway Scan Duration to Receive User Request Packet

The probability of successful reception of the user request packet at the BLE gateway can be given as:

$$\rho_{sr,rq} = 1 - (1 - \rho_{st,rq})^{\gamma_3} \tag{3.25}$$

Where, $\gamma_3 = \zeta_{sd,rq}/\zeta_{ei,g}$, $\zeta_{sd,rq}$ is the scan duration of BLE gateway to receive user request packet, $\rho_{st,rq}$ is the probability of successful transmission (without collision) of the user request packet.
Rearranging the above equation, we can get the expression for the scan duration of the BLE gateway ($\zeta_{sd,rq}$) to receive the user request packets as:

$$\zeta_{sd,rq} = \frac{ln\,(1 - \rho_{st,rq})}{ln\,(1 - \rho_{sr,rq})}\zeta_{ei,g} \tag{3.26}$$

The above equation can directly be used to find the scan duration of the BLE gateway for successful reception of the user request packets as per the required QoS defined by $\rho_{sr,rq}$.

3.3.4.4 BLE Gateway Scheduling

The BLE gateway schedule determines how long and in which sequence the BLE gateway has to scan for the different advertising packets. The BLE gateway scans three advertising packets, i.e., one extended and one periodic advertising packet from BLE sensor nodes and one request packet from users. The scan duration's for each event, i.e., $\zeta_{sd,eb}$, $\zeta_{sd,pb}$, $\zeta_{sd,rq}$

are calculated from (3.22), (3.24), (3.26) respectively. The extended advertising packet from the BLE sensor node is required only once to initiate the BLE sensor nodes periodic advertising process. Hence, a timer $t = T$ is initiated to scan extended advertising once every T (e.g., $t = 24h$). For the rest of the time, periodic advertisements from the BLE sensor node and request packets from users are scanned round robin. The Algorithm 4 running in the BLE gateway implements the scheduling of the BLE gateway.

Algorithm 4 BLE Gateway Scheduling.

Input: $\rho_{st,eb}$, $\rho_{st,pb}$, $\rho_{st,rq}$ from (3.1), (3.2), (3.3) and $\zeta_{ei,b}^{opt}$, $\zeta_{pi,b}^{opt}$, ζ_{tri}^{opt} from (3.8), (3.12), (3.20), and timer 't' value.
1: Calculate $\zeta_{sd,eb}$, $\zeta_{sd,pb}$, $\zeta_{sd,rq}$ from (3.22), (3.24), (3.26).
2: **Task A:** Scan BLE sensor node extended advertisement packet for $\zeta_{sd,eb}$ duration.
3: **Task B:** Scan BLE sensor node periodic advertisement packet for $\zeta_{sd,pb}$ duration.
4: **Task C:** Broadcast at $\zeta_{ei,g}$ to users.
5: **Task D:** Scan user request packet for $\zeta_{sd,rq}$ duration.
6: **Task D:** Send response packet after ζ_{ri}^{opt}.
7: **If** (t=T), **go to Step 2**.
8: **Else** keep performing **Step 4, Step 5, and Step 6**.

3.3.5 Energy Evaluation Model for Cluster 1 and Cluster 2

Based on the proposed service architecture, this section derives the energy consumption model for BLE sensor nodes and users.

3.3.5.1 Energy Modeling for BLE Sensor Nodes

In the proposed service architecture, the BLE sensor node transmits using BLE periodic advertising. Each packet transmission in BLE consists of three subevents: pre processing, data transmission, and post processing [74, 76]. Pre processing and post processing subevents consumes fixed amount of energy [74, 76] i.e., 8.84ms*mA ($E_{syc,pre}$) and 7.03ms*mA ($E_{syc,post}$), respectively. However, the energy required for the data transmission subevent depends on the packet duration. It can be determined by c$\zeta_{syc,b}$ (E_{syc}), where c (=17.5mA) is the current consumption during the data transmission subevent. Hence, the total energy required for one periodic advertisement packet transmission of the BLE sensor node ($E_{p,b}^{tot}$) can be calculated as the sum of the energy required for all three subevents:

$$E_{p,b}^{tot} = E_{syc,pre} + E_{syc} + E_{syc,post} \tag{3.27}$$

However, the transmissions from BLE sensor nodes suffer from collisions, consequently requiring retransmissions for successful data transmission; hence, the average energy consumption ($E_{p,b}$) for one transmission of a BLE sensor node can be calculated as follows;

$$E_{p,b} = \frac{E_{p,b}^{tot}}{\rho_{st,pb}} \tag{3.28}$$

where $\rho_{st,pb}$ is the probability of successful transmission of the BLE sensor node periodic advertisement packet. Hence, (3.28) can directly be used to calculate BLE sensor node energy consumption and battery life estimation in a BLE network.

3.3.5.2 Energy modeling for users

The user undergoes multiple steps to get information from the BLE gateway. At first, the user has to receive the ADV_EXT_IND packet transmitted by the BLE gateway. Second, the user has to receive an AUX_ADV_IND packet transmitted by the BLE gateway. Upon successful reception of AUX_ADV_IND, the user sends the request to the BLE gateway. After this, the user receives AUX_SCAN_RSP (actual data packet) transmitted by the BLE gateway. The pre processing ($E_{adv,pre}$, $E_{aux,pre}$, $E_{req,pre}$, $E_{res,pre}$) and post processing ($E_{adv,post}$, $E_{aux,post}$,, $E_{req,post}$, $E_{res,post}$) events requires fixed energy i.e., 8.84ms*mA and 7.03ms*mA respectively [74, 76]. Hence, the average energy consumption of the user to receive a response from the BLE gateway ($E_{u,r}$) can be given as:

$$\begin{aligned} E_{u,r} = {} & E_{adv,pre} + c\tau_{u,r} + E_{adv,post} \\ & + \frac{E_{aux,pre} + E_{aux,g} + E_{aux,post}}{\rho_{st,rq}} \\ & + \frac{E_{req,pre} + E_{req,g} + E_{req,post}}{\rho_{st,rq}} \\ & + \frac{E_{res,pre} + E_{res,g} + E_{res,post}}{\rho_{st,rq}} \end{aligned} \tag{3.29}$$

where $\rho_{st,rq}$ is the probability of successful transmission of the user request packet. Hence, (3.29) can directly be used to calculate users' energy consumption. All the notations are summarized in Table. 3.2.

Table 3.1: Simulation parameters.

Parameter	Value
ζ_{adv}	0.144ms [85]
$\zeta_{aux,b}, \zeta_{aux,g}, \zeta_{req,u}$	0.176ms [85]
$\zeta_{syc,b}, \zeta_{res,g}$	0.16ms, 0.64ms, 1.28ms, 2.12ms [86]
$\zeta_{ei,b}, \zeta_{pi,b}, \zeta_{ei,g}$	1000ms, (20 to 500ms), 500 ms
ζ_{ri}	(100 to 1000ms)
$\Delta_{ifs}, \Delta_{37}$	0.15 ms, 30ms [86]
$\kappa_{e,b}, \kappa_{p,b}$	3, 33
λ_b, λ_u	(1 to 500), (1 to 500)

Table 3.2: Summary of notations.

Notation	Description
ζ_{adv}	Control packet size
$\zeta_{aux,b}$	Beacon extended advertising auxiliary packet size
$\zeta_{aux,g}$	Gateway auxiliary packet size
$\zeta_{syc,b}$	Beacon periodic advertising data packet size
$\zeta_{req,u}$	User request packet size
$\zeta_{res,g}$	Gateway response packet size
Δ_{37}	Offset channel 37
$\zeta_{ei,b}$	Beacon extended advertising interval
$\zeta_{pi,b}$	Beacon periodic advertising interval
$\zeta_{ei,g}$	Gateway extended advertising interval
Δ_{ifs}, ζ_{ri}	Inter frame space, random interval
$\kappa_{e,b}$	Secondary channels for beacon extended advertisement
$\kappa_{p,b}$	Secondary channels for beacon periodic advertisement
λ_b, λ_u, μ_s	Number of beacons, number of users, number of slots
$\rho_{st,lb}$	Probability of successful transmission of beacon legacy packet
$\rho_{st,eb}$	Probability of successful transmission of beacon extended packet
$\rho_{st,pb}$	Probability of successful transmission of beacon periodic packet
$\rho_{sr,eb}$	Probability of successful reception of beacon extended packet
$\rho_{sr,pb}$	Probability of successful reception of beacon periodic packet
$\rho_{sr,rq}$	User request packet successful reception probability
$\zeta_{sd,eb}$	Gateway scan duration to receive beacon extended packet
$\zeta_{sd,pb}$	Gateway scan duration to receive beacon periodic packet
$\zeta_{sd,rq}$	Gateway scan duration to receive user request packet
c	Current consumption for BLE receive and transmit event
$E_{p,b}$	Beacon energy consumption to transmit periodic packet
$E_{u,r}$	User energy consumption to receive response from gateway

3.4 Results and Discussion

This section discusses the analytical results of the proposed service architecture. In particular, we have investigated the impact of the number of BLE sensor nodes, advertising interval, packet size, and number of channels on the delay experienced and energy consumed by BLE sensor nodes. Further, we investigated the impact of the number of users, channels, slots, and the size of random window on the delay experienced and energy consumed by users. In this context, we considered two cluster scenarios with λ_b and λ_u number of BLE sensor nodes and users. BLE sensor nodes are transmitting ζ_{adv}, $\zeta_{aux,b}$, $\zeta_{syc,b}$, at $\zeta_{ei,b}$, $\zeta_{pi,b}$, and users are transmitting at ζ_{adv}, $\zeta_{aux,g}$, $\zeta_{req,u}$, $\zeta_{res,g}$, at $\zeta_{ei,g}$ respectively. The detailed simulation parameters are listed in Table 3.1. The BLE gateway is configured in continuous scanning mode with scan interval ($\zeta_{sd,eb}$, $\zeta_{sd,pb}$) greater than the advertising period ($\zeta_{ei,b}$) and ($\zeta_{pi,b}$) for BLE sensor nodes and ($\zeta_{sd,eg}$) greater than the advertising period ($\zeta_{ei,g}$) for users, to achieve maximal performance [74]. Further, analytical results are also compared with simulation results, which are in good agreement

with simulation results that validate the proposed service architecture. The analytical results are verified using the simulator developed in [60]. For convenience, the notations are summarized in Table 3.2.

3.4.1 Delay Analysis for Cluster 1

In this subsection, the impact of $\zeta_{pi,b}$ on the $\tau_{p,b}$ for different values of $\zeta_{syc,b}$, $\kappa_{e,b}$, $\kappa_{p,b}$ and λ_b is discussed and is shown in Figure 3.4a, Figure 3.4b, and Figure 3.4c respectively. This section also shows the simulation results, which closely match the analytical results.

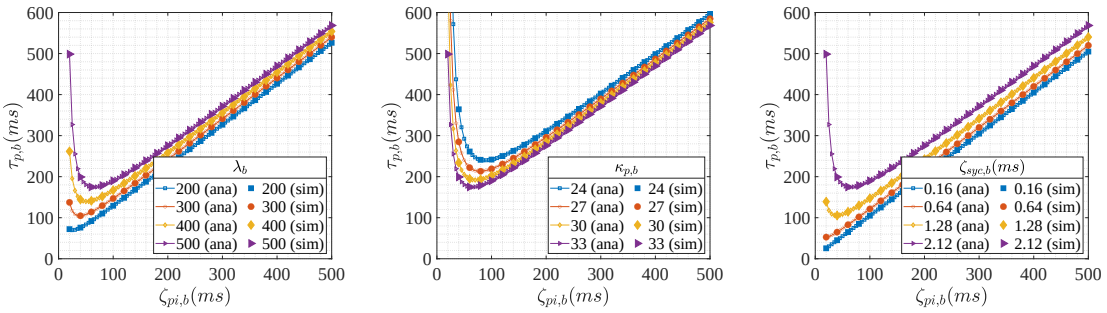

(a) (b) (c)

Figure 3.4: Impact of $\zeta_{pi,b}$ on $\tau_{p,b}$, (a) for different λ_b, (b) for different $\kappa_{p,b}$, and (c) for different $\zeta_{syc,b}$.

3.4.1.1 Impact of $\zeta_{pi,b}$ on the $\tau_{p,b}$ for Different λ_b

Figure 3.4a shows the impact of $\zeta_{pi,b}$ on $\tau_{p,b}$ for different values of λ_b with with $\zeta_{syc,b} = 2.12ms$, $\kappa_{p,b} = 33$. From Figure 3.4a, it can be observed that the lower values of $\zeta_{pi,b}$ cause higher $\tau_{p,b}$, however, on increasing $\zeta_{pi,b}$ further, $\tau_{p,b}$ decreases first, attains minimum and then increases again. Also, the increase in λ_b increases the overall $\tau_{p,b}$. This is because the lower values of $\zeta_{pi,b}$ and higher values of λ_b cause increased collisions, hence more retransmissions and consequently higher $\tau_{p,b}$.

3.4.1.2 Impact of $\zeta_{pi,b}$ on the $\tau_{p,b}$ for Different $\kappa_{p,b}$

Figure 3.4b shows the impact of $\zeta_{pi,b}$ on $\tau_{p,b}$ for different values of $\kappa_{p,b}$ with $\zeta_{syc,b} = 2.12ms$, $\lambda_b = 500$. From Figure 3.4b, it can be observed that the lower values of $\zeta_{pi,b}$ cause higher $\tau_{p,b}$, however, on increasing $\zeta_{pi,b}$ further, $\tau_{p,b}$ decreases first, attains minimum and then increases again. Also, the lower values of $\kappa_{p,b}$ have higher $\tau_{p,b}$. This is because the lower values of $\zeta_{pi,b}$ and $\kappa_{e,b}$ cause increased collisions, hence more retransmissions and consequently higher $\tau_{p,b}$.

3.4.1.3 Impact of $\zeta_{pi,b}$ on the $\tau_{p,b}$ for Different $\zeta_{syc,b}$

Figure 3.4c shows the impact of $\zeta_{pi,b}$ on $\tau_{p,b}$ for different values of $\zeta_{syc,b}$, with $\kappa_{p,b} = 33$, $\lambda_b = 500$. From Figure 3.4c, it can be observed that the lower values of $\zeta_{pi,b}$ cause higher

$\tau_{p,b}$, however, on increasing $\zeta_{pi,b}$ further, $\tau_{p,b}$ decreases first, attains minimum and then increases again. Also, the higher values of $\zeta_{syc,b}$ have higher $\tau_{p,b}$. This is because the lower values of $\zeta_{pi,b}$ and higher $\zeta_{syc,b}$ cause increased collisions, hence more retransmissions and consequently higher $\tau_{p,b}$.

3.4.1.4 Impact of λ_b and $\kappa_{p,b}$ on $\zeta_{pi,b}^{opt}$

In this subsection, the impact of λ_b and $\kappa_{p,b}$ on $\zeta_{pi,b}^{opt}$ is discussed and is shown in Figure 3.5a and Figure 3.5b respectively. In particular, Figure 3.5a shows the impact of λ_b on $\zeta_{pi,b}^{opt}$ for

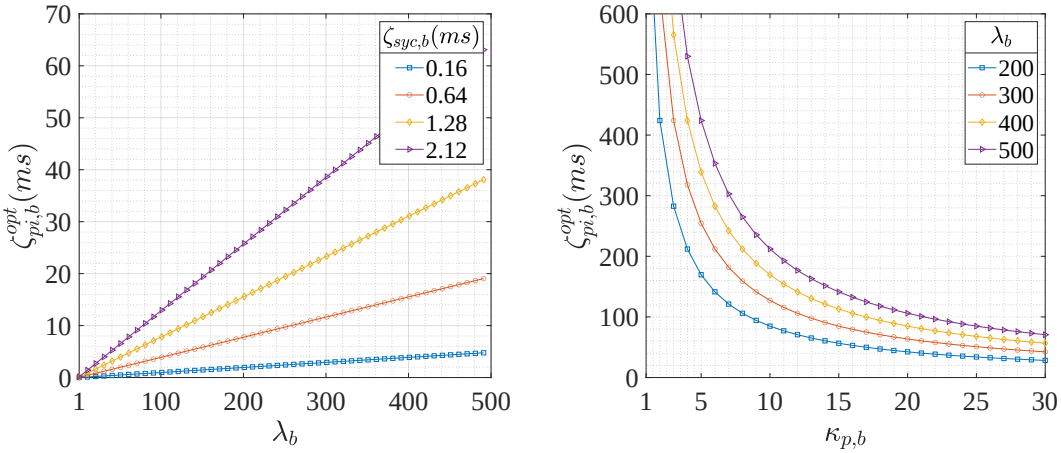

(a) (b)

Figure 3.5: (a) Impact of λ_b on $\zeta_{pi,b}^{opt}$ for different $\zeta_{syc,b}$, (b) impact of $\kappa_{p,b}$ on $\zeta_{pi,b}^{opt}$ for different λ_b.

different values of $\zeta_{syc,b}$ with $\kappa_{p,b} = 33$. From Figure 3.5a, it can be observed that $\zeta_{pi,b}^{opt}$ increase linearly with the increases the λ_b. This is because the increase in λ_b increases the total transmissions, causing more collisions, hence higher $\zeta_{pi,b}^{opt}$. Also, higher $\zeta_{syc,b}$ has higher $\zeta_{pi,b}^{opt}$. On the other hand, the increase in $\kappa_{p,b}$ decreases the $\zeta_{pi,b}^{opt}$ as shown in Figure 3.5b with $\zeta_{syc,b} = 2.12ms$. This is because larger values $\kappa_{p,b}$ avails more channels for transmission, hence decreasing collisions, consequently lowering $\zeta_{pi,b}^{opt}$. However, the more the λ_b, the more will the transmissions and more collisions, consequently, higher $\zeta_{pi,b}^{opt}$. On the other hand, the increase in $\kappa_{p,b}$ decreases the $\zeta_{pi,b}^{opt}$ as shown in Figure 3.5b. This is because larger values $\kappa_{p,b}$ avails more channels for transmission, hence decreasing collisions, consequently lowering $\zeta_{pi,b}^{opt}$. However, more λ_b, more will be transmissions and more collisions consequently higher $\zeta_{pi,b}^{opt}$.

3.4.2 Delay Analysis for Cluster 2

In this subsection, the impact of ζ_{ri} on the $\tau_{u,r}$ for different values of λ_u is discussed and is shown in Figure 3.6. Further the impact of λ_u on the μ_s^{opt} and ζ_{ri}^{opt} for different values of $\zeta_{ei,g}$ is discussed and is shown in Figure 3.7.

3.4.2.1 Impact of ζ_{ri} on the $\tau_{u,r}$ for Different Values of λ_u

Figure 3.6 shows the impact of ζ_{ri} on the $\tau_{u,r}$ for different values of λ_u with $\zeta_{res,g} = 2.12ms$, $\zeta_{ei,b} = 1000ms$, $\lambda_b = 500$. From Figure 3.6, it can be observed that the lower values of ζ_{ri} causes higher $\tau_{u,r}$; however, on increasing ζ_{ri} further, $\tau_{u,r}$ decreases first, attains minimum and then increases again. Also, the increase in λ_u increases the overall $\tau_{u,r}$. This is because the lower values of ζ_{ri} and higher values of λ_u cause increased collisions, hence more retransmissions and consequently higher $\tau_{u,r}$.

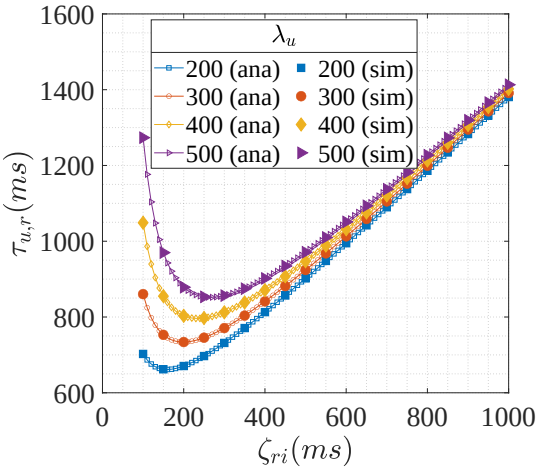

Figure 3.6: Impact of ζ_{ri} on $\tau_{u,r}$ for different λ_u

3.4.2.2 Impact of λ_u on the μ_s^{opt} and ζ_{ri}^{opt}

Figure 3.7 shows the impact of λ_u on the μ_s^{opt} and ζ_{ri}^{opt} with $\zeta_{res,g} = 2.12ms$, $\zeta_{ei,b} = 1000ms$, $\lambda_b = 500$. From Figure 3.7, it can be observed that μ_s^{opt} and ζ_{ri}^{opt} has same trend with λ_u

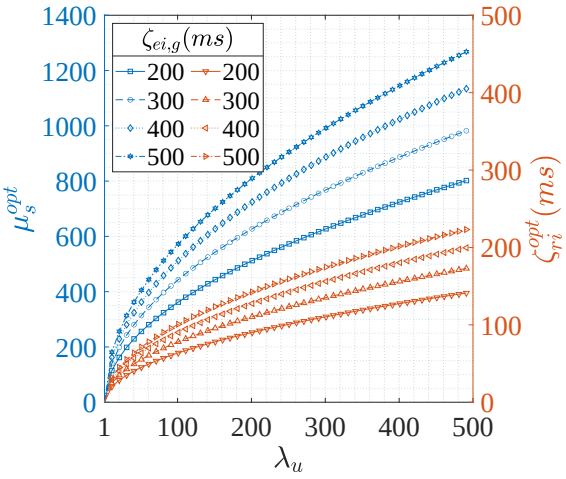

Figure 3.7: Impact of λ_u on μ_s^{opt} and $\zeta_{ri}^{opt}$for different $\zeta_{ei,g}$.

i.e., as the λ_u increases μ_s^{opt} and ζ_{ri}^{opt} also increases and almost linearly which means we need to select μ_s^{opt} roughly equal to λ_u.

3.4.3 Impact of $\zeta_{sd,eb}$, $\zeta_{sd,pb}$, $\zeta_{sd,rq}$ on $\rho_{sr,eb}$, $\rho_{sr,pb}$, $\rho_{sr,rq}$

Figure 3.8 shows the impact of $\zeta_{sd,x}$ on $\rho_{sr,x}$ with $\kappa_{e,b} = 3$, $\kappa_{p,b} = 33$, $\zeta_{syc,b} = 2.120ms$, $\zeta_{res,g} = 2.12ms$, $\zeta_{ei,b} = \zeta_{ei,b}^{opt}$, $\zeta_{pi,b} = \zeta_{pi,b}^{opt}$, $\zeta_{ri} = \zeta_{ri}^{opt}$, $\zeta_{ei,g} = 500ms$, $\lambda_b = 500$, $\lambda_u = 500$. From Figure 3.8, it can be observed that $\rho_{sr,x}$ (success probability of extended packet of

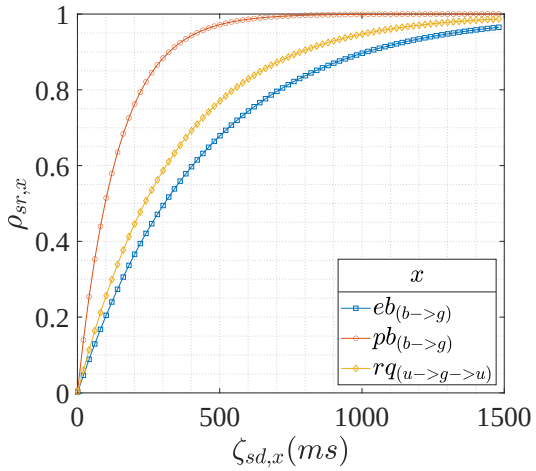

Figure 3.8: Impact of $\zeta_{sd,X}$ on $\rho_{sr,x}$.

BLE sensor node, periodic packet of BLE sensor node and request packet of the user) increases with $\zeta_{sd,x}$ (scan duration of BLE gateway for the extended packet of BLE sensor node, periodic packet of BLE sensor node and request packet of user). The periodic packet of the BLE sensor node has a higher probability of success among the three advertisements.

3.4.4 Energy Analysis for Cluster 1

Figure 3.9 shows the impact of $\zeta_{pi,b}$ on $E_{p,b}$ with $\zeta_{syc,b} = 2.12ms$, $\kappa_{p,b} = 33$. From

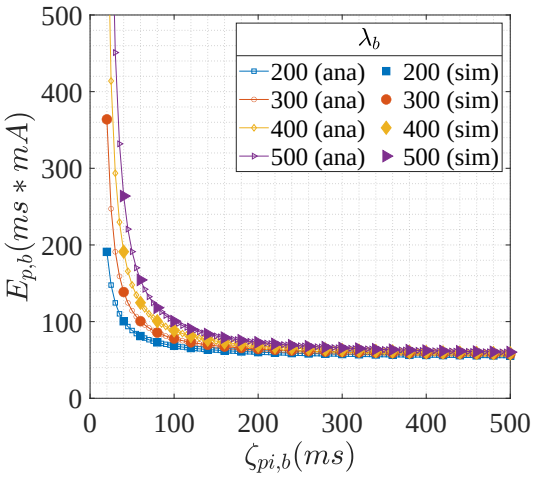

Figure 3.9: Impact of $\zeta_{pi,b}$ on $E_{p,b}$ for different λ_b.

Figure 3.9, it can be observed that lower values of $\zeta_{p,b}$ causes higher $E_{p,b}$, however on increasing $\zeta_{p,b}$ further, $E_{p,b}$ attains almost a constant value. Also, the increase in λ_b

increases the overall $E_{p,b}$. It is because lower values of $\zeta_{p,b}$ and higher values of λ_b increase total transmissions, hence more collisions, consequently requiring more retransmission, thus more energy; however, for larger values of $\zeta_{p,b}$, there are few transmissions and hence few collisions, consequently few retransmission thus energy consumption remains almost constant.

3.4.5 Energy Analysis for Cluster 2

Figure 3.10 shows the impact of ζ_{ri} on the $E_{u,r}$ for different values of λ_u with $\zeta_{res,g} = 2.12ms$, $\zeta_{ei,g} = 500ms$, $\zeta_{ei,b} = 1000ms$, $\lambda_b = 500$. From Figure 3.10, it can be observed that

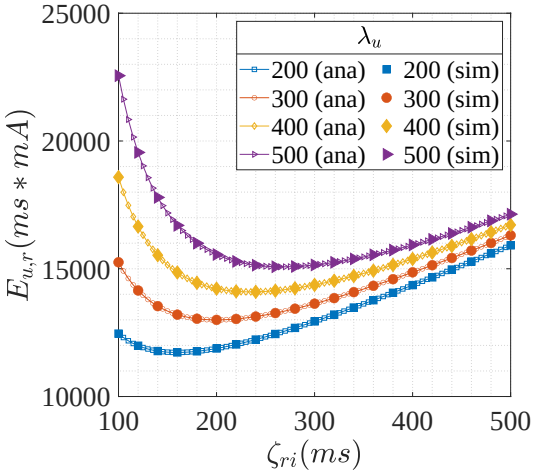

Figure 3.10: Impact of ζ_{ri} on $E_{u,r}$ for different λ_u.

the lower values of ζ_{ri} cause higher $E_{u,r}$; however, on increasing ζ_{ri} further, $E_{u,r}$ decreases first, attains minimum and then increases again. Also, the increase in λ_u increases the overall $E_{u,r}$. This is because the lower values of ζ_{ri} and higher values of λ_u cause increased collisions, hence more retransmissions and consequently higher $E_{u,r}$.

3.5 Comparison with Existing Works

This section demonstrates the performance comparison of the proposed work with existing works in terms of delay and energy. In particular, the delay experienced and energy consumed by the BLE sensor nodes is compared with the recent work proposed in [68], and the delay experienced and energy consumed by users is compared with the recent work proposed in [83].

3.5.1 Delay and Energy Consumption Comparison for BLE Sensor Nodes

This subsection discusses the BLE sensor nodes delay and energy consumption comparison results of the proposed architecture with the existing works with $\kappa_{p,b} = 33$, $\zeta_{p,b} = 20ms$, $\zeta_{a,b} = 20ms$. The comparison results are shown in Figure 3.11.

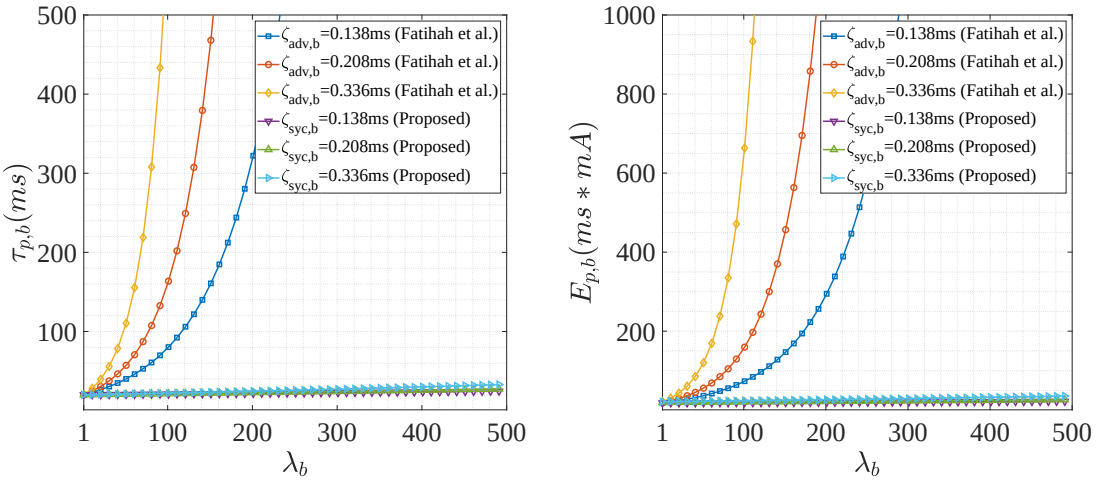

Figure 3.11: BLE sensor nodes delay and energy comparison results of the proposed architecture with the existing works, (a) delay comparison, (b) energy comparison; for different $\zeta_{syc,b}$ and $\zeta_{adv,b}$.

In particular, from Figure 3.11a and Figure 3.11b, it can be observed that the BLE sensor nodes with the proposed architecture experience much lower delays and energy consumption compared to the existing works [68]. It is because the delay analysis model proposed in [68] is based on BLE legacy advertising, which utilizes three channels for data transmission and hence requires more retransmission for successful data transmission, consequently increasing delay and energy consumption. In contrast, the proposed architecture model is based on BLE periodic advertisement, which utilizes 37 channels for data transmission and hence requires fewer retransmissions for successful data transmission, consequently lowering delay and energy consumption.

3.5.2 Delay and Energy Consumption Comparison for Users

This subsection discusses the user's delay and energy consumption comparison results of the proposed architecture with the existing works for different ζ_{gap} with $\zeta_{res,g} = 2.12ms$, $\zeta_{ei,g} = 500ms$, $\zeta_{ei,b} = 1000ms$, $\lambda_b = 500$. The comparison results are shown in Figure 3.12. In particular, from Figure 3.12a and Figure 3.12b, it can be observed that the users with the proposed architecture experience much lower delay compared to the existing works [83]. It is because the delay analysis model proposed in [83] utilizes the gap between ADV_EXT_IND packets (ζ_{gap}) to receive user requests. However, ζ_{gap} can attain a maximum value of 9.824ms, hence can receive requests successfully for few users only. In contrast, a random window has been introduced in the proposed service architecture, the size of which depends on the number of users, hence resulting in lower delays and energy consumption.

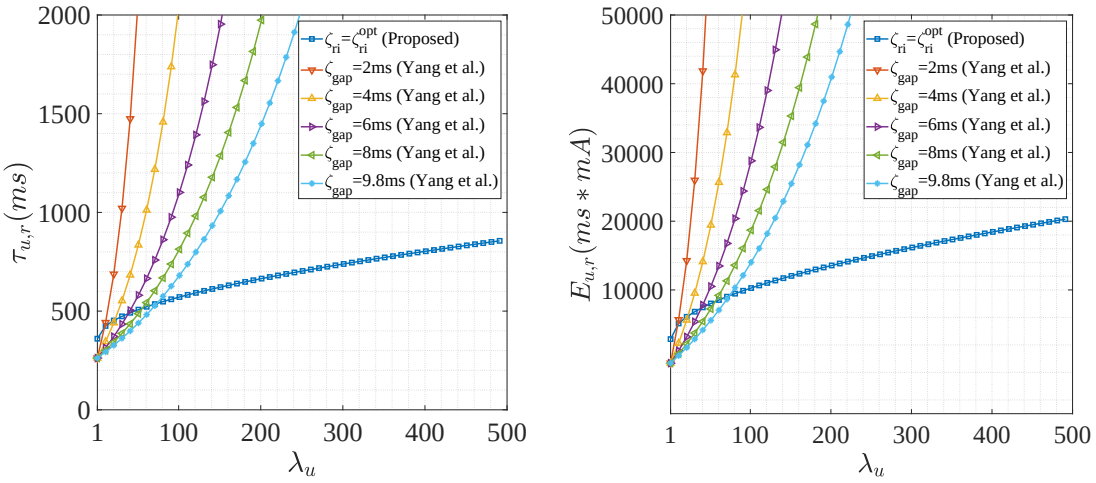

(a) (b)

Figure 3.12: User's delay and energy comparison results of the proposed architecture with the existing works, (a) delay comparison, (b) energy comparison.

3.6 Applications and Network Design

This section discusses different applications where the proposed service architecture can be utilized. Afterward, we discussed developing an application using the proposed service architecture.

3.6.1 Key Applications of the Proposed Service architecture

The proposed service architecture can have numerous applications. However, in this section, we discussed a few prominent applications from them.

3.6.1.1 BLE based Smart Parking Solution

The proposed service architecture facilitates the development of an advanced BLE based smart parking solution that delivers users real time parking slot information and navigation assistance. This system leverages BLE technology to overcome the limitations of traditional solutions that rely on the Internet and GPS, which often fail in underground parking environments. By utilizing BLE technology, the proposed architecture effectively addresses connectivity issues inherent in underground parking environments, providing users with reliable slot booking and navigation capabilities. In this solution, BLE sensor nodes will send the parking slot information to the BLE gateway. The BLE gateway will collect the parking slot information from all the BLE sensor nodes. The BLE gateway will then broadcast the parking slot information to the users. The user will then send the request to the gateway to book the preferred slot. The system's reliance on BLE ensures robust and uninterrupted connectivity, even in areas with poor internet or cellular reception, such as underground parking facilities.

3.6.1.2 BLE based Smart Airport

The proposed service architecture enables the development of an advanced BLE based system tailored for airport applications, offering travelers real time flight information and navigation assistance. This system harnesses BLE technology to overcome the challenges faced by traditional solutions that depend on the internet and GPS, which can be unreliable in certain airport environments, such as underground terminals or areas with weak signal coverage. In this application, BLE sensor nodes will transmit essential flight and gate information to a central BLE gateway. The gateway will aggregate this data from all the BLE sensor nodes and broadcast it to users. Travelers can then request specific flight details or gate information from the gateway. The system use of BLE ensures consistent and reliable connectivity, even in areas with limited internet or cellular reception, such as underground or heavily enclosed spaces within airports. This approach guarantees travelers timely updates and accurate navigation support throughout their airport journey.

3.6.1.3 BLE based Smart Super Market

The proposed service architecture enables developing a cutting edge BLE based system for supermarkets, enhancing the shopping experience by delivering real time product information and in store navigation assistance. This system utilizes BLE technology to overcome the limitations of conventional methods that depend on the internet and GPS, which can be less effective in the complex indoor environments of large supermarkets. In this setup, BLE sensor nodes placed throughout the store transmit detailed information about product locations, promotions, and store layouts to a central BLE gateway. The gateway aggregates this data and broadcasts it to shoppers' mobile devices, providing them with up to date product information and guiding them to specific aisles or items. By relying on BLE technology, the system ensures consistent and reliable connectivity throughout the supermarket, even in areas where internet or cellular signals might be weak. This approach allows for seamless navigation and enhanced shopping convenience, regardless of the store's layout or signal conditions.

3.6.2 BLE based Smart Parking Solution Design

In this section, we discussed developing a BLE based smart parking solution using the proposed service architecture. We also discussed how we can achieve different service requirements for such applications.

3.6.2.1 BLE Parking Solution Design

In this subsection, we discussed developing a BLE-based parking solution using the proposed service architecture. A smart parking solution provides users with parking slot information and navigation information. So, we can deploy BLE sensor nodes embedded with sensors to detect the occupancy state. The occupancy state is then transmitted to the BLE gateway. After receiving the occupancy state from all the BLE sensor nodes, the

BLE gateway will broadcast to the users. The users can then request to book the slots. This procedure is shown in Figure 3.13. Using the service architecture proposed in this

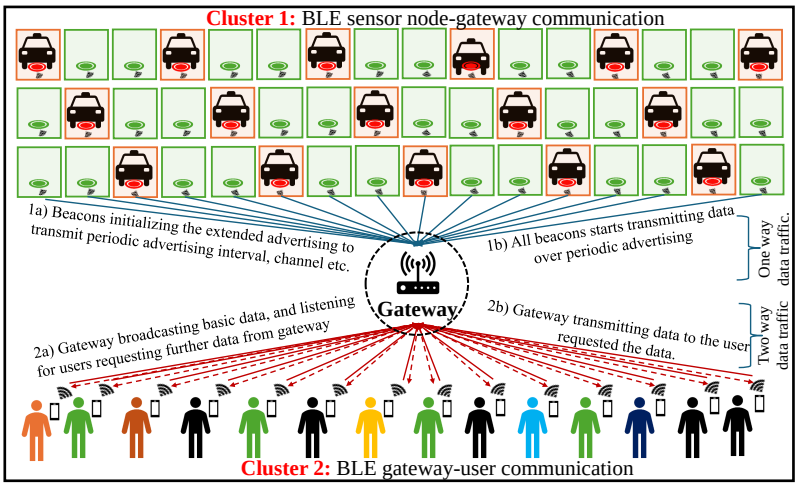

Figure 3.13: Illustration of cluster formation and communication in BLE based parking system.

chapter, we can minimize the delay experienced by users and maximize the battery life of BLE sensor nodes.

3.6.2.2 How to select $\zeta_{pi,b}$

There can be a requirement where we have to select the $\zeta_{pi,b}$ for a given set of QoS requirements. Such an example is shown in Figure 3.14, where QoS 1 requires $\tau_{p,b} < 400ms$ and $\rho_{sr,b} > 0.5$, QoS 2 requires $\tau_{p,b} < 600ms$ and $\rho_{sr,b} > 0.95$ and QoS 3 has $\tau_{p,b} < 500ms$ and $\rho_{sr,b} > 0.8$ respectively. For QoS 1, the service provider can select $\zeta_{pi,b}$ between 60 ms to 320ms; however, $\zeta_{pi,b}$=60ms can be chosen for minimal delay, and $\zeta_{pi,b}$=320ms can be chosen for higher $\rho_{sr,pb}$. Similarly for QoS 2 $\zeta_{pi,b}$ between 420ms to 500ms, and QoS 3 $\zeta_{pi,b}$ between 145ms to 420ms can be chosen.

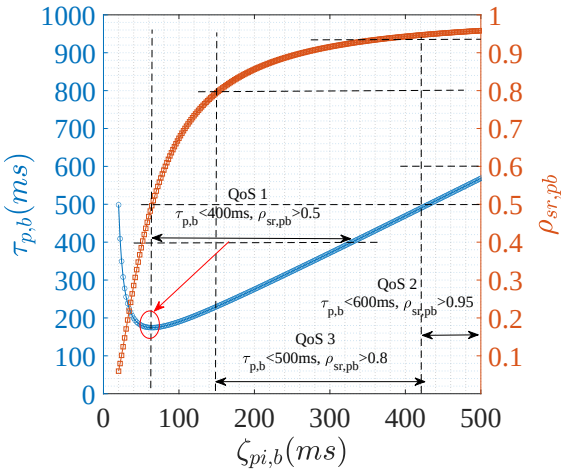

Figure 3.14: Variation of $\tau_{p,b}$ and $\rho_{sr,pb}$ with $\zeta_{pi,b}$.

3.6.2.3 How to Select μ_s and ζ_{ri}

Similarly there can be a requirement where we have to select the ζ_{ri} for a given set of QoS requirements as shown in Figure 3.15a, where QoS 1 requires $\tau_{u,r} < 1000ms$ and $\rho_{sr,rq} > 0.7$, QoS 2 requires $\tau_{u,r} < 1500ms$ and $\rho_{sr,rq} > 0.9$ respectively. For QoS 1, the service provider can select ζ_{ri} between 200ms to 550ms, however, ζ_{ri}=275ms can be chosen for minimal $\tau_{u,r}$ and ζ_{ri}=550ms can be chosen for higher $\rho_{sr,rq}$. Similarly for QoS 2 ζ_{ri} between 750ms to 1000ms can be chosen. Also, Figure 3.15b shows how many λ_u the

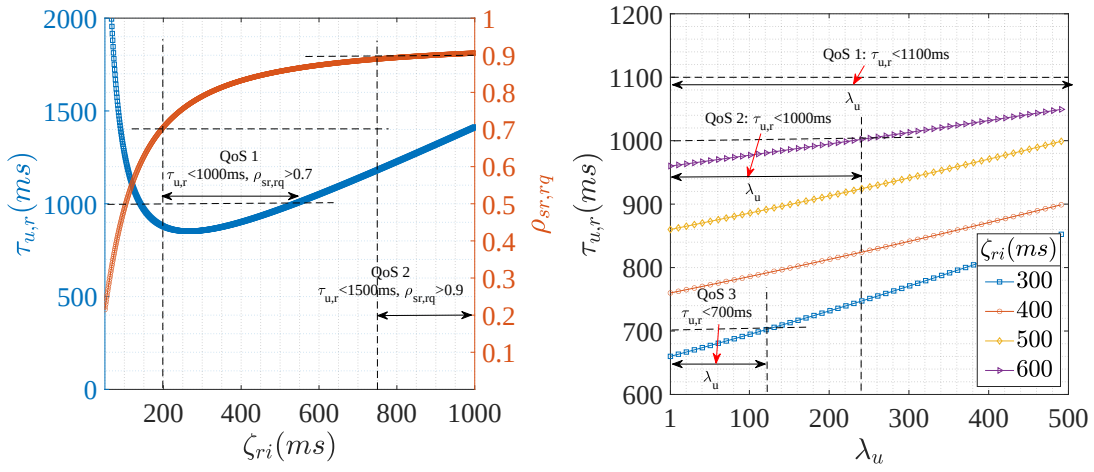

Figure 3.15: (a) Variation of $\tau_{u,r}$ and $\rho_{sr,rq}$ with ζ_{ri}, (b) variation of $\tau_{u,r}$ with λ_u for different ζ_{ri}.

network can support for a given set of QoS requirements. It can be observed that QoS 1 can support $\lambda_u = 500$, whereas QoS 2 can only support $\lambda_u = 240$ and QoS 3 can support $\lambda_u = 120$ respectively.

3.7 Conclusion

This chapter minimizes the delay for sensor nodes-gateway-user communication scenario considering a smart parking use case. At first, a performance model considering a heterogeneous scenario is developed to analyze delay. Using this model, analytical expression for selecting optimal advertising interval are derived. Based on these analytical expressions, algorithms are proposed that autonomously optimize the network and ensure minimal latency. In addition to the above, an energy consumption model that helps in estimating the battery lifetime of the sensing nodes along with suitable parameter selection is developed and discussed. Further, this chapter provides insights into various quality of service (QoS) needs for a BLE based heterogeneous network, along with the process of selecting parameters to meet those requirements. This analysis would help the service provider establish the network with such QoS requirements. Further, this chapter presents the simulations to verify the proposed model and analysis.

Chapter 4

Battery Life Enhancement Through Effective Hardware Design and Efficient Utilization

Most of the IoT applications deployed at remote locations have constraints on energy, hence require higher energy efficiency for longer battery life [87]. Therefore, in this chapter, we proposed a battery life enhancement strategy through integrated hardware design, efficient hardware utilization, and optimal configuration. Among the IoT applications mentioned and discussed in Chapter 1, one of the crucial cold chain monitoring IoT use cases from the logistics & retail domain, requiring higher energy efficiency and longer battery life, has been considered for energy efficiency analysis, evaluation, and enhancement. To begin with, we first identified the general issues in existing cold chain monitoring solutions, followed by investigating the root factors causing a reduction in energy efficiency, which, as a result, reduced the overall battery life of the device. Among the general issues, it is found that most of the existing solutions are based on general purpose microcontroller boards and sensor breakout boards, which affect accuracy, increase size, and reduce energy efficiency, thereby reducing overall battery life [61, 62]. Besides, in the existing solutions the sensors are powered directly from the power supply which makes the sensor to consumes few µA's of current even in the sleep mode. These issues are identified as the root factors causing significant degradation in energy efficiency, thereby significantly reducing battery life. To address the aforementioned issues, we first designed, developed, and validated the integrated sensing and logging solution called THERMOD (TemperatuRE, Humidity, and MOvement Data logger), addressing the general issues, including cost, size, and data accuracy. Further, the proposed solution utilizes the GPIOs to power sensors and an optimal clock configuration. A brief review of existing works and how our proposed work differs from the existing works is introduced below.

4.1 Related Work and Motivation

The authors in [88] proposed a real time cold chain tracking system in which the data is processed and transmitted to the authenticated person using 5G along with GPS location. Moreover, the authors in [89] have proposed a drone operated medicines and vaccine delivery system with a temperature monitoring and logging system. However, being power hungry technologies, 5G/GPS based solutions may affect the vaccine potency due

to the frequent opening of vaccine containers for battery replacement. In contrast, some researchers solely focused on self sustained solar energy based monitoring and logging solutions. For instance, the authors in [90] and [91], have designed solar power vaccine backpacks for remote areas providing self sustainable energy solutions for vaccine cold storage and data logging respectively. However, exposure to sunlight/UV rays may affect the vaccine's potency.

Indeed, several innovative solutions have been developed to assure vaccine storage and distribution under specified limits. For instance, the authors in [92], have surveyed different data loggers, and proposed a basic model of temperature data logger system, whereas, the authors in [93], have designed a temperature & humidity data logger based on cypress CY8C29566 microcontroller. Furthermore, the authors in [94] have proposed a data logger system based on Atmel atmega32 microcontroller, which allows the use of any microcontroller with and without a universal serial bus (USB) host/USB On-the-Go (OTG) for accessing USB drive. Besides it, the authors in [61], have designed a multi point data logger based on the texas instrument LM35 temperature sensor and arduino uno microcontroller board. Moreover, the authors in [62], have designed an arduino based logging platform, which consists of three breakout boards i.e., DS3231 real time clock (RTC) module, AT24C512 electrically erasable programmable read-only memory (EEPROM) module. However, the aforementioned methods have certain limitations that restrict them from becoming effective solutions for vaccine storage and temperature monitoring. For instance, the hardware of [93] is limited to 4000 logs and microcontroller have high current consumption in sleep and standby modes, whereas in [94] no hardware is realized and based on atmega32 which have high current consumption. Moreover, [61] is based on LM35 temperature, which has a high response time, and Arduino Uno board, which can affect the sensed data (since the generic board doesn't have temperature-specific components). Besides it, [62], is designed using breakout boards which affect the sensed data accuracy and also consumes considerable energy in sleep mode which is quite high for battery operated temperature data loggers.

It can be observed from the above discussion that most of the existing solutions are based on development and generic breakout boards, which contain generalized hardware and temperature sensitive passive components, which can affect overall device accuracy and can increase energy consumption. Also, the existing solutions focus on the stationary environment cold chain monitoring, while vaccines and other pharmaceuticals require proper in transit monitoring.

In contrast, this chapter focuses on the design and development of cost efficient integrated sensing and power efficient logging solution for dynamic environment cold chain monitoring. In particular, the device can measure temperature & humidity, and 3 dimensional movement, and is able to log 16000 data points with 10 minutes logging intervals for 9 months on a single 220mAh CR2032 coin cell. Further, the logged data can be retrieved in tabular and graphical format with min/max readings along with temperature excursion.

In this chapter, we address the above challenges by proposing an integrated sensing and logging solution. To date, hardly any of the existing work studied the integrated sensing and logging solution to the best of our knowledge. Moreover, a hardware design has been formulated within the institution lab along with test results. Further, it is shown that the proposed hardware is not only significantly inexpensive as compared to the available industrial solutions but also energy efficient with a battery life of 4.6 years at 10 minutes logging intervals and can log 240000 data points.

4.2 Contribution

Specifically, the contribution of this work can be summarized as;

- Designing and development of integrated and compact, sensing and logging solution for monitoring sensitive vaccines, including COVID 19. Unlike existing works, the device can sense and store temperature & humidity and movement data with max/min temperature & humidity indication.
- Extensive experiments have been conducted to validate the realization of THERMOD. Moreover, the experimental data obtained after retrieval proves the accuracy of the proposed THERMOD. However, in existing works, no real time experiments have been conducted.
- User friendly configuration tool design, where the parameters like start delay, alarm for low & high thresholds, and logging interval can be configured easily, whereas in existing solutions no configuration tool is designed.
- Efficient hardware utilization by integrated circuits (ICs) only integration of microcontroller and related sensing units to achieve cost and energy efficiency, which is a critical bottleneck in the implementation of the existing solutions.
- Further, extensive efforts have been made towards energy efficiency enhancement followed by various experiments which show that the device can achieve a long battery life of 4.6 years at 10 minutes logging interval, and a maximum of 240000 data points can be logged with CR2032 coin cell of 220mAh capacity. Moreover, it is recommended to use the device for 9 months with 16000 data points at 10 minute logging interval.

Indeed, the proposed THERMOD can sense, store, temperature & humidity down to -40°C, which covers frozen (-25°C and -15°C) and refrigerated storage (2°C to 8°C) [95]. Moreover, to support ultra low temperature storage (-80°C and -60°C) monitoring, the proposed THERMOD is equipped with the provision for an external sensor which can be utilized to connect the external sensor to the THERMOD. However, for ultra low temperature monitoring, the device should be kept out of the vaccine container since the sensors, microcontroller, and flash memory have operating range down to -40°C. Moreover,

the proposed THERMOD is reusable data logger, hence it can be used repetitively for frozen and refrigerated storage vaccines monitoring. Furthermore, the comparisons shown in Table 4.1 with the existing solutions emphasize the novelty of the proposed THERMOD.

Table 4.1: Technical comparison of the proposed THERMOD with most prominent works.

Novelty	[93]	[94]	[61]	[62]	Proposed
Size	Moderate	Large	Large	Moderate	Compact
Accuracy	Low	Low	Low	Low	High
Complexity	Low	Moderate	Low	High	Low
System Cost ($)	Moderate	High	Moderate	Low	Least
Monitoring	Stationary cold chain	Stationary cold chain	Stationary cold chain	Stationary cold chain	Dynamic & stationary cold chain
Battery Life	Low	Low	Low	Low	High
Data Reports	Simple data	Simple data	Simple data	Simple data	Graphical & tabular format

4.3 System Model

The proposed solution consists of a battery operated device (THERMOD) that senses the temperature & humidity and movement data with the help of a digital temperature & humidity sensor and accelerometer and stores the data in the flash memory. Further, this data can be retrieved by plugging the device into the computer and can be downloaded into .pdf and .csv format.

4.3.1 Sensor Node Design

Figure 4.1 illustrates the block diagram, along with the interconnections among different sub units and the designed hardware of the proposed THERMOD.
In addition to the minimum path circuitry, the layout places the interacting units, including temp/humidity sensors and power supply, at the edges of the PCB to prevent the sensors from thermal energy generated from the power supply. Moreover, dual power support is provided to ensure smooth operation, i.e., USB power and CR2032 coin cell. As shown, the metal-oxide-semiconductor field-effect-transistor (MOSFET) switches between the input power via coin cell and USB. Moreover, the Schottky diode has been added to protect the low dropout regulator (LDO) from reverse polarity, i.e., when the device is powered by a CR2032 coin cell. Besides, a seamless interconnection is developed among the other units; i.e., the accelerometer, temperature & humidity data are communicated to the microcontroller unit (MCU) via an inter-integrated circuit (I2C). The MCU transfers the data to flash memory over the serial peripheral interface (SPI).

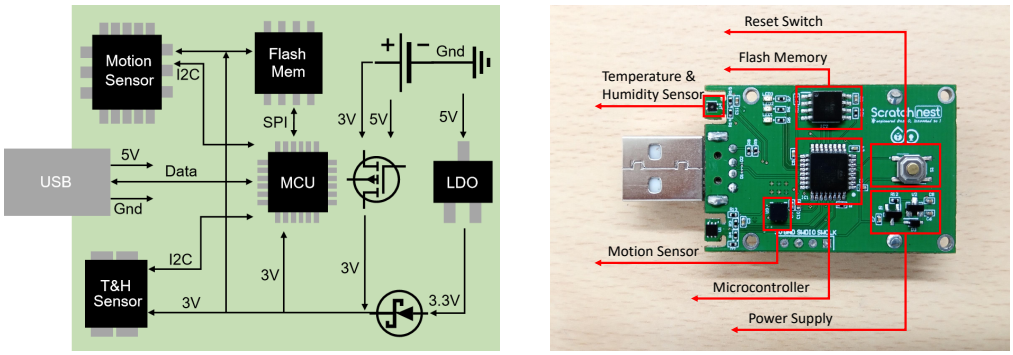

(a) (b)

Figure 4.1: (a) Block diagram of the proposed THERMOD, (b) hardware design of the proposed THERMOD.

Moreover, the key components are listed in the Table. 4.2, which performs different operations as; temperature & humidity, and movement monitoring.

Table 4.2: Major components of the proposed THERMOD and their key functions.

Components	**Manufacturer**	**Functions**
STM32L412KB	STMicroelectronics	Data Processing
LIS3DHTR	STMicroelectronics	In transit motion monitoring
W25Q16JVSNIQ	Winbond	Stores the sensed data
SHT40	Sensirion	Senses ambient temperature & humidity
USB A	Zenric	Power & pdf generation
AO3401	Alpha & Omega	5V/3V Switching
XC6206P332MR	Torex	Regulated 3.3V output

Furthermore, the below components are chosen mainly due to the following key specifications:

- **Microcontroller:** The device has STM32L412KBT6, an ultra low power arm cortex M4 based microcontroller from STMicroelectronics. This controller is shortlisted due to several attractive features from the perspective of the mentioned applications. For instance, the low current consumption in shutdown and standby mode to achieve longer battery life. Besides, it is built over one full speed crystal less USB interface required for retrieving the logged data.

- **Temperature & Humidity Sensor:** Assuring the compatibility of the above microcontroller, the device has SHT40, an ultra low power & high accuracy temperature & humidity sensor from the well known venture Sensirion. Moreover, the sensors were chosen keeping the operating voltage (i.e., down to 1.08V), accuracy (±0.2°C, ±1.8%RH), and resolution (0.01) into consideration, Altogether the industry calibrated digital SHT40 sensor has relatively good accuracy and resolution at the low cost. Besides, it can also operate down to 0.08µA current.

- **Accelerometer:** Coming to the highly sensitive motion sensing, the device is loaded with LIS3DHTR, an ultra low power high performance three axis linear

accelerometer from STMicroelectronics. Specifically, the accelerometer is used for orientation & free fall detection, vibration & movement monitoring. Another reason for choosing the mentioned accelerometer over others is its ultra low current feature (i.e., down to 0.5µA) among available commercial accelerometers. Besides it also supports dual interface, i.e., I2C/SPI.

- **Flash Memory:** The device has W25Q16JVSNIQ, serial flash memory from Winbond. It has storage up to 2MB. The serial flash memory stores the temperature & humidity and accelerometer data. The memory is called frequently on every user defined logging interval; thus, it must have a low operating current. It has a low operating current, i.e., down to 1µA. Besides, it can also operate down to 2.7V.

- **Voltage Regulator:** Keeping a view of the required electrical specifications, the device is powered with XC6206P332MR, a low dropout regulator (LDO with 250mV dropout voltage) from Torex. LDO converts USB 5V to 3.3V, followed by a Schottky diode which gives 3V. The 3V output is supplied to the whole circuitry.

- **ESD Diode:** The device has ESDAXLC6, an electrostatic discharge (ESD) diode from STMicroelectronics. ESD diode is used to protect the device from ESD, which may strike on external exposed peripherals, i.e., USB. The diode capacitance introduces delay in signals; hence, the ESD diode with low diode capacitance (0.5pF) is preferred over others.

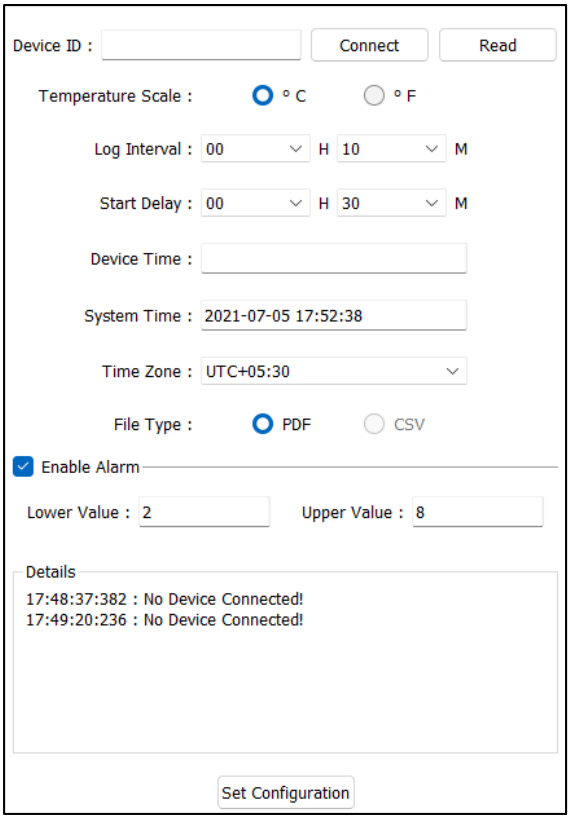

Figure 4.2: Configuration tool.

4.3.2 Sensor Node Working

The THERMOD is activated by pressing the switch for 5 seconds, the activation is confirmed by three led's blinking three times. Once the activation is done, the sensor will start sensing. The temperature & humidity sensor senses the immediate surroundings temperature & humidity, and if the device is in motion, the accelerometer will sense the 3 dimensional movement data. All the sensed data will be stored in flash memory. Pressing the switch again for 5 seconds will deactivate the logging mode, and THERMOD will stop sensing and logging. The sensed data can be retrieved by plugging the device into any computer/laptop. It also generated alerts when the temperature & humidity go beyond the predefined limits. The temperature & humidity limits, logging interval, and date/time/zone can be set using the interface shown in Figure 4.2.

4.4 Results and Discussion

In this section, the performance of the proposed THERMOD is analyzed by performing numerous experiments. For instance, for data validation, we have considered a fridge as a reference temperature device, operating at very low temperatures. On completion of logging, the logged data is retrieved in .pdf format. The cost of THERMOD is compared with the state of art solutions, and it is found that the proposed THERMOD is quite inexpensive compared to the existing solutions. Further, an experimental setup is formed for current consumption measurements in different operating modes and overall battery life evaluation.

4.4.1 Logged Data Reports

We performed extensive experiments to validate the data obtained from THERMOD. For instance, THERMOD is placed in a fridge operating at 4°C for data acquisition as shown in Figure 4.3. Once the data logging is completed, the logged data can be retrieved in

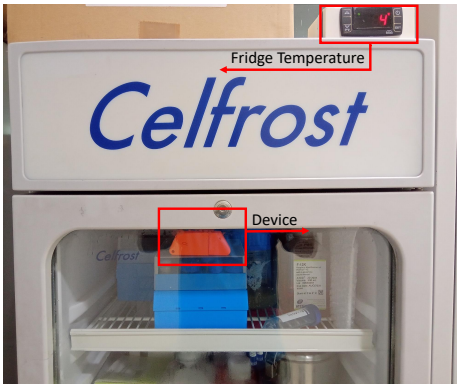

Figure 4.3: Experimental setup for THERMOD data validation.

.pdf or .csv format. Figure 4.4a, shows the pdf of the retrieved temperature & humidity along with the other parameters. For instance, the red and black dotted lines in the pdf

show user defined limits for temperature & humidity; similarly, blue and yellow curves shows the logged temperature & humidity values in addition to the date and time stamps, which are essential parameters for cold chain monitoring applications. The temperature data so obtained is close to fridge temperature over the entire experiment duration, which confirms the temperature accuracy. The correct PCB layout and component placement, in addition to temperature sensor accuracy, assures the overall temperature accuracy. Moreover, the Figure 4.4b, shows the 3 dimensional movement data with respect to time. The curve so obtained is almost flat, which assures the accuracy and shows the THERMOD is in rest mode.

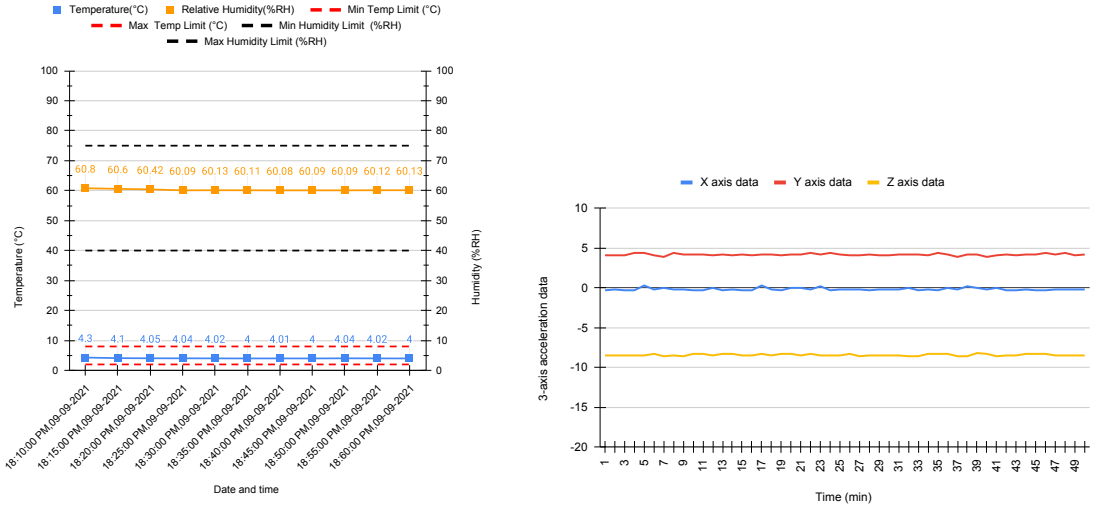

(a) (b)

Figure 4.4: (a) Retrieved temperature & relative humidity pdf data, (b) retrieved accelerometer pdf data plot.

4.4.2 Cost Comparison

The existing temperature & humidity data loggers are based on general purpose development boards, i.e., microcontroller development boards, and breakout boards, i.e., temperature & humidity sensor, memory/SD card and RTC modules, hence possessing redundant hardware and consequently higher cost. In contrast, the proposed THERMOD is designed using integrated chips directly that avoids redundancy and, at the same time, possesses low cost. Besides, the cost is reduced further by a selection of ICs with optimum specifications. For example, the MCU with a required number of GPIO's, SPI, and I2C interfaces in addition to a crystal less USB interface, which cuts external circuitry cost, and the temperature sensor with only the I2C interface and flash memory with the SPI interface. Furthermore, the reduced power circuitry with less number of components altogether reduces the cost of the proposed THERMOD. Moreover, Table 4.3 includes the approximate cost of the main components used in the temperature & humidity data loggers. However, from Table 4.3, it can be seen that the proposed THERMOD is much

more efficient than the existing systems to date.

Table 4.3: Cost comparison of the state of the art and the proposed THERMOD.

Reference	**Components**	**Features**	**Cost ($)**
[93]	CY8C29566 DS18B20 DHT22	Temperature Humidity	54.40
[61]	Arduino Uno LM35 MicroSD shield	Temperature	224
[62]	Arduino Pro Mini DS18B20 MicroSD card DS3231 RTC	Temperature	34
Proposed	STM32L412 SHT40 W25Q16 LIS3DH	Temperature Humidity 3D Accelerometer	5

4.4.3 Effective Power Utilization

The THERMOD is a standalone battery operated device, hence power optimization is essential. Unlike existing solutions, STM32L412KB MCU assures effective power utilization, availing one of the available power saving modes. While measurements, the following observations have been made:

- The THERMOD enters in run mode once the logging starts and consumes 34µA/MHz.
- After data logging, the device enters in standby mode and consumes 105nA with wake up time of 16.1µsec.
- Finally, once the pdf is generated, MCU goes back to shutdown mode. The current consumption is 16nA with wake up time of 256µsec.

The THERMOD can be wake up from shutdown and standby mode with an interrupt on the GPIO pin.
Further, in the existing systems, the sensors are powered directly by the power supply. Due to the continuous power supply, sensors consume few µA's of current even in the sleep mode. We have found two solutions for this. First, the sensors can be powered directly from GPIO pins, as GPIO pins can source a maximum of 20mA current. Second, if the sensor current requirement exceeds 20mA, a MOSFET can be used as a switch, which will disconnect the power supply and will save a few µA's of current. Besides this, we have utilized the following to save more power.

- The current consumption of MCU in run mode is dependent on clock frequency. Except memory, all sensors can run on low clock frequency. So, we have reduced the clock frequency in standby and run mode to 16MHz except when memory is used, which requires 80MHz.

4.4.4 Battery Life Calculation

The experimental setup shown in Figure 4.5 is used to evaluate the battery performance matrices of the proposed THERMOD. In particular, Figure 4.5a shows the device connection with a digital multimeter for current measurement, while the current consumption waveform for sleep and active modes is shown in Figure 4.5b where the peak and horizontal line represents the active and sleep mode currents respectively. Note the Figure 4.5b is the zoomed version of Figure 4.5a. Furthermore, the battery life can be calculated by summing up the current contribution of the THERMOD in active and sleep modes with respect to time duration. The current waveform in Figure 4.5b has two peaks, i.e., the first peak occurs when MCU enters active mode and activates the peripherals like GPIO, I2C, and SPI. Once the peripherals are activated, the MCU goes back to standby mode, shown by dip in Figure 4.5b, hence further reduction in current consumption, whereas the second peak is obtained when the data is transmitted from MCU and is stored in memory.

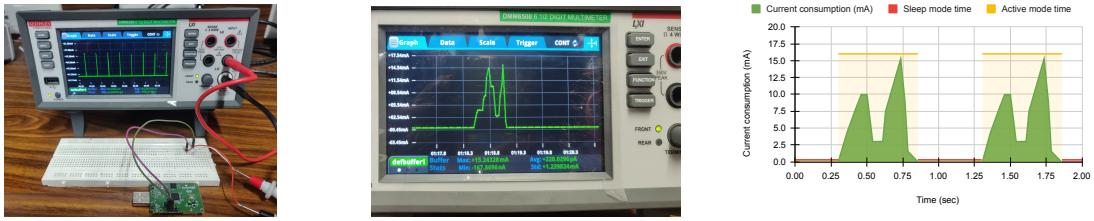

(a) (b) (c)

Figure 4.5: Experimental setup for THERMOD battery life evaluation: (a) experimental setup for current consumption evaluation, (b) current consumption waveform for sleep and active mode, (c) current consumption plot for sleep and active mode.

Moreover, the power rating measurements lead to the following observations:

- The device consumes 1uA in sleep mode and 6mA average current for 0.45sec in data logging mode with a peak of 15.3mA as shown in Figure 4.5c.

- Accordingly, the device can operate for approximately 4.6 years on a single coin cell with 220mAh battery capacity.

Since the vaccines like Moderna and Pfizer have refrigerated storage (2°C to 8°C) up to 30 days, hence, to achieve the re-usability of the device, the battery life of the THERMOD design has been optimized and can last for 4.6 years. Accordingly, once a lot of vaccine is delivered and consumed, the same device can be used to monitor another lot of vaccines.

4.4.4.1 Maximum Battery Life

The active and sleep mode current contribution is calculated as follows:

$$\begin{aligned} Q_{Active}^{Device} &= I_{Active} \times T_{Active} \\ &= 6 \times 0.45 \\ &= 2.7mAs \end{aligned} \tag{4.1}$$

where Q_{Active}^{Device} is the current contribution of the device in active mode.

$$\begin{aligned} Q_{Sleep}^{Device} &= I_{Sleep} \times T_{Sleep} \\ &= 0.001 \times 599.55 \\ &= 0.599mAs \end{aligned} \tag{4.2}$$

where Q_{Sleep}^{Device} is the current contribution of the device in sleep mode.

Now, the average current consumption of the device during 10min interval can be calculated as:

$$\begin{aligned} I_{Average}^{Device} &= \frac{Q_{Active}^{Device} + Q_{Sleep}^{Device}}{T} \\ &= \frac{2.7mAs + 0.599mAs}{600s} \\ &= 5.499 \times 10^{-3}mA \end{aligned} \tag{4.3}$$

where $I_{Average}^{Device}$ is the average current consumption of the device and T is the logging interval.

The battery life of the device can be calculated as:

$$\begin{aligned} N_{Days}^{Total} &= \frac{Q_B}{I_{Average}^{Device}} \\ &= \frac{220mAh}{5.499 \times 10^{-3}mA} \\ &= 4000.455hrs \\ &\approx 1666days \\ &\approx 4.6years \end{aligned} \tag{4.4}$$

where N_{Days}^{Total} is the total number of days the THERMOD can operate and Q_B is the total battery capacity in mAh.

4.4.4.2 Maximum Number of Logs

The maximum number of logs the device can store can be calculated as follows:

$$\begin{aligned} I_{OneLog}^{Total} &= Q_{Active}^{Device} + Q_{Sleep}^{Device} \\ &= 2.7mAs + 0.599mAs \\ &= 3.299mAs \end{aligned} \tag{4.5}$$

where I_{OneLog}^{Total} is the total current contribution required for one log with a 10minute interval.
Now, the total number of logs can be given by the following equation:

$$\begin{aligned} N_{Logs}^{Total} &= \frac{Q_B}{I_{onelog}} \\ &= \frac{220mAh}{3.299mAs} \\ &\approx 240000 \end{aligned} \tag{4.6}$$

where, N_{Logs}^{Total} is total number of logs the THERMOD can log with 220mAh CR2032 coin cell battery and I_{onelog} is the average current contribution required for one log.

4.5 Applications

The proposed reusable THERMOD is not limited to COVID-19 vaccines but can also be used in various applications, including:

4.5.1 Foods, Beverages, Dairy, and Meat Transportation

The perishable food items like milk, eggs, meat, fish, poultry, fruits, and green leafy vegetables should be kept out of the danger zone (5°C to 63°C) as per Food Safety and Standards Authority of India (FSSAI). The microorganisms multiply themselves by a process known as the binary fission process and become dormant below 5°C above 63°C. Hence, the perishable food items are refrigerated below 5°C, and thus, the monitoring required during transport can be fulfilled by THERMOD.

4.5.2 Vaccines and Pharmaceuticals Transportation

Vaccines and pharmaceuticals are the key components for the prevention of diseases. It is important that they are precisely handled and are kept at accurate temperatures. THERMOD is configurable and allows you to take readings at particular intervals for a complete overview.

4.5.3 Chemical and Paints Transportation

The chemicals, epoxy, and varnishes are temperature sensitive products. If these products are kept outside the temperature range, they get degraded and sometimes reduce their shelf lives. The THERMOD can record the temperature, thus allowing us to model the degradation.

4.5.4 Environmental Monitoring

The THERMOD can be taken to diverse locations that cannot easily support fixed temperature monitoring equipment. They can be mountains, deserts, jungles, mines, ice flows, caves, etc.

4.6 Conclusion

This chapter proposes a battery life enhancement strategy through optimal design and efficient hardware utilization. The proposed methodology has been investigated on a cold chain monitoring application. In this regard, first, we have designed and developed an integrated sensing and logging solution addressing general issues like cost, size, and data accuracy. Thereafter, the proposed strategy has been applied for enhancing energy efficiency and achieving a longer battery life. It involves (a) utilizing GPIOs to power sensors and (b) optimizing controller clock configuration. As a result, the proposed sensing device (THERMOD) can operate continuously for 4.6 years with a maximum log count of 240000 on a 220mAH coin cell battery, outperforming the state of the art solutions.

Chapter 5

Battery Life Enhancement Through Hardware Miniaturization

Generally, battery replacement in IoT applications deployed at remote sites is difficult, expensive, and sometimes impractical. Hence, these solutions must possess higher energy efficiency to achieve longer battery life. Therefore, in this chapter, we proposed a battery life enhancement strategy through hardware miniaturization. Among the IoT applications mentioned and discussed in Chapter 1, one of the crucial water quality monitoring IoT use case from the smart farming domain, requiring higher energy efficiency, has been considered for energy efficiency analysis, evaluation, and enhancement. To begin with, we first identified the general issues in existing water quality monitoring solutions, followed by investigating the major factors reducing energy efficiency and, consequently, reducing the overall battery life of the device. Among the general issues, it is found that most of the existing solutions are based on general purpose microcontroller boards and sensor breakout boards, which affect accuracy, increase size and cost, and use conventional cellular technologies (2G/3G/4G/5G) whose performance varies with local connectivity and requires more energy. Besides, it is observed that existing solutions utilize GPS for real time location estimation even when high accuracy is not desired or high errors in real time locations can be tolerated. Since it is a known fact that GPS requires a significant energy budget for its operation, hence affects overall battery life significantly [63]. This issue is identified as the root factor causing significant degradation in energy efficiency, thereby affecting and reducing the battery life significantly. To address the aforementioned issues, we first designed, developed, and validated the LoRa based integrated sensing and localization solution called TEMPSENSE (Tds (total dissolved solids), Ec (electrical conductivity), teMperature, pH (potential of hydrogen) monitoring SystEm with integrated localizatioN Solution), addressing the general issues including data accuracy, size, and cost. Further, the proposed TEMPSENSE replaces the GPS completely with the RSSI based localization algorithm running at the gateway facilitating the real time location at much lower energy budget, this as a result increases energy efficiency significantly and hence leading to a longer battery life. A brief review of existing works and their shortcomings, as well as how our proposed work differs from the existing works, is introduced below.

5.0.1 Related Work and Motivation

Water quality monitoring and related transmission have gained significant research spotlight. For instance, the authors in [63] and [96], have focused on the sensing performance targeting data quality, data gathering, and intelligent data analysis. Likewise, the authors in [97] have utilized data driven approach for predicting urban water quality. On the other hand, some existing works solely focused on energy efficiency and cost of the developed solutions. For instance, the authors in [98], utilized deep neural networks (DNN) to propose an energy efficient water quality monitoring system. While, the authors in [99], have developed a low cost water quality monitoring system which also includes the development of nitrates, phosphates sensors. However, the aforementioned methods seem under optimized, especially in this modern era with a quite impressive sensing and communication techniques. For instance, [100] is pillared on the terrestrial network, while [63] and [96] are based on GPS, and hence suffer from low reliability and energy inefficiency. On the other hand, though few existing solutions, like [98, 99, 101], are based on energy efficient platforms like LoRa, none of them provide real time location information of the water quality monitoring device. Since the real time location of the water quality monitoring device plays a critical role in corrective actions, locating the water quality monitoring device is becoming essential, especially in the upcoming high density sensor environments.

Indeed, satellite based GPS solutions have revolutionized outdoor navigation and positioning. However, GPS based solutions suffer from higher energy consumption [102] and require line of sight (LoS) between sensor node and GPS satellite, which is the critical limitation in their implementation. Moreover, some existing works revealed the fact that the LPWAN can also be utilized for localization, however their implementation methods are still underway and have numerous limitations [103, 104, 105, 102]. For instance, angle of arrival (AoA) techniques use an antenna array to determine the angle of arrival at the receiver [106, 107, 108]. However, the angle calculation involves complex hardware and calibration. Also, for larger distances, small errors in angle estimation are translated to huge distance estimation errors [109]. Whereas, in time of arrival (ToA), distances are measured based on the time that the transmitted signal takes to arrive at the receiver [110, 109, 107]. Likewise, in time difference of arrival (TDoA), distance measurement is based on the difference in propagation times of two different signals. Again, time based techniques require accurate synchronization of clocks [109]. Besides, they also require line of sight between transmitter and receiver along with large bandwidth and sampling rates for better resolution [109, 108]. Similarly, fingerprinting requires obtaining RSSI fingerprints at fixed locations before deploying the system. Nevertheless, it can yield accurate results, but the fingerprint map needs to be rebuilt if there is any change in the environment [109].

In this chapter, we have addressed the aforementioned challenges by proposing the TEMPSENSE: *a)* an integrated sensing & localization solution. To the best of our knowledge, integrated sensing & localization solution and their study have not yet been

presented to date, especially from the purview of noncellular based solutions. *b)* a hardware design has been formulated within the institution lab along with test results. Further, it is shown that the hardware of the proposed TEMPSENSE is significantly inexpensive as compared to the available industrial solutions. Furthermore, the results of the extensive experiments conducted in high and low density scenarios show that the proposed algorithm is better than the existing solutions in terms of cost effectiveness, localization accuracy, and energy efficiency.

5.1 Contribution

Specifically, the contribution of this work can be summarized as:

- An integrated energy efficient and cost effective hardware for sensing & localization, along with assured data accuracy, provided by a selection of application specific low noise and low tolerance discrete passive components.
- Further, extensive efforts have been made towards real time location estimation of the proposed TEMPSENSE using RSSI based localization algorithm. Moreover, the estimated real time location obtained after experimentation is close to the true location, which shows that the proposed TEMPSENSE can replace existing GPS based location solutions and can estimate real time location precisely and more energy efficiently.
- Efficient power/chip area utilization with IC only integration of controllers and related sensing units to achieve cost and energy efficiency, which is a critical bottleneck in the implementation of the existing solutions.
- Extensive real time experiments have been conducted on different types of samples including river water to validate the realization of TEMPSENSE. Moreover, the experimental data obtained after sensing proves the accuracy of the proposed TEMPSENSE. However, in existing works, no real time experiments have been conducted.

5.2 System Model

The proposed integrated sensing and localization solution primarily consists of a sensing node (TEMPSENSE hardware), LoRa gateway, and a server, as shown in Figure 5.1. The proposed TEMPSENSE senses and transmits the crucial water quality parameters, i.e., pH, temperature, TDS, and EC, to the LoRa gateway. The LoRa gateway receives the sensor data and also makes a note of the RSSI value of the signal received at the gateway. These RSSI values are then fed to the localization algorithm running in the gateway. The LoRa gateway then transmits the sensor data and the location of the sensing node (TEMPSENSE) to the server. The end user can access the data from this server. The

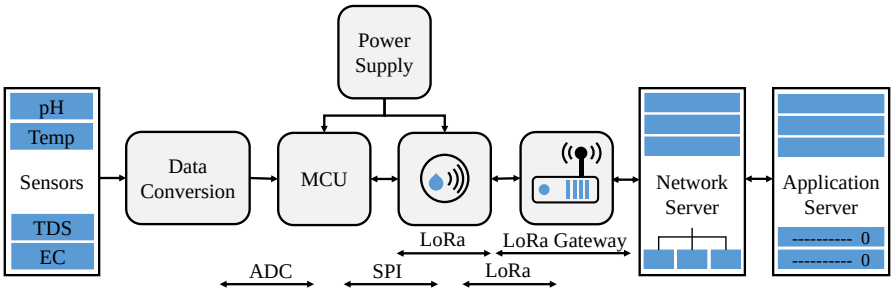

Figure 5.1: The architecture of the proposed system.

sensing node design, overview of sensing and communication, localization algorithm, and experimental setup are discussed in the subsequent sections.

5.2.1 Sensor Node Design

The hardware of the proposed TEMPSENSE mainly consists of a power supply, microcontroller, LoRa module, and different water quality monitoring sensors, i.e., pH, temperature, TDS, and EC as shown in Figure 5.2b and Figure 5.2c. Whereas the Figure 5.2a and Figure 5.2b show the hardware differences between state of the art and proposed integrated sensing and localization solutions. The key components of the

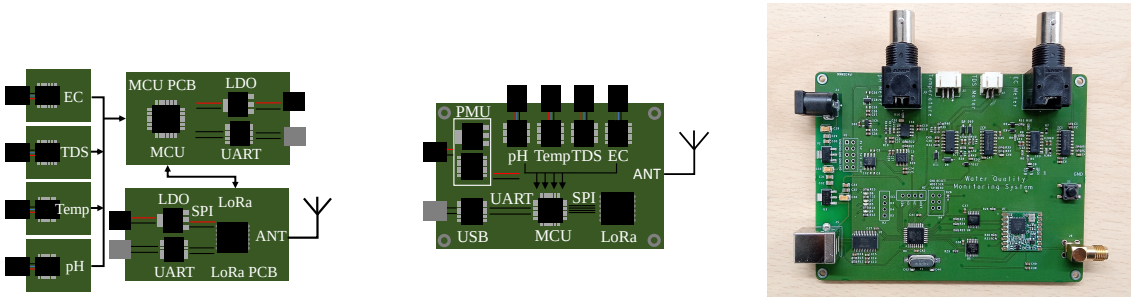

(a) (b) (c)

Figure 5.2: Illustration of the hardware differences between state of the art and the proposed integrated sensing & localization solution: (a) state of the art solutions, (b) proposed solution, (c) TEMPSENSE hardware.

proposed TEMPSENSE are described below as:

Power supply: The device operates at 3.3 V. Hence a buck-boost voltage regulator (i.e., a regulator which can increase and decrease voltage based on the required output voltage), with 3.3 V output voltage, is used. In addition to the battery, the device also has the provision of solar panel incorporation, and hence, the device can also utilize solar power.

- **Microcontroller:** The device utilizes Atmel's 8 bit microcontroller labeled as atmega328P-AU. The microcontroller has 32 kilobyte (32 KB) flash memory. The code running in the microcontroller is stored in flash memory. The incorporated

microcontroller has various interfaces, i.e., I2C, SPI, universal asynchronous receiver transmitter (UART), universal synchronous and asynchronous receiver transmitter (USART), and 2 Wire. The microcontroller and LoRa module utilize SPI to interface the LoRa module to the microcontroller.

- **LoRa:** The device utilizes the RFM95W LoRa module by HopeRF. RFM95W incorporates Sx1276 LoRa transceiver by Semtech. It supports various modulations, including minimum shift keying (MSK), gaussian minimum shift keying (GMSK), frequency shift keying (FSK), gaussian frequency shift keying (GFSK), on off keying (OOK), and LoRa. The LoRa module facilitates the transmission of data received from different sensors to the LoRa gateway.

- **LoRa Gateway:** The experiments were performed on the RAK7258 indoor and RAK7249 outdoor gateway by RAK Wireless. The LoRa gateway has multiple connectivity options, i.e., local area network (LAN), WiFi, and long term evolution (LTE) for cloud connectivity. The LoRa gateway mainly incorporates two chips i.e., Sx1301 and Sx1257 by Semtech. Sx1301 is used for digital signal processing, while Sx1257 is the RF front end and is used for modulation/demodulation.

- **Antenna:** The device is equipped with an external dipole antenna. The dipole antenna operates in the industrial scientific and medical (ISM) band, i.e., at 865 MHz (860-880 MHz). It has an omnidirectional radiation pattern with 2 dBi gain.

- **Temperature:** The temperature sensor is based on a negative temperature coefficient of resistance, i.e., the resistance decreases as the temperature increases. This temperature sensor can be used in the temperature range -55 °C $\sim$ 125 °C to provide -10 °C to +85 °C temperature detection with an accuracy of $\pm$0.5 °C. The temperature is calculated using the following equation known as parameter equation which is derived from Steinhart–Hart equation.

$$\beta = \frac{T2 \times T1}{T2 - T1} ln\left(\frac{R1}{R2}\right) \tag{5.1}$$

  where β defines the variation of resistance with temperature, T1 and T2 are temperatures in K. R1 and R2 are the resistances at temperature T1 and T2 respectively.

- **pH:** pH is also called the hydrogen ion concentration index. It is a measure of hydrogen ion concentration in a solution. Usually, the pH is a number between 0 and 14, where a pH=7 means the solution is neutral, a pH<7 means the solution is acidic, and a pH>7 means the solution is alkaline. Prior to the measurements, the sensor probe is calibrated using pH 4.0 and pH 7.0 standard buffer solution.

- **TDS:** TDS indicates how many milligrams of soluble solids are dissolved in one liter of water. In general, the higher the TDS value, the more soluble solids are dissolved

in water, and the less clean the water is. The probe is calibrated using a standard 707 ppm buffer solution.

- **Electrical Conductivity:** An electrical conductivity sensor helps measure impurities. The impurities can be dissolved substances, chemicals, and minerals. The higher the amount of these impurities, the higher the conductivity. The EC probe is calibrated using a standard buffer solution of 12.88 ms/cm.

5.2.2 Sensor Node Working

Pressing the switch for 5s activates the TEMPSENSE. On successful activation, the TEMPSESNE sensors are dipped in river water as shown in Figure 5.3a. The sensed data is then transmitted to the LoRa gateway installed at the river site as shown in Figure 5.3b. The data received at the LoRa gateway can be seen on the TEMPSENSE website, as shown in Figure 5.3c.

(a) (b) (c)

Figure 5.3: Experimental setup of integrated sensing & localization solution: (a) sensors dipped in water, (b) LoRa gateway, (c) sensor data on TEMPSENSE website (fetched from TTN server).

5.2.3 Overview of RSSI Based Localization

Localization refers to the process of determining either the relative (proximity) or exact (positioning) position of an asset/person in a given environment. Proximity solutions require only one gateway, whereas inferring the location of a node requires multiple gateways.

The distance of the sensor node from a gateway is determined using the RSSI values received at the gateway. Log distance path loss model gives the RSSI $P(d)$ as a function of distance, as described by (5.2) [111].

$$P(d) = C - 10nlog_{10}(\frac{d}{d_0}) + X \tag{5.2}$$

d is the distance between transmitter and receiver, d_0 is the reference distance, C is the average RSSI at the reference distance d_0, n is the path loss exponent which depends on the environment, and X is a zero-mean Gaussian random variable which accounts for shadowing. When $P(d)$ is known, distance d is estimated using (5.3).

$$d = 10^{\left(\frac{C-P(d)}{10n}\right)} \tag{5.3}$$

Further, based on these estimated distance values, the location of the reference node can be estimated using trilateration, as shown in Figure 5.4. In Figure 5.4, a two dimensional network having a target node with an unknown coordinate (x_t, y_t) and a set of gateways nodes ($\mathbf{x}^{\Gamma}$, $\mathbf{y}^{\Gamma}$) is considered.

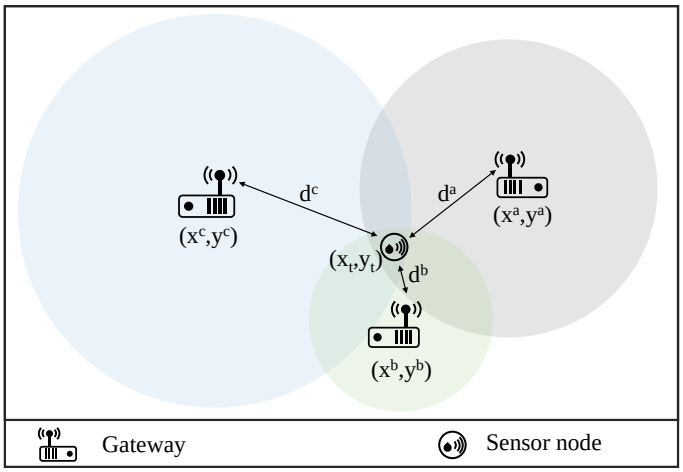

Figure 5.4: Illustration of trilateration for the estimation of the real time location of the proposed TEMPSENSE.

5.3 Experimental Setup for Localization

The experimental setup for RSSI based localization is shown in this section. Experiments were carried out in two different scenarios, i.e., *i)* Low density scenario: Inside IIT Ropar Campus, and *ii)* High density scenario: At Satluj River Barrage. We have opted for RSSI based technique for distance estimation as it does not require any extra hardware, is cost effective, and is energy efficient [102, 109] in comparison to existing techniques. Since the RSSI values are affected by multipath fading [109, 112], hence large fluctuations in RSSI values are observed at a fixed distance from the transmitter. These fluctuations can be controlled using filtering techniques. Unlike the existing solutions, we have filtered RSSI values received at gateways prior to the distance estimation using the Kalman filter. In this chapter, first, we have estimated the distance of the sensor node from three gateways based on RSSI values by using the log distance path loss model. Later, trilateration was performed using the estimated distances to determine the position of the sensor node.

5.3.1 Kalman Filter

Noisy RSSI measurements were filtered using a Kalman filter. Considering that multiple RSSI values are recorded at any fixed location, the true RSSI value at each timestamp is unknown, while all we have is the noisy measurements. Since both the gateway and sensor node are static, it is expected that the RSSI values collected at a fixed location do

not vary with time. However, there is some process noise due to phenomena like fading, reflection, and diffraction, which bring about RSSI fluctuations. Thus, we model the RSSI estimation problem as a one dimensional Kalman filter using the following equations:

$$s_k = s_{k-1} + w;$$

$$z_k = s_k + v$$

where

$$w \sim \mathcal{N}(0, Q)$$

$$v \sim \mathcal{N}(0, R)$$

s_k and z_k represent the true state and measurement, respectively, at k^{th} timestamp. w and v represent process and measurement noise, respectively. R and Q are the measurement noise and process noise variance respectively, which are kept constant for all timestamps.

5.3.2 Kalman Filter Algorithm

Algorithm 5 covers the 1D Kalman filter process. ${P_k}^-$ and P_k are the a-priori and a-posteriori estimate error variances and are given by (5.4) and (5.5) respectively. $\hat{s}_k^-$ is the a-priori state estimate, and $\hat{s}_k$ is the a-posteriori state estimate. The predict step gives the a-priori estimates for estimate error variance and state without seeing the measurement z_k. The update step calculates the final a-posteriori state estimate by inculcating the measurement at the k^{th} timestamp. Kalman gain K_k allocates a weight value which decides whether $\hat{s}_k^-$ or z_k should be trusted more for giving the final state estimate $\hat{s}_k$.

Algorithm 5 Covariance matching based 1D Kalman filter

Initialize x_0, P_0, Q, R

for k= 1 to N:

Predict equations:

$\hat{s}_k^- = \hat{s}_{k-1}$

${P_k}^- = P_{k-1} + Q$

Update equations:

$K_k = \frac{{P_k}^-}{{P_k}^- + R}$

$\hat{s}_k = \hat{s}_k^- + K_k(z_k - \hat{s}_k^-)$

$P_k = (1 - K_k){P_k}^-$

$$P_k = E[(s_k - \hat{s}_k)^2] \tag{5.4}$$

$${P_k}^- = E[(s_k - \hat{s}_k^-)^2] \tag{5.5}$$

Through trial and error, the initial parameters were set to $x_0 = 0$, $P_0 = 10$, $Q = 0.1$ and $R = 10^3$.

5.3.3 Experimental Setup for Low-density Scenario: Inside IIT Ropar Campus

5.3.3.1 Path Loss Model Parameters

2000 RSSI values were collected by moving the device away from the gateway at intervals of 0.2 m up to a distance of 10 m. Beyond 10 m, the interval was increased to 1 m, and a total distance of 30 m was covered and is represented by the area around location PL, shown in Figure 5.5a. Average RSSI was obtained at each location, and least squares based curve fitting was applied as shown in Figure 5.5b. C and n values were estimated as -79.68 dBm and 1.364, respectively.

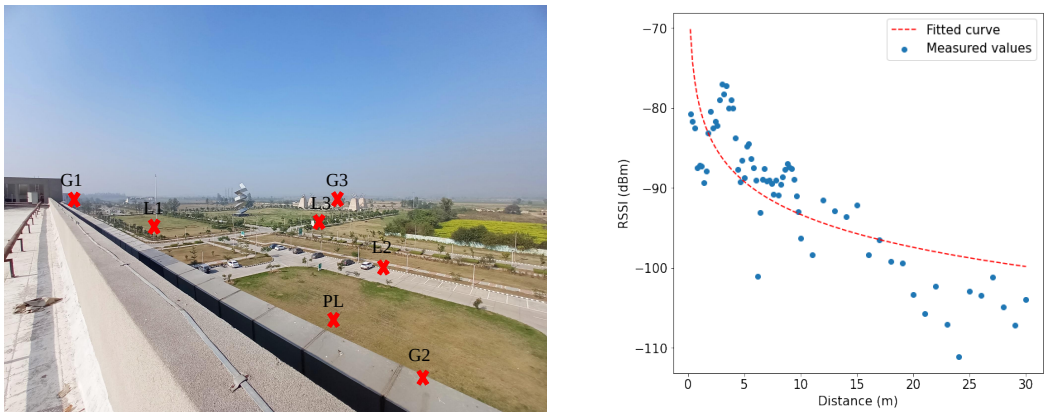

(a) (b)

Figure 5.5: (a) Gateway positioning inside IIT Ropar campus for the low density indoor scenario, (b) curve fitting for low density indoor scenario.

5.3.3.2 Trilateration

For simplicity and better interpretability, equivalent cartesian coordinates were created based on the GPS locations of the device and three gateways as depicted in Figure 5.6, where L1, L2, L3 are the three device locations, and G1, G2, G3 indicate the fixed positions of the three gateways. The coordinates highlighted in red are the GPS coordinates, while those in black are their equivalent cartesian coordinates.

The distances estimated using averaging, histogram approximation [113], and Kalman filter have been summarized in Table 5.1. 2000 RSSI readings were collected at each gateway, to which averaging, histogram approximation, and Kalman filter were applied. Trilateration was applied using the distance values obtained from Table 5.1. Table 5.2 shows the predicted device positions and corresponding positioning errors. Mean errors of 7.1 m, 13.7 m, 10 m, and 8.2 m were observed using the GPS, averaging, histogram approximation, and Kalman filter technique, respectively. Kalman filter improved the positioning accuracy for all three device locations and also yielded a smaller mean error than the averaging and histogram approximation technique.

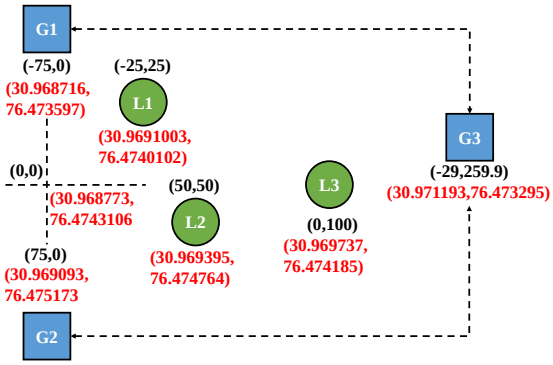

Figure 5.6: Cartesian and GPS coordinates for the device and gateway locations: Low density indoor scenario.

Table 5.1: True and estimated distance values (in meters) between the three gateways and three device locations (low density indoor scenario).

Device	Gateway	Distance (m)				
		True	GPS	Average	Hist.	Kalman
L1	G1	55.9	58.1	54.9	54.0	53.1
	G2	103.0	111.1	91.6	97.2	96.7
	G3	234.9	241.9	212.3	219.6	224.1
L2	G1	134.6	134.5	121.7	122.7	130.1
	G2	55.9	51.5	55.8	51.8	55.9
	G3	224.3	243.8	199.3	202.7	213.6
L3	G1	125	126.4	72.2	96.3	107.4
	G2	125	118.4	87.7	100.4	106.5
	G3	162.6	182.4	93.1	126.2	126.4

Table 5.2: Estimated position and positioning error for the three device locations (low density indoor scenario).

Device	Position (cartesian coordinates)					Error (m)			
	True	GPS	Average	Hist.	Kalman	GPS	Average	Hist.	Kalman
L1	(-25.0, 25.0)	(-20.2, 19.8)	(-17.9, 43.0)	(-21.7, 37.4)	(-21.8, 33.4)	7.1	16.5	12.0	7.8
L2	(50.0, 50.0)	(46.8, 55.2)	(38.9, 65.9)	(41.2, 63.4)	(-46.0, 57.4)	6.1	11.5	10.1	6.3
L3	(0.0, 100.0)	(-5.3, 93.6)	(-8.2, 115.6)	(-2.7, 108.4)	(0.6, 110.6)	8.3	13.2	8.0	10.6

5.3.4 Experimental Setup for the high density scenario: At Satluj River Barrage

Localization performance was evaluated through experimentation using three gateways at the riverside, as shown in Figure 5.7a. Trilateration was performed to infer the

position of the TEMPSENSE at three different locations shown in Figure 5.8. Averaging, histogram approximation, and Kalman filter were used to filter the RSSI values, followed by trilateration for the aforementioned filtering schemes.

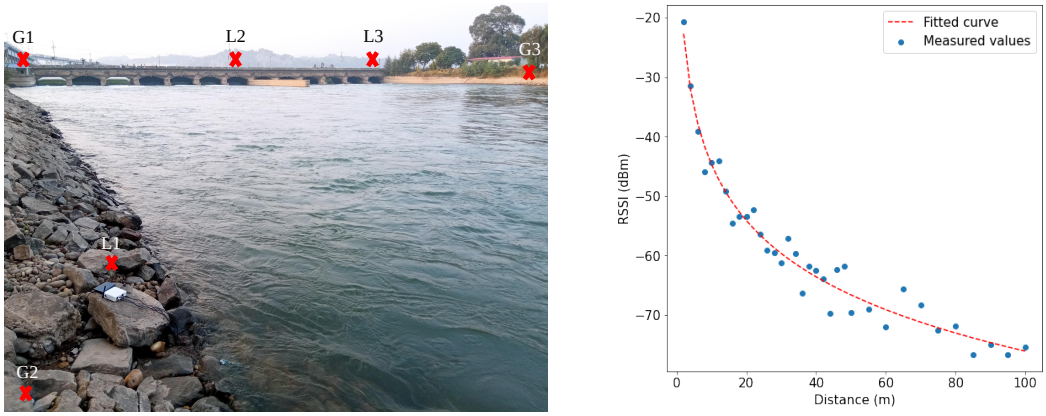

(a) (b)

Figure 5.7: (a) Experimental setup for data acquisition and device positioning at river, (b) curve fitting for high density outdoor scenario.

5.3.4.1 Path Loss Model Parameters

The path loss parameters C and n for the Satluj River Barrage were estimated using least squares based curve fitting applied to averaged RSSI values collected at the riverside, which had trees on one side. RSSI values were collected from the sensor node by moving it away from the gateway in intervals of 2 m up to a distance of 50 m. Beyond 50 m, the interval was increased to 5 m, and a total distance of 100 m was covered. 2000 RSSI values were collected at each location. The C value was estimated to be -12.805 dBm for d_0=1 m, and the n value was estimated to be 2.769. The path loss exponent curve so obtained has been shown in Figure 5.7b.

5.3.4.2 Trilateration

For simplicity and better interpretability, equivalent cartesian coordinates were created based on the GPS locations of the device and three gateways as depicted in Figure 5.8, where L1, L2, L3 are the three device locations, and G1, G2, G3 indicate the fixed positions of the three gateways. The coordinates highlighted in red are the GPS coordinates, while those in black are their equivalent cartesian coordinates.

The distances estimated using averaging, histogram approximation, and Kalman filter have been summarized in Table 5.3. 2000 RSSI readings were collected at each gateway, to which averaging, histogram approximation, and Kalman filter was applied. Trilateration were applied using the distance values obtained in Table 5.3.

Table 5.4 shows the predicted device positions and corresponding positioning errors. Mean errors of 7.1 m, 13.6 m, 11.4 m, and 9.4 m were observed using the GPS, averaging, histogram approximation, and Kalman filter technique, respectively. Kalman

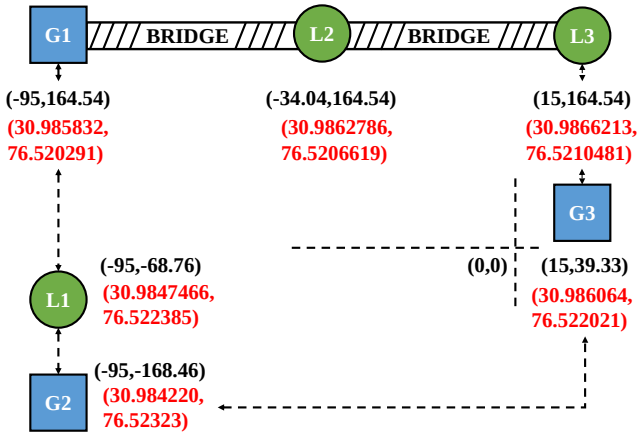

Figure 5.8: Cartesian and GPS coordinates for the device and gateway locations: high density scenario.

Table 5.3: True and estimated distance values (in meters) between the three gateways and three device locations (high density outdoor scenario).

Device	Gateway	Distance (m)				
		True	GPS	Average	Hist.	Kalman
L1	G1	233.3	105.2	226.6	230.4	238.0
	G2	99.7	105.2	90.9	97.2	107.4
	G3	154.2	160.4	152.9	144.3	154.2
L2	G1	60.9	64.9	58.0	54.3	54.9
	G2	338.5	351.9	323.4	302.6	330.2
	G3	134.5	140.7	124.2	125.8	133.3
L3	G1	110.0	115.5	83.9	84.0	110.1
	G2	350.7	364.1	268.8	271.1	371.7
	G3	125.2	130.8	95.2	94.4	125.2

filter improved the positioning accuracy for all three device locations and also yielded a smaller mean error than the averaging and histogram approximation technique.

Table 5.4: Estimated position and positioning error for the three device locations (high density outdoor scenario).

Device	Position (cartesian coordinates)					Error (m)			
	True	GPS	Average.	Hist.	Kalman	GPS	Average	Hist.	Kalman
L1	(-95.0, -68.7)	(-101.3, -75.3)	(-104.8, -66.6)	(-86.1, -67.5)	(-85.9, -69.7)	9.1	9.6	8.7	8.9
L2	(-34.0, 164.5)	(-29.8, 169.1)	(-40.1, 150.1)	(-65.4, 131.1)	(-44.2, 157.2)	6.2	13.2	11.7	7.0
L3	(15.0, 164.5)	(-19.1, 169.1)	(-55.9, 95.9)	(-53.2, 97.7)	(40.9, 187.3)	6.2	18.1	13.9	12.3

5.4 Results and Discussion

5.5 Results and Discussion

In this section, the accuracy of the sensed data and localization, cost comparison of the proposed solution with state of the art solutions, and battery life evaluation are discussed.

5.5.1 Sensed Data Accuracy

Considering the output of pH, temperature, TDS, and EC sensors, which varies from millivolt to a few volts, the hardware of the proposed TEMPSENSE is designed with low tolerance and low noise passive components in addition to the recommended layout for power supply and mixed signals. This, in turn, ensures the accuracy of the acquired data. Moreover, the sensors are calibrated with standard solutions prior to measurements. Several experiments were performed on different samples containing normal water, river water, orange water, and biscuit solution as shown in Figure 5.9a and Figure 5.9b respectively. Further, experimental data obtained in Table 5.5 is in good agreement with

(a) (b)

Figure 5.9: Experimental setup of for sensed data accuracy evaluation: (a) design validation and testing with different solutions, (b) setup for river water sensing.

the practical values. For instance, while measuring normal water, we obtained pH values of 7.01 and 7.06 using TEMPSENSE and a reference sensor. This altogether ensures the accuracy of the proposed TEMPSENSE.

5.5.2 Localization Accuracy in Low and High density Scenarios

Since the water quality monitoring systems are typically deployed at remote river sites, so the requirement of a low cost and energy efficient solution for real time location is addressed by the proposed TEMPSENSE that replaces the GPS with the RSSI based algorithm and hence demands low energy. Moreover, the localization data so obtained from the experiments conducted for different scenarios is in good agreement with the true locations. For instance, the mean errors of 7.1 m, 13.7 m, 10 m, and 8.2 m were observed using the GPS, averaging, histogram approximation, and Kalman filter technique for low density indoor scenario. In contrast, the mean errors of 7.1 m, 13.6 m, 11.4 m, and 9.4

Table 5.5: Water quality parameter measurement for different samples.

Sample type	Parameters calculated			
	pH	**Temp (°C)**	**TDS (ppm)**	**EC (ms/cm)**
Orange water	6.38	29.5	252	0.26
	6.35	29.40	251	0.25
	6.38	29.60	254	0.28
	6.4	29.50	253	0.30
Biscuit water	6.81	28.85	650	1.61
	6.88	29.80	651	1.90
	6.86	29.60	657	1.85
	6.85	29.70	655	1.88
Normal water	7.01	28.50	104.8	0.24
	6.90	28.60	104.6	0.20
	7.02	27.90	104.9	0.25
	7.10	28.40	105.1	0.23
River Water	6.78	18.10	137.7	0.61
	6.70	17.80	137.2	0.65
	6.75	17.90	136.8	0.67
	6.72	18.20	137.3	0.66

m were observed using the GPS, averaging, histogram approximation, and Kalman filter technique for high density outdoor scenario. This altogether ensures that the proposed TEMPSENSE can estimate real time location precisely, cost, and energy efficiently.

5.5.3 Cost Comparison

From Figure 5.2a, it can be seen that state of the art solutions are designed mostly using modules i.e., pH, temperature, TDS and EC, and development boards i.e., power supply, microcontroller, and LoRa board, hence posses the redundant hardware. While the proposed TEMPSENSE is designed using dedicated integrated chips (can be seen from Figure 5.2b) that avoid redundancy and, at the same time, possess low cost. Moreover, Table 5.6 includes the approximate cost of the main components used in the water quality monitoring systems. Apart from pH, TDS, temperature, and EC, some of the existing solutions measure additional parameters. Hence, to get a better cost comparison, the cost of additional sensors is not considered. However, from Table 5.6, it can be seen that the proposed TEMPSENSE is much more cost efficient than the existing systems to date.

5.5.4 Battery Life Calculation

The experimental setup shown in Figure 5.10, is used to evaluate the battery performance of the proposed TEMPSENSE. In particular, Figure 5.10a, shows the device connection with digital multi-meter for current measurement, while the current consumption waveform for sleep and active modes are shown in Figure 5.10b, where the peak and the horizontal line represent the active and sleep mode currents respectively. The battery

Table 5.6: Cost, performance, and localization accuracy comparison of state of the art and the proposed integrated sensing & localization solution.

Ref.	**Tech.**	**Parameters**	**Data accuracy**	**Positioning accuracy (m)**	**Cost ($)**
[100]	LTE	pH, DO, EC, Temp & TDS	Low	Not defined	80
[114]	GSM	pH, DO, T&H	Low	Not defined	122
[63]	LoRa	pH, DO, EC, Temp, & Pressure	High	2.5m (ideal)	130
[96]	LoRa	pH, DO, EC & Turbidity	High	10 m	215
[98]	LoRa	pH, DO, EC & Turbidity	High	10 m	215
[101]	LoRa	Pressure & Pulse sensor	Low	Not defined	40
[115]	LoRa	pH, Salinity, & Temperature	Low	2.5 m (ideal)	116
[116]	LoRa	Turbidity, pH & Conductivity	Moderate	2.5 m (ideal)	102
[117]	BLE	pH	Low	2.5 m (ideal)	53
Prop.	LoRa	pH, EC, Temp & TDS	Moderate	8.8 m (practical)	13.5

life can be calculated by summing up the current contribution of the TEMPSENSE in active and sleep modes with respect to time duration. Note that Figure 5.10c is the zoomed version of Figure 5.10a. The measurements lead to the following observations:

- The TEMPSENSE consumes 0.33 mA in sleep mode and 8.4 mA average current for 0.5 s in data acquisition and transmission mode with a peak of 18.5 mA as shown in Figure 5.10c.
- Accordingly, the device can operate for approximately 2 years on a battery with 20000 mAh capacity.

Moreover, the detailed calculations for TEMPSENSE battery life estimation are given below: The active and sleep mode current contribution of TEMPSENSE is as follows:

$$\begin{aligned} C_{Active}^{TEMPSENSE} &= I_{Active} \times T_{Active} \\ &= 8.4 \times 0.5 \\ &= 4.2\, mAs \end{aligned} \tag{5.6}$$

where $C_{Active}^{TEMPSENSE}$ is the current contribution of the TEMPSENSE in active mode.

$$\begin{aligned} C_{Sleep}^{TEMPSENSE} &= I_{Sleep} \times T_{Sleep} \\ &= 0.33 \times 4.5 \\ &= 1.485\, mAs \end{aligned} \tag{5.7}$$

where $C_{Sleep}^{TEMPSENSE}$ is the current contribution of the TEMPSENSE in sleep mode.

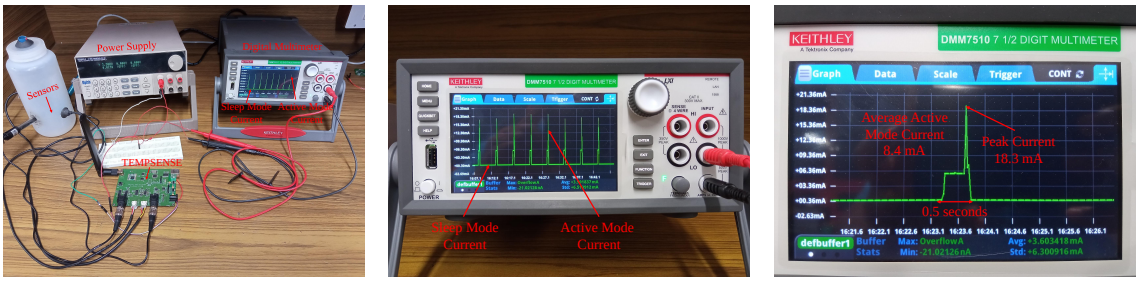

(a) (b) (c)

Figure 5.10: Experimental setup for TEMPSENSE energy consumption and battery life evaluation: (a) setup for TEMPSENSE current evaluation, (b) current waveform for sleep and active modes, (c) current consumption while data acquisition and transmission.

Now, the average current consumption of the TEMPSENSE during one transmission interval can be calculated as:

$$\begin{aligned} I_{Average}^{TEMPSENSE} &= \frac{C_{Active}^{TEMPSENSE} + C_{Sleep}^{TEMPSENSE}}{T} \\ &= \frac{4.2\,mAs + 1.485\,mAs}{5\,s} \\ &= 1.137\,mA \end{aligned} \tag{5.8}$$

where, $I_{Average}^{TEMPSENSE}$ is the average current consumption of the TEMPSENSE and T is the transmission interval.

The battery life of the TEMPSENSE can be calculated as:

$$\begin{aligned} N_{Days}^{Total} &= \frac{B_C}{I_{Average}^{TEMPSENSE}} \\ &= \frac{20000\,mAh}{1.137\,mA} \\ &= 17590.1495\,hrs \\ &\approx 733\,days \\ &\approx 24\,months \\ &\approx 2\,years \end{aligned} \tag{5.9}$$

where N_{Days}^{Total} is the total number of days the TEMPSENSE can operate, and B_C is the total battery capacity in mAh.

5.6 Applications

The proposed TEMPSENSE can have various applications, including water quality monitoring in rivers and lakes, agriculture, and aquaculture. Since the TEMPSENSE enables real time location, corrective measures can be taken in time. Therefore, the device

can significantly reduce water pollution. In agriculture, soil parameters like pH, electrical conductivity, and temperature can be measured, and hence, unnecessary watering of the fields can be avoided. Further, the proposed solution can also monitor essential parameters required for aquaculture, especially fisheries.

5.7 Challenges and Practical Constraints

In high-density environments, several challenges arise that significantly impact the performance of RSSI-based localization solutions. A primary issue is the large fluctuations in RSSI values, which degrade localization accuracy. Additionally, limited cellular coverage impairs the data transmission reliability between the gateway and the cloud, negatively affecting system performance. Practical constraints include the need for stable cellular connectivity between the gateway and the cloud, as well as a reliable grid power supply to ensure continuous gateway operation. Moreover, periodic sensor calibration is essential to maintain accurate measurements. From a hardware perspective, optimal performance often requires the deployment of three gateways, which slightly increases the overall cost.

5.8 Conclusion

This chapter proposes a battery life enhancement strategy through hardware miniaturization. The proposed methodology has been investigated on a river water quality monitoring solution requiring real time location. In this regard, first, we have designed and developed an integrated sensing and localization solution addressing general issues like cost, size, and data accuracy. Thereafter, the proposed strategy has been applied to enhance energy efficiency and achieve a longer battery life. It involves replacing expensive and energy intensive GPS with an RSSI based real time localization algorithm that estimates real time locations without incorporating additional positioning hardware, thus saving significant energy. As a result, the proposed sensing device (TEMPSENSE) can operate continuously for 2 years on a 20000 mAh battery, outperforming the existing solutions.

Chapter 6

Battery Life Enhancement Through Aggregated Data Transmission

In general, remotely deployed IoT solutions require longer battery life due to numerous reasons. Replacing the batteries requires manpower and money; sometimes, it is difficult and impractical to replace batteries due to the nature of the remote sites. Therefore, in this chapter, we proposed a battery life enhancement strategy through aggregated data transmission. Among the IoT applications mentioned and discussed in Chapter 1, one of the crucial livestock monitoring (cattle health and activity monitoring) IoT use cases from the smart farming domain, requiring higher energy efficiency, has been considered for energy efficiency analysis, evaluation, and enhancement. To begin with, we first identified the general issues in existing cattle health monitoring solutions, followed by investigating the root factors causing a reduction in energy efficiency, which, as a result, reduces the overall battery life of the sensing node. Among the general issues, it is found that most of the existing solutions rely primarily on parametric energy optimization, however cattle health and activity monitoring system may have parametric requirements that are non optimized. Besides, the existing solutions transmit raw data, which is usually generated frequently, consequently increasing total transmission and causing high energy consumption. Also, the existing solutions transmit the fixed number of copies to overcome packet loss issues. However, transmitting the fixed number of copies may not completely overcome packet loss and may also lead to redundant transmissions. These issues are identified as the root factors causing significant degradation in energy efficiency, thereby significantly reducing battery life. To address the aforementioned issues, we first designed, developed, and validated the integrated sensing and logging solution called BlueEYE (Bluetooth-based monitoring device), which addressed general issues, including size and cost. Further, a thresholding method was proposed that reduces the total number of transmissions and saves a significant amount of energy by only transmitting parametric data over raw data, which is usually sensed and transmitted very frequently. Additionally, analytical expression for selecting number of copies required to overcome the packet loss and redundant transmissions have been derived, this further enhances the energy efficiency. A brief review of existing works and how our proposed work differs from the existing works is introduced below.

6.1 Related work and Motivation

Indeed, significant research efforts have been made to design and develop cattle health and activity monitoring systems. Primarily two technology types are deployed for remote monitoring *a)* cellular, e.g., global system for mobile communication (GSM), NBIoT [65, 118], *b)* non cellular, e.g., RFID, WiFI, LoRa, ZigBee, BLE [119, 120, 121, 122, 123, 124, 54, 125, 126]. The GSM and NBIoT based solutions proposed in [65, 118], may not work in remote areas with bad network coverage, additionally, cellular based solutions have a comparatively high energy consumption footprint. Hence, noncellular technologies are investigated and adopted for such applications [119, 120]. Indeed, noncellular based solutions outperform cellular based solutions, which have *a)* bad network coverage in remote areas and a high energy consumption footprint; however, they also have certain limitations. For instance, RFID [121, 122] and WiFi based solutions [124] require high energy, whereas LoRa and Zigbee [126, 123] solutions require complex setups and also possess duty cycle restrictions.

However, the recent developments in BLE, i.e., low energy, less complex, and good coexistence, make it more suitable over other noncellular technologies (e.g., WiFi, ZigBee, Sigfox, NBIoT, etc.) and hence is utilized in most of the health and activity monitoring solutions and related applications, e.g., smartwatches, BLE beacons, wearable, cattle health and activity monitoring solutions, et.c [127, 54, 128, 129, 130, 131, 125, 64]. A BLE based cattle health and activity monitoring solution consists of two main components, i.e., *a)* sensing device with BLE functionality and *b)* BLE scanner. The sensing device has an accelerometer sensor that measures acceleration due to movement in 3 dimensional space. The 3 axis acceleration data is then transmitted to the BLE scanner (BLE gateway). The authors in [132] have suggested a sensing frequency of 10-20Hz (every 50-100ms) as best for cattle activity recognition, causing increased transmission requirements. The 3 axis acceleration data received at the gateway is further analyzed to predict the cattle activity corresponding to that data using different algorithms running in the BLE scanner.

Indeed, efforts have been made toward energy optimization in BLE based IoT solutions. For instance, the authors in [133, 134, 135] investigated parametric energy optimization (e.g., advertising interval, transmitted energy, etc.). However, a cattle health and activity monitoring application may have different parametric requirements (which may not be optimized), e.g., advertising interval, scanning interval, transmitted energy, payload size, etc.

Further, the raw data received from the sensors is used for classification and activity prediction. To do so, various machine learning (ML) algorithms are used [136]. In particular, the ML algorithms take the raw accelerometer data obtained from sensors, train the model, and predict the cattle activities. For instance, the BLE based solution proposed in [137] uses a gradient boost decision tree model that classifies resting, moving, and eating and possesses only 288 days of battery life on a 230 mAh battery. Similarly, the authors in [66] proposed a LoRa based solution using a random forest classifier (RF)

for walking, feeding, standing, and lying classification and possess 15 days of battery life on a 660mAh battery. Further, the authors in [65] proposed a GSM-based solution that uses a gradient boost and random forest classifier for standing, lying, ruminating, grazing, and walking classification and possesses 11 hours of battery life on an 850mAh battery. Further, the authors in [138] proposed WiFi based solution, which uses a support vector machine (SVM) and decision tree for standing, lying down, and eating classification, and possesses 10 days battery life on a 3400mAh battery. The aforementioned solutions transmit the raw acceleration data. However, transmitting the raw data requires more transmissions (since it is sensed very frequently, i.e., every 50-100ms), resulting in higher energy consumption/lower battery life.

Additionally, the BLE based solution suffers data loss when the number of devices in the network increases significantly, which is a highly likely case for a big cattle farm. To address this, some authors [139] used the previous data points to send with the current data, which increases the chances of reception up to a certain extent. However, it may not be efficient when numerous sensors are utilized for activity monitoring, collectively creating large amounts of data.

It is evident from the above discussion that the existing solutions have numerous limitations, including relying on parametric energy optimization, which might not be applicable, frequent data transmission, causing more energy consumption, and a lack of proper mechanisms to overcome data loss.

To address the aforementioned issues, in this chapter, we first investigated the root cause of higher energy consumption. However, none of the existing BLE based cattle health monitoring systems emphasizes the root cause of higher energy consumption/lower battery life, which can be the collective effect of inappropriate sensor configuration, inefficient utilization of BLE resources, etc. Further, proposed a thresholding based approach that decreases the total number of transmissions required, consequently decreasing the total energy consumption and increasing the battery life. In addition to the above, to further enhance energy efficiency, we have analytically derived the close form expression, which helps in selecting an exact number of transmissions required to overcome data loss and redundancy in transmissions.

6.2 Contribution

Specifically, the contributions of this chapter are summarized as follows:

- Thresholding based low energy mode is proposed which doubles the battery life by significantly reducing the number of transmissions.
- Network congestion occurs when devices in the network grow. Simplified close form expression is derived to choose the number of transmissions required to transmit data in a congested network. The simplified close form expression will help the service providers to choose the parameters efficiently.

- Experimentally we found that sense, store, and advertise when the packet is full, is significantly more energy efficient than simple sense and advertising, which was not utilized in most of the existing works. Hence, implement, sense, store, and advertise the data when the packet is full.

6.3 System Model

The proposed solution primarily consists of BlueEYE hardware, a BLE gateway, and a server, as shown in Figure 6.1. The BlueEYE sensing node is attached to the cow neck with the help of a belt. It senses and transmits temperature, movement, and orientation data to the BLE gateway. Further, for remote processing and analyses of the data, the BLE gateway uploads the data to the server using an internet connection. Moreover, this data can also be fetched by the user directly from BlueEYE in real time.

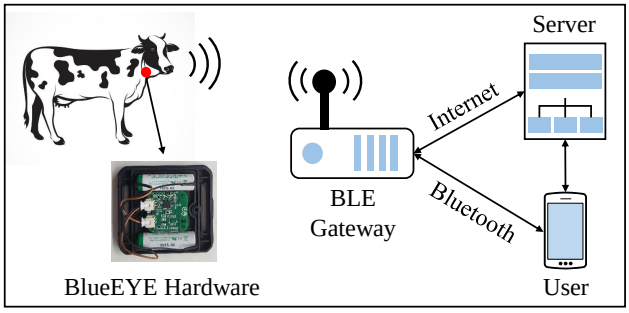

Figure 6.1: The architecture of the BlueEYE based cattle health monitoring system.

6.3.1 Sensor Node Design

Figure 6.2 shows the block diagram and the designed and developed sensing node (BlueEYE). The BlueEYE mainly consists of a BLE system on chip (SoC), sensors, light emitting diodes (LEDs), a button, and a customized 2.45 GHz antenna. The device is equipped with two sensors, i.e., motion (orientation and movement), temperature, and humidity. The sensor data so obtained is processed and advertised by BLE SoC. The LEDs are used for start, stop, and advertising indications, whereas the button is used to switch ON/OFF the device. The customized compact monopole antenna is matched to 50 ohms and hence doesn't require additional matching components, thereby possessing low cost and long range. The key specifications of each component are given below:
BlueEYE mainly consists of BLE SoC, motion sensor, temperature, and humidity sensor. The motion sensor senses movement and orientation, whereas the temperature and humidity sensor senses the ambient temperature, which is communicated to BLE SoC over I2C communication. The data is then advertised by BLE SoC and can be received and analyzed by the user.
The selection of components plays an important role in the energy optimization of the device. Hence, the components are selected considering low energy battery operated IoT device requirements.

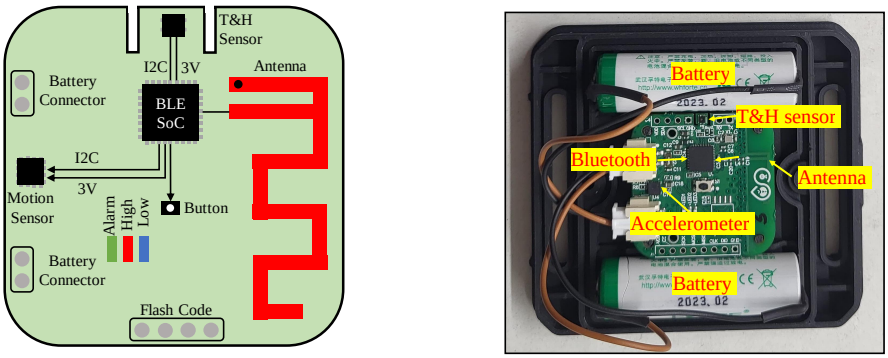

(a) (b)

Figure 6.2: (a) Block diagram of the proposed BlueEYE, (b) fabricated hardware of the proposed BlueEYE at the institution lab

- **BLE SoC** BlueEYE has Nordic's nRF52 series Arm Cortex M4 processor termed as nRF52832 BLE SoC, which is among the best low energy system on a chip that has a 2.4 GHz radio along with the inbuilt controller. The key electrical specifications are as follows.
  - Current consumption in system OFF mode: 0.3 µA
  - Current consumption in system ON mode with wake on RTC: 1.9 µA
  - Fully automatic low drop regulator (LDO) and DC/DC regulator system.

  For any general application, the BLE SoC resides mainly in two modes, i.e., system ON sleep mode and system OFF mode; hence, it must consume low current in these modes. The selected BLE SoC consumes the lowest current among the available BLE radios, i.e., 0.3 µA and 1.9 µA, in system ON sleep and system OFF mode, respectively. Also, the SoC is equipped with an inbuilt LDO, a highly efficient DC-DC converter, and balanced to the unbalanced converter (BALUN), which reduces the additional cost and space.

- **Temperature and Humidity Sensor** BlueEYE incorporates the ultra low energy and high accuracy SHT40 temperature and humidity sensor from the well known venture Sensirion. SHT40 is selected due to the following key electrical specifications.
  - Idle state current consumption: down to 0.08 µA
  - Current consumption during sensing and measurement: down to 0.4 µA.

  Besides the low operating current in idle and measurement state, the sensor also possesses the temperature and humidity accuracy of ± 0.2 °C, ± 1.8 %RH, respectively.

- **Motion Sensor** BlueEYE has a LIS3DH motion sensor from STMicroelectronics. Key electrical specifications are as follows:
  - Idle state current consumption: down to 0.5 µA

– Current consumption during sensing and measurement: down to 2 µA.

In addition to low current consumption, LIS3DH has an integrated 32 level first in first out (FIFO) buffer, allowing the user to store data to limit intervention by the host processor, saving significant energy.

6.3.2 Sensor Node Working

Initially, the BlueEYE resides in system OFF mode, and all the sensors are in an OFF state. When the button is pressed for 5 seconds, the device switches to system ON low-power mode, and Timer 1 is activated with a timeout of T_1 seconds. During this time, data from the temperature sensor is collected and stored. Once T_1 expires, Timer 2 starts with a timeout of T_2 seconds, during which readings from the accelerometer are captured and stored. After T_2 expires, Timer 3 is initiated with a timeout of T_3 seconds, and during this interval, the battery status is sensed and stored. Once the data from the temperature sensor, accelerometer, and battery status are ready, Timer 4 begins. During this period, packet formation is triggered, followed by the transmission of the collected data. Once the advertisement is complete, Timer 4 stops, and the cycle repeats.

6.4 Overview of BLE Communication

The data can be communicated to the host Bluetooth device using one of the two link layer states, i.e., either advertising or connection state. The advertising state can be entered directly from the standby state (lowest energy state, no transmission, and reception), whereas the connection state requires one intermediate state, i.e., either the advertising or initiating state, as shown in Figure 6.3.

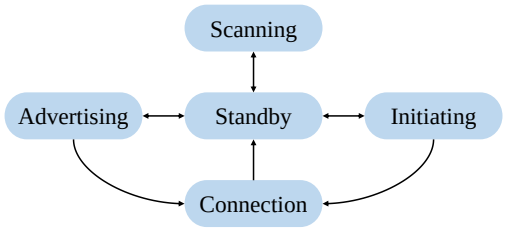

Figure 6.3: BLE link layer states.

The link layer in the advertising state transmits advertising channel packets and possibly listens and responds to responses triggered by the advertising packets. Whereas in the connection state, the data communication is initiated once the connection is established. Within the connection state, two roles are defined, i.e., master (when entered from the initiating state) and slave (when entered from the advertising state).
The data transfer using a connection state comes at the cost of high energy consumption. Also, if the connection drops, reconnection occurs at the cost of increased energy consumption. As a result, advertisement data communication is preferred over the

connection for battery operated applications [54, 55]. In particular, in this chapter, we opted BLE legacy advertisement.

BLE link layer packet structure is shown in Figure 6.4. The preamble field is used for frequency synchronization, automatic gain control, and symbol time estimation. All the advertising channel packets have the same access address, i.e., 0x8E89BE06. The cyclic redundancy check (CRC) field is used for error correction and detection. AdvA and AdvData fields contain the advertiser/transmitter address and the data to be transmitted.

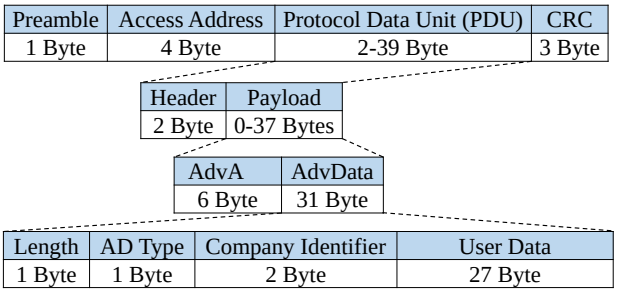

Figure 6.4: BLE link layer packet structure for non-connectable undirected advertising.

The data can be advertised on the advertising channels having channel indexes 37, 38, and 39, respectively. The advertising events are shown in Figure 6.5. The advertising period can be calculated as:

$$T_{AP} = T_{AI} + T_{RD} \tag{6.1}$$

where T_{AP} is the advertising interval and can take any value between 20 ms - 10.24 s in the multiples of 0.625 ms, T_{RD} is the pseudo random value between 0 - 10 ms generated by the link layer for each advertising event, T_{AP} is the total time of an advertising event.

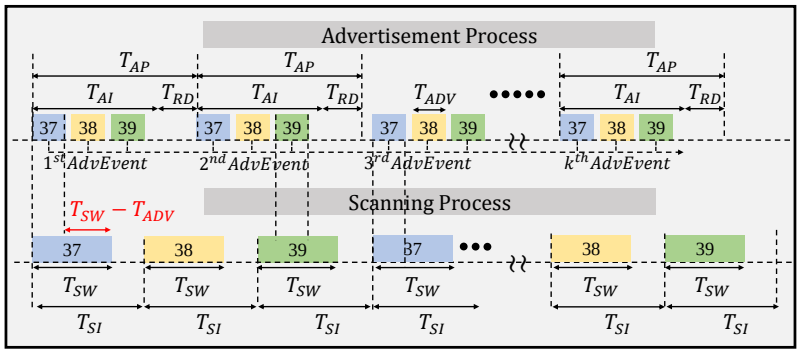

Figure 6.5: Illustration of advertising events and scanning process in BLE.

6.5 Proposed Methodology, Results, and Discussion

In this section, first, the root factors causing higher energy consumption are investigated, then derivation for number of transmissions required to overcome packet loss and redundancy in transmissions is derived and discussed, followed by a discussion on thresholding methodology and battery life analysis.

6.5.1 Investigating Root Cause of Higher Energy Consumption

6.5.1.1 Sense, Store, and Advertise

Generally, the monitoring devices sense and read the sensor unit sample data, followed by advertisements. However, the in depth experiments performed show that this is not an energy efficient approach. Since the sensor unit sample, data size is usually less than the advertising packet payload size (a manufacturer specific advertisement packet can have 27 bytes of user data), hence, resources are not utilized efficiently. Contrarily, the proposed BlueEYE firmware is designed in such a way that it advertises the data only when the packet is full, i.e., 27 bytes. Moreover, the experiments performed on the temperature sensor (of 2 byte unit sample data size) show that sense, store, and advertise when the packet is full is 19 % more energy efficient than simple sense and advertise unit sample, as shown in Table. 6.1.

Table 6.1: Current consumption for sense & advertise and sense, store & advertise.

Sense & advertise	Sense, store, & advertise	Change (%)
4.55 µA	3.67 µA	19.3
4.55 µA	3.67 µA	19.3
4.53 µA	3.68 µA	18.7

Moreover, the current consumption waveforms for sense, store, and advertise and conventional sense and advertise are shown in Figure 6.6.

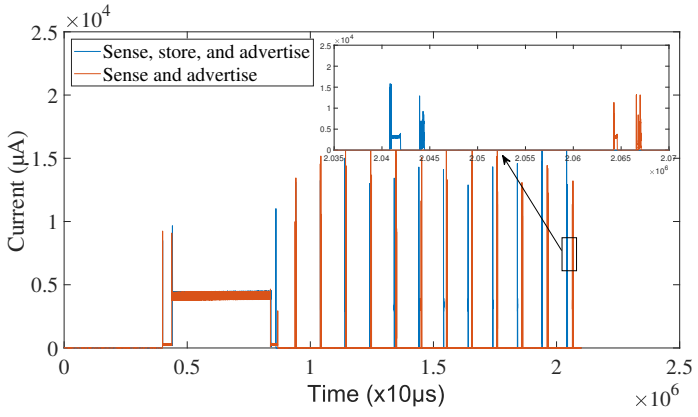

Figure 6.6: Current waveforms for sense, store, and advertisement and sense and advertisement scenario.

6.5.1.2 First in First Out (FIFO) Buffer

Accelerometer unit sample data is 6 bytes (2 bytes on each axis, i.e., x, y, and z). Conventionally, as soon as the sample is sensed and is available to read, it is read by BLE SoC using I2C communication. Since the I2C communication between the BLE SoC and accelerometer sensor involves BLE SoC central processing unit (CPU) intervention, therefore the frequent read involving BLE SoC CPU intervention will result in increased energy consumption. The proposed BlueEYE addresses this issue by utilizing the FIFO buffer, which is able to store 32 samples within the sensor registers (i.e., 32 sample data) and reduces the number of reading cycles from thirty two to one for each buffer containing 32 samples. The buffer status (i.e., whether the buffer is full or not) is indicated by the watermark (WTM)/ overrun (OVRN) flag. The flags can be read in two ways:

- Checking the status of the WTM/OVRN flag continuously and reading the data once the WTM/OVRN flag is high.

- Generating an interrupt on the GPIO pin of the BLE SoC on the WTM/OVRN flag status and then reading the buffer data.

However, reading the flag status, either way, involves the BLE SoC CPU intervention continuously and hence causes comparatively high energy consumption. The proposed BlueEYE solved this problem using a timer (the timer doesn't require BLE SoC CPU intervention) whose timeout depends on the sampling rate, i.e., suppose the sampling interval is 100 ms, and buffers stores 32 samples hence, a total time of 3200 ms can be set as the timeout of the timer. Moreover, the experiments performed using the proposed method have shown excellent results, i.e., the data is received without any problem almost at negligible energy, as shown in Table 6.2. Also, the current waveforms for conventional

Table 6.2: Current consumption analysis for conventional sense & read and sense, FIFO store & read.

Sense, FIFO store, and read		
With OVRN/ WTM flag status read	**With interrupt on OVRN/ WTM flag**	**Without OVRN/ WTM status and interrupt read**
2.88 mA	3.03 mA	23.78 µA
2.90 mA	3.09 mA	23.87 µA
2.85 mA	3.06 mA	23.65 µA

read, FIFO read with if/else/interrupt, and FIFO read with timer are shown in Figure 6.7.

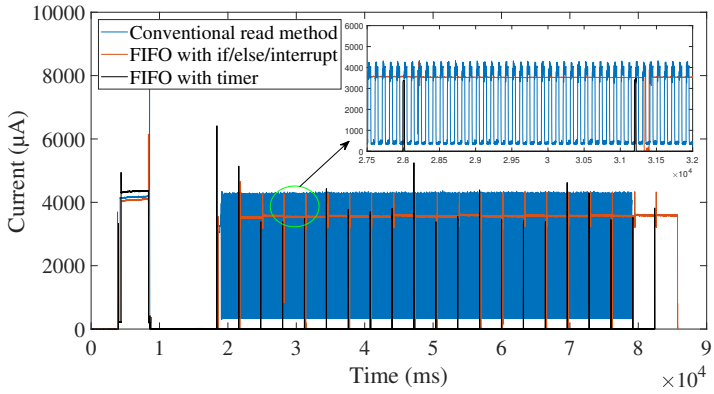

Figure 6.7: Current waveforms for conventional read, FIFO read with if/else/interrupt read, and FIFO read with timer.

6.5.2 BLE Packet Transmission

6.5.2.1 Packet Success Probability Derivation

The packet from a sensor node is said to be successful only when the following conditions are satisfied:

1. *Condition 1 (C1)* The packet from the reference sensor node must not collide with the other sensor nodes in the network.

2. *Condition 1 (C2)* Both the channels used to transmit and receive data must be the same, and the entire duration of the packet should lie within the scanning window T_{SW} of the BLE gateway.

The probability of collision when only two sensor nodes are advertising can be obtained as $2T_{ADV}/T_{AP}$, now if there are N sensor nodes in total, then the packet from the reference sensor node may collide with the packets from other $N-1$ sensor nodes, then the probability which satisfies *Condition 1 (C1)* can be given as:

$$P_{C1} = \left(1 - \frac{2T_{ADV}}{T_{AP}}\right)^{N-1} \tag{6.2}$$

where P_{C1} is the probability of no collision, T_{ADV} is the packet duration, T_{AP} is the advertising period, and N is the total number of sensor nodes in the network. Similarly, the probability which satisfies the *Condition 2 (C2)* can be given as:

$$P_{C2} = \left(\frac{T_{SW} - T_{ADV}}{T_{SI}}\right) \tag{6.3}$$

where P_{C2} is the probability of successful reception of uncollided packet on the scanner/gateway side, T_{SW} is the scan window, and T_{SI} is the scan interval.
Now, the probability of successful packet reception can be obtained by multiplying P_{C1} and P_{C2},

$$P_{SUCC} = \left(\frac{T_{SW} - T_{ADV}}{T_{SI}}\right)\left(1 - \frac{2T_{ADV}}{T_{AP}}\right)^{N-1} \tag{6.4}$$

where P_{SUCC} is the probability that the reference BLE device transmission is successfully received at the BLE gateway.

6.5.2.2 Average Number of Packets

The BLE advertising does not have any feedback mechanism to ensure data reception at the gateway. The transmission of a packet from a reference sensor node is either successful or failure (Bernoulli trail). The probability of success in a repeated Bernoulli trial can be given as:

$$P(x = k) = (1 - p)^{k-1}p \tag{6.5}$$

where, k represents number of trails needed to get first success and p=P_{SUCC}. We can derive the expression of the average number of trials needed to get the first success (expected value of geometric distribution) below:

$$E(k) = \sum_{k=1}^{\infty} k(1 - p)^{k-1}p \tag{6.6}$$

$$E(k) = p\sum_{k=1}^{\infty} k(1 - p)^{k-1} \tag{6.7}$$

$$E(k) = p[1 + 2(1 - p) + 3(1 - p)^2 + 4(1 - p)^3 + ...] \tag{6.8}$$

$$\begin{aligned}(1 - p)E(k) = p[(1 - p) + 2(1 - p)^2 + 3(1 - p)^3 + \\ 4(1 - p)^4 + ...]\end{aligned} \tag{6.9}$$

Subtracting equation 6.9 from equation 6.8, we get,

$$\begin{aligned}E(k)[1 - (1 - p)] = p[(1 + (1 - p) + (1 - p)^2 + \\ (1 - p)^3 + (1 - p)^4 + ...]\end{aligned} \tag{6.10}$$

$$\begin{aligned}E(k) = [(1 + (1 - p) + (1 - p)^2 + (1 - p)^3 + \\ (1 - p)^4 + ...]\end{aligned} \tag{6.11}$$

Using the sum of infinite terms of geometric series identity, we get,

$$E(k) = \frac{1}{(1 - (1 - p))} \tag{6.12}$$

$$E(k) = \frac{1}{p} \tag{6.13}$$

where, p=P_{SUCC} is the probability of success.

Hence, the average number of trails (N_{AVG}) needed to get first success can be given as:

$$N_{AVG} = \frac{1}{P_{SUCC}} = \frac{1}{\left(\frac{T_{SW} - T_{ADV}}{T_{SI}}\right)\left(1 - \frac{2T_{ADV}}{T_{AP}}\right)^{N-1}} \tag{6.14}$$

Using this expression, one can easily determine the number of transmissions required for successful data reception at the gateway for a reference sensor node in a network consisting of N devices, transmitting packets of T_{ADV} duration with the T_{AP} interval.

6.5.2.3 Analytical Results Showing the Impact of BLE Parameters on N_{AVG} and P_{SUCC}

Figure 6.8a, shows the variation N_{AVG} and P_{SUCC} with T_{AP} for different values of N with $T_{ADV} = 0.248ms$ and $T_{SW} = T_{SI} = 10s$. For a given value of N, P_{SUCC} increases, and N_{AVG} decreases with the increase in T_{AP}. This is because the higher values of T_{AP}

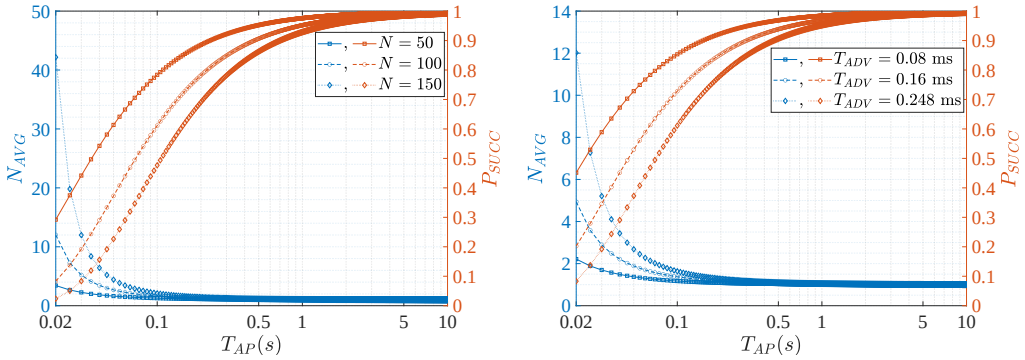

Figure 6.8: (a) Impact of the number of devices N, (b) impact of packet size T_{ADV}.

decrease collision, increase P_{SUCC}, and hence decrease N_{AVG}. It can also be observed that the increase in N increases N_{AVG}, especially at lower T_{AP}. It is because the increase in N increases the network size, resulting in more collisions, which decreases the P_{SUCC}. Similarly, the increase in BLE packet size (T_{ADV}) causes more collisions, consequently decreasing the P_{SUCC}, hence increasing the average number of transmissions (N_{AVG}) as shown in Figure 6.8b with $N = 100$ and $T_{SW} = T_{SI} = 10s$. Likewise, Figure 6.9a shows the impact of the scan window (T_{SW}) on N_{AVG} for $N = 100$ and $T_{ADV} = 0.248ms$. It can be seen that smaller scan windows cause less P_{SUCC} hence, more N_{AVG}. $T_{SW} \geq T_{AP}$ is the best choice. Hence, $T_{SW} = 10s$ has more P_{SUCC}, then $T_{SW} = 5s, 7s$ cases.
This analysis can be used by the service provider to select the BLE parameters to handle data loss efficiently. Such a use case is shown in Figure 6.9b for given $N = 100$, $T_{ADV} = 0.248ms$ and $T_{SW} = T_{SI} = 10s$. As per the quality of service (QoS) requirement, the user does want to send more than two packets (since each transmission comes at the cost of power) and needs $P_{SUCC} \geq 0.9$. An advertising period (T_{AP}) of greater than

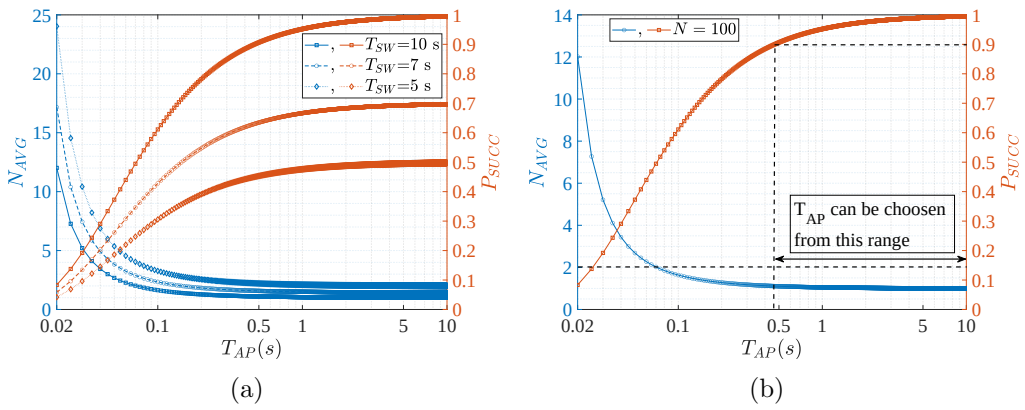

Figure 6.9: (a) Impact of scan window T_{SW}, (b) steps to choose T_{AP}.

0.5s can easily fulfill such a requirement. However, a higher interval causes less energy consumption; hence, a period of 10 s can be chosen for such a use case. Hence, the above analyses can be used to select the optimal T_{AP}. In particular, one can use the close form expression obtained in (6.14) to choose T_{AP} for a required N_{AVG} and P_{SUCC}.

6.5.3 Statistical analyses

This section discusses the statistical parameter based thresholding approach adopted in this chapter to decrease the total number of transmissions. In this approach, we calculate the mean, median, maximum, sum, mode, and RMS values of the 3-axis accelerometer data obtained from the sensor over a fixed period known as the window size. Typically, a 3-30s window size is recommended in the literature [132]. The calculated mean, median, maximum, sum, mode, and RMS values over this window are transmitted directly to the BLE gateway. In this way, we can reduce the total number of transmissions and can increase battery life significantly. Apart from decreasing the total transmissions to a very low value, this approach does not require additional classification algorithms running on the gateway side, requiring additional time and resources on the gateway side.

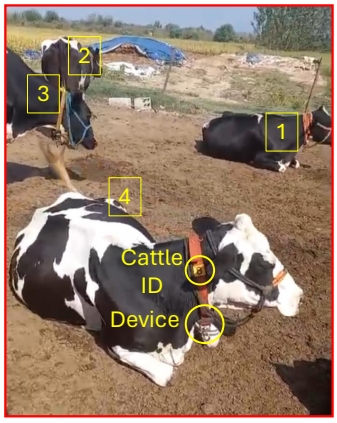

Figure 6.10: Cattles being monitored.

In this direction, we have chosen one cow randomly (marked as 4) from the farm as shown

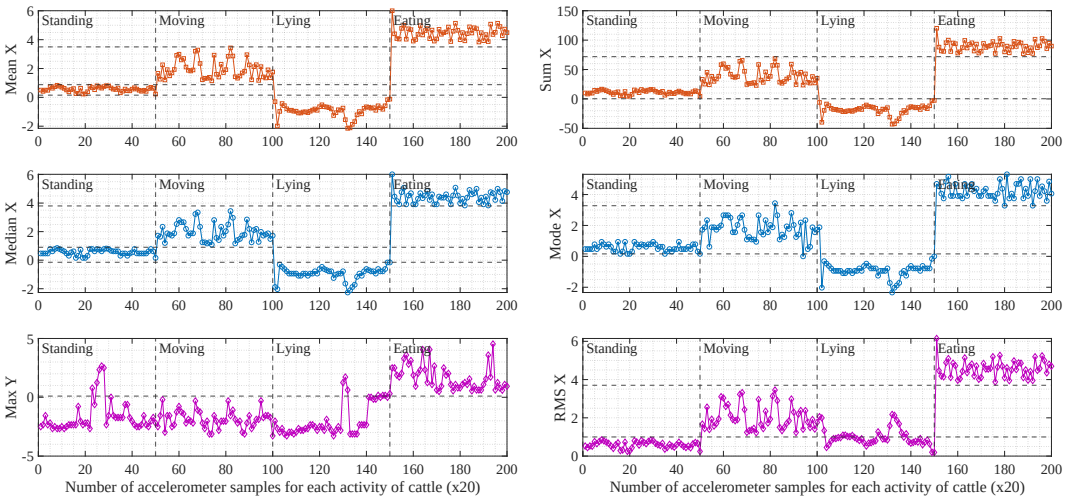

(a) calculated mean X, median X, and max Y. (b) calculated sum X, mode X, and RMS X.

Figure 6.11: Calculation of statistical parameters from accelerometer readings for different activities of cow.

in Figure 6.10, and analyzed four crucial activities [132] (an important indicator of cattle's health), which are shown in Figure 6.11. From Figure 6.11 it can be observed that the mean and median values clearly distinguish between the different activities, such as standing, moving, lying, and eating. Additionally, the maximum values show a distinct threshold for moving and eating, while the sum, mode, and RMS values exhibit clear thresholds for standing and eating activities. The activities obtained after thresholding show a good correlation with the data annotated physically.

6.5.4 Battery Life Analysis

In this section, the current consumption of the proposed solution is analyzed and compared with the existing solutions. The experimental setup is shown in Figure 6.12a.

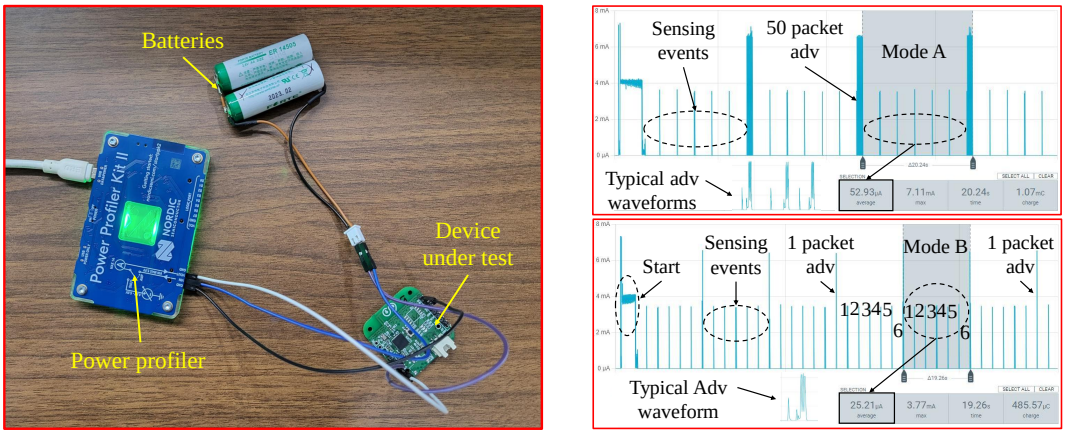

(a) (b)

Figure 6.12: (a) Setup for BlueEYE's current consumption evaluation, (b) BlueEYE current waveforms for Mode A and Mode B.

The expected battery life of a typical sensor node can be calculated as [140]:

$$N_{Days} = \frac{B_C}{I_{Average}} \tag{6.15}$$

where N_{Days} is the total number of days the sensor node can operate, and B_C is the total battery capacity in mAh.

The battery lifetime of a BLE sensor node depends upon various parameters such as advertising interval, advertising protocol data unit (PDU) type, transmitted power, payload size, sensing interval of sensors, battery capacity, etc. Moreover, different parameters have been considered for battery life estimation in the literature. Consequently, it is not fair to compare the estimated battery life. However, the worst case possible parameters should be taken into consideration so as to estimate worst case battery life. Please note that *transmitted power of 0 dBm (least value), battery capacity of 4800 mAh, and sensing interval of 100 ms (continuous sensing)* are considered for BlueEYE battery life estimation.

Mode A generates and transmits a total of 50 packets (raw data mode) in 20s, which are converted to one packet in mode B (thresholding mode), which transmits one packet by calculating mean, median, maximum, sum, mode, and RMS data over the 20s window. The current consumption of the proposed system in mode A and mode B (raw data transmission mode and thresholding mode) is shown in Figure 6.12b:

The battery life in mode A can be obtained as:

$$\begin{aligned} N_{Days}^{ModeA} &= \frac{B_C}{I_{Average}^{BlueEYE}} \\ &= \frac{4800\,mAh}{0.05293\,mA} \\ &= 90685.811\,hrs \\ &\approx 10.3\,years \end{aligned} \tag{6.16}$$

Similarly, the battery life in mode B can be obtained as:

$$\begin{aligned} N_{Days}^{ModeB} &= \frac{B_C}{I_{Average}^{BlueEYE}} \\ &= \frac{4800\,mAh}{0.02521\,mA} \\ &= 190400.63\,hrs \\ &\approx 21.7\,years \end{aligned} \tag{6.17}$$

As shown in Table 6.3, BLE based solutions possess longer battery life among LoRa, WiFi, Zigbee, and GSM based solutions. Hence, we have compared the battery life with existing BLE based solutions. However, they have used different battery life, hence it is not fair to compare directly. Thus, we have considered days/mAh as a fair way for comparison. The BLE based solutions proposed in [137] have 1.25 day/mAh and [64] 1.52 days/mAh. The

Table 6.3: Comparison of the proposed solution with most prominent works.

Ref.	Tech.	Activity	Size	Cost	Interval	Battery Life
[66]	LoRa	Walking, Feeding, Standing, Lying	Large	High	ODR: 10Hz, Window: 10s	6600 mAh, 15 days
[138]	WiFi	Standing, Lying down, Eating	Large	Moderate	Not Mentioned	3400 mAh, 10 days
[141]	Zigbee	Rumination, Body temp., Heart rate, Ambient temp, stress level	Large	High	Not Mentioned	350 mAh, 60 days
[142]	LoRa	Gesture, No. of steps Air pressure, Lying time	Medium	Moderate	ODR:30Hz	7800 mAh, 3.9 years
[143]	LoRa	Cow back inclination, Standing, lying period	Medium	Moderate	ODR: 1Hz, Window: 10s	1000 mAh, 2.21 years
[137]	BLE	Resting, Moving, Eating	Small	Low	ODR:1Hz	230 mAh, 288 days
[64]	BLE	Rumination, Feeding, Walking	Medium	Moderate	ODR: 20Hz, Window: 10s	1200 mAh, 5 years
[65]	GSM	Standing, Lying, Rumination, Grazing, Walking	Large	High	ODR: 1Hz, Window: 60s	850 mAh, 11 hours
Prop.	BLE	Temperature, Bat status, Standing, Moving, Lying, Eating	Small	Low	ODR: 10Hz, Window: 20s	4800 mAh, $>$ 10 years

proposed solution in mode B, monitoring 4 activities, achieves 1.65 days/mAH. Hence, the proposed solution achieves better battery life than existing solutions.

6.6 Conclusion

This chapter proposes a battery life enhancement strategy through aggregated data transmission. The proposed methodology has been investigated on a livestock monitoring application. In this regard, first, we have designed and developed an integrated sensing and logging solution addressing general issues like size and cost. Thereafter, the proposed strategy has been applied to enhance energy efficiency and achieve a longer battery life. It involves (a) a thresholding method that reduces the total number of transmissions and saves a significant amount of energy by only transmitting parametric data over raw data, which is usually sensed and transmitted very frequently, (b) analytical expression for selecting the number of copies required to overcome the packet loss and redundant transmissions, thus saving significant energy. Specifically, transmitting aggregated data over raw data enhances energy efficiency by more than 100%. As a result, the proposed sensing node (BlueEYE) can operate continuously for 21 years on a 4800mAh battery, thereby outperforming the state of the art solutions.

Chapter 7

Conclusion

This chapter concludes the dissertation by summarizing the key findings and the possible future research directions. The key findings are summarized in Section 7.1, whereas, future research directions are presented in Section 7.2.

7.1 Conclusion

IoT has gained significant popularity due to its applications in various domains including industries, healthcare, farming, retail and logistics etc. These applications have different QoS requirements for example, low latency, high energy efficiency, reliability, scalability, security etc. However, most of the IoT applications requires minimal latency and higher energy efficiency. For example, in smart industries low latency is critical to ensure real time control, decision making and safety. Besides, the remote monitoring applications where battery replacement is difficult requires higher energy efficiency and longer battery life. Hence this dissertation focuses on managing and fulfilling these QoS requirements. The key finding and their details are as follow:

Chapter 2 minimizes the latency for sensor nodes-gateway communication scenario considering an industrial automation use case. At first, a performance model considering heterogeneous scenario is developed to analyze latency. Using this mode analytical expression for selecting optimal advertising interval are derived. Based on these analytical expressions, algorithms are proposed that autonomously optimizes the network and ensures minimal latency. In addition to the above, a energy consumption model that helps in estimating the battery lifetime of the sensing nodes along with suitable parameter selection is developed and discussed. Further this chapter presents the simulations to verifies the proposed model and analysis.

Chapter 3 minimizes the delay for sensor nodes-gateway-user communication scenario. At first, a performance model is developed to analyze delay for BLE sensor nodes and delay experienced by user. Using this model analytical expressions are derived for selecting optimal advertising interval. Based on these analytical expressions, algorithms are proposed that autonomously optimizes the network and ensures minimal delay for the data transmitted by BLE sensor nodes and the delay experienced by users. Additionally, this work discusses developing a BLE based smart parking solution using the proposed service architecture and also discusses the step wise procedure to achieve various QoS

requirements. This analysis provides valuable insights for service providers aiming to establish networks with such requirements. Lastly, this chapter also presents the simulations that verifies the proposed model and analysis.

Chapter 4 proposes a battery life enhancement strategy through effective hardware design and efficient utilization. It involves: (a) utilizing GPIOs to power sensors and (b) optimizing controller clock configuration. Specifically, utilizing GPIOs significantly enhances energy efficiency by cutting sleep mode currents of sensors to almost zero.

Chapter 5 proposes a battery life enhancement strategy through hardware miniaturization. It involves, replacing expensive and energy intensive GPS with a RSSI based real time localization algorithm which estimates real time locations without incorporating additional positioning hardware, thus saving significant energy.

Chapter 6 proposes a battery life enhancement strategy through aggregated data transmission. It involves: (a) thresholding method that reduces the total number of transmissions and saves a significant amount of energy by only transmitting parametric data over raw data, which is usually sensed and transmitted very frequently, (b) analytical expression for selecting number of copies required to overcome the packet loss and redundant transmissions, thus saving significant energy. Specifically, transmitting aggregated data over raw data enhances energy efficiency almost by more than 100%.

7.2 Future Scope

The possible future research directions from each chapter of this dissertation are listed below as:

- **Chapter 2** proposed an analytical model to analyze the latency and simplified expressions to chose transmission parameters that ensures minimal latency considering sensor nodes-gateway communication scenario. However, such application may also need to maximize the data rate. Hence, as a future work, a similar performance model can be developed to analyze the data rate, and using this model simplified analytical expressions can be derived for transmission parameter selection that can ensure maximal data rate.
- **Chapter 3** proposed an analytical model to analyze the delay and simplified expressions to chose transmission parameters that ensures minimal delay considering sensor nodes-gateway-user communication scenario. However, such application may also need to maximize the throughput. Hence, as a future work, a similar performance model can be developed to analyze the throughput, and using this model simplified analytical expressions can be derived for transmission parameter selection that can ensure maximal throughput.

- **Chapter 4** proposed battery life enhancement strategy through effective hardware design and efficient utilization considering cold chain monitoring as an use case. The proposed solution effectively stores crucial parameters through monitoring duration. However, certain use cases may require immediate action if specific thresholds are exceeded. Hence as a future work, the same strategy can be extended to develop an enhanced cold chain monitoring solution capable of storing crucial parameters and also giving real time updates.

- **Chapter 5** proposed battery life enhancement strategy that replaces GPS with RSSI based localization for real time location estimation. The proposed work achieves accuracy up to few meters. However, there are various applications that require more accurate real time locations, for example fish farming. Hence, as a future work efforts can be made to improve accuracy up to cm level considering energy constraints.

- **Chapter 6** proposed battery life enhancement strategy through aggregated data transmission for applications generating data very frequently, for example cattle health monitoring. The proposed statistical evaluation is capable of identifying limited activities. However, there are various applications that might need to monitor and identify more activities, for example real time patient activity monitoring in hospitals. Hence, as a future work efforts can be made to replace statistical evaluation through neural network architecture which is capable of detecting large number of activities in addition to actionable events that occur, hence, enabling prolonged battery life while also minimizing energy consumption.

References

[1] Mahmoud Elkhodr, Seyed Shahrestani, and Hon Cheung. The Internet of Things: Vision & Challenges. In *IEEE 2013 Tencon - Spring*, pages 218–222, 2013. doi: 10.1109/TENCONSpring.2013.6584443.

[2] Marieh Talebkhah, Aduwati Sali, Meisam Gordan, Shaiful Jahari Hashim, and Fakhrul Zaman Rokhani. Comprehensive Review on Development of Smart Cities Using Industry 4.0 Technologies. *IEEE Access*, 11:91981–92030, 2023. doi: 10.1109/ACCESS.2023.3302262.

[3] Adam Zielonka, Marcin Woźniak, Sahil Garg, Georges Kaddoum, Md. Jalil Piran, and Ghulam Muhammad. Smart Homes: How Much Will They Support Us? A Research on Recent Trends and Advances. *IEEE Access*, 9:26388–26419, 2021. doi: 10.1109/ACCESS.2021.3054575.

[4] Amir Masoud Rahmani, Wang Szu-Han, Kang Yu-Hsuan, and Majid Haghparast. The Internet of Things for Applications in Wearable Technology. *IEEE Access*, 10: 123579–123594, 2022. doi: 10.1109/ACCESS.2022.3224487.

[5] Juan Carlos Cano, Victor Berrios, Ben Garcia, and Chai K. Toh. Evolution of IoT: An Industry Perspective. *IEEE Internet of Things Magazine*, 1(2):12–17, 2018. doi: 10.1109/IOTM.2019.1900002.

[6] Li Da Xu, Wu He, and Shancang Li. Internet of Things in Industries: A Survey. *IEEE Transactions on Industrial Informatics*, 10(4):2233–2243, 2014. doi: 10.1109/TII.2014.2300753.

[7] Andrea Zanella, Nicola Bui, Angelo Castellani, Lorenzo Vangelista, and Michele Zorzi. Internet of Things for Smart Cities. *IEEE Internet of Things Journal*, 1(1): 22–32, 2014. doi: 10.1109/JIOT.2014.2306328.

[8] Jayavardhana Gubbi, Rajkumar Buyya, Slaven Marusic, and Marimuthu Palaniswami. Internet of Things (IoT): A Vision, Architectural Elements, and Future Directions. *Future generation computer systems*, 29(7):1645–1660, 2013.

[9] Dhananjay Singh, Gaurav Tripathi, and Antonio J Jara. A Survey of Internet-of-Things: Future Vision, Architecture, Challenges and Services. In *2014 IEEE world forum on Internet of Things (WF-IoT)*, pages 287–292. IEEE, 2014.

[10] Shanzhi Chen, Hui Xu, Dake Liu, Bo Hu, and Hucheng Wang. A Vision of IoT: Applications, Challenges, and Opportunities With China Perspective. *IEEE Internet of Things Journal*, 1(4):349–359, 2014. doi: 10.1109/JIOT.2014.2337336.

[11] Yousaf Bin Zikria, Rashid Ali, Muhammad Khalil Afzal, and Sung Won Kim. Next-generation Internet of Things (IoT): Opportunities, Challenges, and Solutions. *Sensors*, 21(4):1174, 2021.

[12] Sanjeevikumar Padmanaban, Mostafa Azimi Nasab, Mohammad Ebrahim Shiri, Hamid Haj Seyyed Javadi, Morteza Azimi Nasab, Mohammad Zand, and Tina Samavat. The Role of Internet of Things in Smart Homes. *Artificial Intelligence-based Smart Power Systems*, pages 259–271, 2023.

[13] Ayca Kirimtat, Ondrej Krejcar, Attila Kertesz, and M. Fatih Tasgetiren. Future Trends and Current State of Smart City Concepts: A Survey. *IEEE Access*, 8: 86448–86467, 2020. doi: 10.1109/ACCESS.2020.2992441.

[14] Yung-Chang Hsiao, Ming-Ho Wu, and Simon Cimin Li. Elevated Performance of the Smart City—A Case Study of the IoT by Innovation Mode. *IEEE Transactions on Engineering Management*, 68(5):1461–1475, 2021. doi: 10.1109/TEM.2019.2908962.

[15] Saraju P. Mohanty, Uma Choppali, and Elias Kougianos. Everything You Wanted to Know about Smart Cities: The Internet of Things is the Backbone. *IEEE Consumer Electronics Magazine*, 5(3):60–70, 2016. doi: 10.1109/MCE.2016.2556879.

[16] Ammar Gharaibeh, Mohammad A. Salahuddin, Sayed Jahed Hussini, Abdallah Khreishah, Issa Khalil, Mohsen Guizani, and Ala Al-Fuqaha. Smart Cities: A Survey on Data Management, Security, and Enabling Technologies. *IEEE Communications Surveys & Tutorials*, 19(4):2456–2501, 2017. doi: 10.1109/COMST.2017.2736886.

[17] Patruni Muralidhara Rao, Saraswathi Pedada, Srinivas Jangirala, Ashok Kumar Das, and Joel J. P. C. Rodrigues. Role of IoT in the Ages of Digital to Smart Cities: Security Challenges and Countermeasures. *IEEE Internet of Things Magazine*, 7 (1):56–64, 2024. doi: 10.1109/IOTM.001.2300124.

[18] Mamoona Humayun, NZ Jhanjhi, Bushra Hamid, and Ghufran Ahmed. Emerging Smart Logistics and Transportation Using IoT and Blockchain. *IEEE Internet of Things Magazine*, 3(2):58–62, 2020. doi: 10.1109/IOTM.0001.1900097.

[19] Zineb Mahrez, Essaid Sabir, Elarbi Badidi, Walid Saad, and Mohamed Sadik. Smart Urban Mobility: When Mobility Systems Meet Smart Data. *IEEE Transactions on Intelligent Transportation Systems*, 23(7):6222–6239, 2022. doi: 10.1109/TITS.2021.3084907.

[20] S. M. Riazul Islam, Daehan Kwak, MD. Humaun Kabir, Mahmud Hossain, and Kyung-Sup Kwak. The Internet of Things for Health Care: A Comprehensive Survey. *IEEE Access*, 3:678–708, 2015. doi: 10.1109/ACCESS.2015.2437951.

[21] Md. Milon Islam, Sheikh Nooruddin, Fakhri Karray, and Ghulam Muhammad. Internet of Things: Device Capabilities, Architectures, Protocols, and Smart

Applications in Healthcare Domain. *IEEE Internet of Things Journal*, 10(4): 3611–3641, 2023. doi: 10.1109/JIOT.2022.3228795.

[22] Mohammad Nuruzzaman Bhuiyan, Md Mahbubur Rahman, Md Masum Billah, and Dipanita Saha. Internet of Things (IoT): A Review of its Enabling Technologies in Healthcare Applications, Standards Protocols, Security, and Market Opportunities. *IEEE Internet of Things Journal*, 8(13):10474–10498, 2021. doi: 10.1109/JIOT.2021.3062630.

[23] Yasir Saleem, Noel Crespi, Mubashir Husain Rehmani, and Rebecca Copeland. Internet of Things-Aided Smart Grid: Technologies, Architectures, Applications, Prototypes, and Future Research Directions. *IEEE Access*, 7:62962–63003, 2019. doi: 10.1109/ACCESS.2019.2913984.

[24] S. M. Abu Adnan Abir, Adnan Anwar, Jinho Choi, and A. S. M. Kayes. IoT-Enabled Smart Energy Grid: Applications and Challenges. *IEEE Access*, 9:50961–50981, 2021. doi: 10.1109/ACCESS.2021.3067331.

[25] Muhammad Haseeb Raza, Yousaf Murtaza Rind, Isma Javed, Muhammad Zubair, Muhammad Qasim Mehmood, and Yehia Massoud. Smart Meters for Smart Energy: A Review of Business Intelligence Applications. *IEEE Access*, 11:120001–120022, 2023. doi: 10.1109/ACCESS.2023.3326724.

[26] Muhammad Shoaib Farooq, Shamyla Riaz, Adnan Abid, Kamran Abid, and Muhammad Azhar Naeem. A Survey on the Role of IoT in Agriculture for the Implementation of Smart Farming. *IEEE Access*, 7:156237–156271, 2019. doi: 10.1109/ACCESS.2019.2949703.

[27] Muhammad Shoaib Farooq, Osama Omar Sohail, Adnan Abid, and Saim Rasheed. A Survey on the Role of IoT in Agriculture for the Implementation of Smart Livestock Environment. *IEEE Access*, 10:9483–9505, 2022. doi: 10.1109/ACCESS.2022.3142848.

[28] N. N. Misra, Yash Dixit, Ahmad Al-Mallahi, Manreet Singh Bhullar, Rohit Upadhyay, and Alex Martynenko. IoT, Big Data, and Artificial Intelligence in Agriculture and Food Industry. *IEEE Internet of Things Journal*, 9(9):6305–6324, 2022. doi: 10.1109/JIOT.2020.2998584.

[29] Yanxing Song, F. Richard Yu, Li Zhou, Xi Yang, and Zefang He. Applications of the Internet of Things (IoT) in Smart Logistics: A Comprehensive Survey. *IEEE Internet of Things Journal*, 8(6):4250–4274, 2021. doi: 10.1109/JIOT.2020.3034385.

[30] Alfredo Arnaud, Martin Marioni, Mario Ortiz, Gisselle Vogel, and Matías R. Miguez. LoRaWAN ESL for Food Retail and Logistics. *IEEE Journal on Emerging and Selected Topics in Circuits and Systems*, 11(3):493–502, 2021. doi: 10.1109/JETCAS.2021.3101367.

[31] Montdher Alabadi, Adib Habbal, and Xian Wei. Industrial Internet of Things: Requirements, Architecture, Challenges, and Future Research Directions. *IEEE Access*, 10:66374–66400, 2022. doi: 10.1109/ACCESS.2022.3185049.

[32] Othmane Friha, Mohamed Amine Ferrag, Lei Shu, Leandros Maglaras, and Xiaochan Wang. Internet of Things for the Future of Smart Agriculture: A Comprehensive Survey of Emerging Technologies. *IEEE/CAA Journal of Automatica Sinica*, 8(4): 718–752, 2021. doi: 10.1109/JAS.2021.1003925.

[33] Nader Mohamed, Jameela Al-Jaroodi, and Sanja Lazarova-Molnar. Leveraging the Capabilities of Industry 4.0 for Improving Energy Efficiency in Smart Factories. *IEEE Access*, 7:18008–18020, 2019. doi: 10.1109/ACCESS.2019.2897045.

[34] Martin Wollschlaeger, Thilo Sauter, and Juergen Jasperneite. The Future of Industrial Communication: Automation Networks in the Era of the Internet of Things and Industry 4.0. *IEEE Industrial Electronics Magazine*, 11(1):17–27, 2017. doi: 10.1109/MIE.2017.2649104.

[35] Montdher Alabadi, Adib Habbal, and Xian Wei. Industrial Internet of Things: Requirements, Architecture, Challenges, and Future Research Directions. *IEEE Access*, 10:66374–66400, 2022. doi: 10.1109/ACCESS.2022.3185049.

[36] Selma Dilek, Kerem Irgan, Metehan Guzel, Suat Ozdemir, Sebnem Baydere, and Chalermpol Charnsripinyo. QoS-aware IoT Networks and Protocols: A Comprehensive Survey. *International Journal of Communication Systems*, 35(10): e5156, 2022.

[37] Philipp Schulz, Maximilian Matthe, Henrik Klessig, Meryem Simsek, Gerhard Fettweis, Junaid Ansari, Shehzad Ali Ashraf, Bjoern Almeroth, Jens Voigt, Ines Riedel, Andre Puschmann, Andreas Mitschele-Thiel, Michael Muller, Thomas Elste, and Marcus Windisch. Latency Critical IoT Applications in 5G: Perspective on the Design of Radio Interface and Network Architecture. *IEEE Communications Magazine*, 55(2):70–78, 2017. doi: 10.1109/MCOM.2017.1600435CM.

[38] Jie Ding, Mahyar Nemati, Chathurika Ranaweera, and Jinho Choi. IoT Connectivity Technologies and Applications: A Survey. *IEEE Access*, 8:67646–67673, 2020. doi: 10.1109/ACCESS.2020.2985932.

[39] Vikas Hassija, Vinay Chamola, Vikas Saxena, Divyansh Jain, Pranav Goyal, and Biplab Sikdar. A Survey on IoT Security: Application Areas, Security Threats, and Solution Architectures. *IEEE Access*, 7:82721–82743, 2019. doi: 10.1109/ACCESS.2019.2924045.

[40] Mumin Adam, Mohammad Hammoudeh, Rana Alrawashdeh, and Basil Alsulaimy. A Survey on Security, Privacy, Trust, and Architectural Challenges in IoT Systems. *IEEE Access*, 12:57128–57149, 2024. doi: 10.1109/ACCESS.2024.3382709.

[41] Francesca Meneghello, Matteo Calore, Daniel Zucchetto, Michele Polese, and Andrea Zanella. IoT: Internet of Threats? A Survey of Practical Security Vulnerabilities in Real IoT Devices. *IEEE Internet of Things Journal*, 6(5):8182–8201, 2019. doi: 10.1109/JIOT.2019.2935189.

[42] Boonyarith Saovapakhiran, Wibhada Naruephiphat, Chalermpol Charnsripinyo, Sebnem Baydere, and Suat Özdemir. QoE-Driven IoT Architecture: A Comprehensive Review on System and Resource Management. *IEEE Access*, 10: 84579–84621, 2022. doi: 10.1109/ACCESS.2022.3197585.

[43] Ala Al-Fuqaha, Mohsen Guizani, Mehdi Mohammadi, Mohammed Aledhari, and Moussa Ayyash. Internet of things: A survey on enabling technologies, protocols, and applications. *IEEE Communications Surveys & Tutorials*, 17(4):2347–2376, 2015. doi: 10.1109/COMST.2015.2444095.

[44] Jie Lin, Wei Yu, Nan Zhang, Xinyu Yang, Hanlin Zhang, and Wei Zhao. A Survey on Internet of Things: Architecture, Enabling Technologies, Security and Privacy, and Applications. *IEEE Internet of Things Journal*, 4(5):1125–1142, 2017. doi: 10.1109/JIOT.2017.2683200.

[45] Mario Collotta, Giovanni Pau, Timothy Talty, and Ozan K. Tonguz. Bluetooth 5: A Concrete Step Forward toward the IoT. *IEEE Communications Magazine*, 56(7): 125–131, 2018. doi: 10.1109/MCOM.2018.1700053.

[46] Zhijin Qin, Frank Y. Li, Geoffrey Ye Li, Julie A. McCann, and Qiang Ni. Low-Power Wide-Area Networks for Sustainable IoT. *IEEE Wireless Communications*, 26(3): 140–145, 2019. doi: 10.1109/MWC.2018.1800264.

[47] Ali Nikoukar, Saleem Raza, Angelina Poole, Mesut Güneş, and Behnam Dezfouli. Low-Power Wireless for the Internet of Things: Standards and Applications. *IEEE Access*, 6:67893–67926, 2018. doi: 10.1109/ACCESS.2018.2879189.

[48] Jothi Prasanna Shanmuga Sundaram, Wan Du, and Zhiwei Zhao. A Survey on LoRa Networking: Research Problems, Current Solutions, and Open Issues. *IEEE Communications Surveys & Tutorials*, 22(1):371–388, 2020. doi: 10.1109/COMST.2019.2949598.

[49] Alexandru Lavric, Adrian I. Petrariu, and Valentin Popa. Long Range SigFox Communication Protocol Scalability Analysis Under Large-Scale, High-Density Conditions. *IEEE Access*, 7:35816–35825, 2019. doi: 10.1109/ACCESS.2019.2903157.

[50] Emmanuel M. Migabo, Karim D. Djouani, and Anish M. Kurien. The Narrowband Internet of Things (NB-IoT) Resources Management Performance State of Art, Challenges, and Opportunities. *IEEE Access*, 8:97658–97675, 2020. doi: 10.1109/ACCESS.2020.2995938.

[51] Usman Raza, Parag Kulkarni, and Mahesh Sooriyabandara. Low Power Wide Area Networks: An Overview. *IEEE Communications Surveys & Tutorials*, 19(2): 855–873, 2017. doi: 10.1109/COMST.2017.2652320.

[52] Augustine Ikpehai, Bamidele Adebisi, Khaled M. Rabie, Kelvin Anoh, Ruth E. Ande, Mohammad Hammoudeh, Haris Gacanin, and Uche M. Mbanaso. Low-Power Wide Area Network Technologies for Internet-of-Things: A Comparative Review. *IEEE Internet of Things Journal*, 6(2):2225–2240, 2019. doi: 10.1109/JIOT.2018.2883728.

[53] Bluetooth Special Interest Group (SIG). Bluetooth Core Specification Version 4.0. *https://www.bluetooth.com/*, 2010.

[54] Kunal Shyamadas Burman, Sven Schmidt, Dhouha El Houssaini, and Olfa Kanoun. Design and Evaluation of a Low Energy Bluetooth Sensor Node for Animal Monitoring. In *2021 18th International Multi-Conference on Systems, Signals & Devices (SSD)*, pages 971–978, 2021. doi: 10.1109/SSD52085.2021.9429390.

[55] Maciej Nikodem and Marek Bawiec. Experimental Evaluation of Advertisement-based Bluetooth Low Energy Communication. *Sensors*, 20(1): 107, 2019.

[56] Panagiotis Gkotsiopoulos, Dimitrios Zorbas, and Christos Douligeris. Performance Determinants in LoRa Networks: A Literature Review. *IEEE Communications Surveys & Tutorials*, 23(3):1721–1758, 2021. doi: 10.1109/COMST.2021.3090409.

[57] Hongxu Zhu, Kim Fung Tsang, Yucheng Liu, Yang Wei, Hao Wang, Chung Kit Wu, and Wai Hin Wan. Index of low-power wide area networks: A ranking solution toward best practice. *IEEE Communications Magazine*, 59(4):139–144, 2021. doi: 10.1109/MCOM.001.2000873.

[58] Gaoyang Shan, Sun young Im, and Byeong hee Roh. Optimal AdvInterval for BLE Scanning in Different Number of BLE Devices Environment. In *2016 IEEE Conference on Computer Communications Workshops (INFOCOM WKSHPS)*, pages 1031–1032, 2016. doi: 10.1109/INFCOMW.2016.7562238.

[59] Bingqing Luo, Feng Xiang, Zhixin Sun, and Yudong Yao. BLE Neighbor Discovery Parameter Configuration for IoT Applications. *IEEE Access*, 7:54097–54105, 2019. doi: 10.1109/ACCESS.2019.2912493.

[60] Gaoyang Shan and Byeong-Hee Roh. Advertisement Interval to Minimize Discovery Time of Whole BLE Advertisers. *IEEE Access*, 6:17817–17825, 2018. doi: 10.1109/ACCESS.2018.2817343.

[61] O Ojike, CC Mbajiorgu, E Anoliefo, and WI Okonkwo. Design and Analysis of a Multipoint Temperature Datalogger. *Nigerian Journal of Technology*, 35(2):458–464, 2016.

[62] Patricia A Beddows and Edward K Mallon. Cave Pearl Data Logger: A Flexible Arduino-based Logging Platform for Long-Term Monitoring in Harsh Environments. *Sensors*, 18(2):530, 2018.

[63] Libu Manjakkal, Srinjoy Mitra, Y Petillo, Jamie Shutler, M Scott, Magnus Willander, and Ravinder Dahiya. Connected Sensors, Innovative Sensor Deployment and Intelligent Data Analysis for Online Water Quality Monitoring. *IEEE Internet of Things Journal*, 2021.

[64] Olgierd Unold, Maciej Nikodem, Marek Piasecki, Kamil Szyc, Henryk Maciejewski, Marek Bawiec, Paweł Dobrowolski, and Michał Zdunek. IoT-based Cow Health Monitoring System. In *International Conference on Computational Science*, pages 344–356. Springer, 2020.

[65] Debeshi Dutta, Dwipjyoti Natta, Soumen Mandal, and Nilotpal Ghosh. MOOnitor: An IoT based Multi-sensory Intelligent Device for Cattle Activity Monitoring. *Sensors and Actuators A: Physical*, 333:113271, 2022.

[66] Duc-Nghia Tran, Tu N. Nguyen, Phung Cong Phi Khanh, and Duc-Tan Tran. An IoT-Based Design Using Accelerometers in Animal Behavior Recognition Systems. *IEEE Sensors Journal*, 22(18):17515–17528, 2022. doi: 10.1109/JSEN.2021.3051194.

[67] Chongtao Guo, Xijun Wang, Le Liang, and Geoffrey Ye Li. Age of Information, Latency, and Reliability in Intelligent Vehicular Networks. *IEEE Network*, 37(6): 109–116, 2023. doi: 10.1109/MNET.124.2200132.

[68] Siti Nur Fatihah, Gilang Raka Rayuda Dewa, Cheolsoo Park, and Illsoo Sohn. Self-Optimizing Bluetooth Low Energy Networks for Industrial IoT Applications. *IEEE Communications Letters*, 27(1):386–390, 2023. doi: 10.1109/LCOMM.2022.3215158.

[69] Andrew Mackey, Petros Spachos, and Konstantinos N. Plataniotis. Smart Parking System Based on Bluetooth Low Energy Beacons With Particle Filtering. *IEEE Systems Journal*, 14(3):3371–3382, 2020. doi: 10.1109/JSYST.2020.2968883.

[70] Dinh C. Nguyen, Ming Ding, Pubudu N. Pathirana, Aruna Seneviratne, Jun Li, Dusit Niyato, Octavia Dobre, and H. Vincent Poor. 6G Internet of Things: A Comprehensive Survey. *IEEE Internet of Things Journal*, 9(1):359–383, 2022. doi: 10.1109/JIOT.2021.3103320.

[71] Gaoyang Shan and Byeong-hee Roh. Performance Model for Advanced Neighbor Discovery Process in Bluetooth Low Energy 5.0-Enabled Internet of Things Networks. *IEEE Transactions on Industrial Electronics*, 67(12):10965–10974, 2020. doi: 10.1109/TIE.2019.2962401.

[72] Ángela HernáNdez-Solana, David PéRez-DíAz-De-Cerio, Antonio Valdovinos, and Jose Luis Valenzuela. Anti-Collision Adaptations of BLE Active Scanning for

Dense IoT Tracking Applications. *IEEE Access*, 6:53620–53637, 2018. doi: 10.1109/ACCESS.2018.2870691.

[73] David Perez-Diaz de Cerio, Ángela Hernández, Jose Luis Valenzuela, and Antonio Valdovinos. Analytical and Experimental Performance Evaluation of BLE Neighbor Discovery Process including Non-idealities of Real Chipsets. *Sensors*, 17(3):499, 2017.

[74] Wha Sook Jeon, Made Harta Dwijaksara, and Dong Geun Jeong. Performance Analysis of Neighbor Discovery Process in Bluetooth Low-Energy Networks. *IEEE Transactions on Vehicular Technology*, 66(2):1865–1871, 2017. doi: 10.1109/TVT.2016.2558194.

[75] Bluetooth Special Interest Group (SIG). Bluetooth Core Specification Version 5.0. *https://www.bluetooth.com/*, 2016.

[76] Bingqing Luo, Jia Xu, and Zhixin Sun. Neighbor Discovery Latency in Bluetooth Low Energy Networks. *Wireless Networks*, 26:1773–1780, 2020.

[77] Mohammad Ghamari, Emma Villeneuve, Cinna Soltanpur, Javad Khangosstar, Balazs Janko, R. Simon Sherratt, and William Harwin. Detailed Examination of a Packet Collision Model for Bluetooth Low Energy Advertising Mode. *IEEE Access*, 6:46066–46073, 2018. doi: 10.1109/ACCESS.2018.2866323.

[78] Chi-Fang Chien, Hui-Tzu Chen, and Chi-Yi Lin. A Low-Cost On-Street Parking Management System Based on Bluetooth Beacons. *Sensors*, 20(16):4559, 2020.

[79] Petar Solic, Alfiero Leoni, Riccardo Colella, Toni Perkovic, Luca Catarinucci, and Vincenzo Stornelli. IoT-Ready Energy-Autonomous Parking Sensor Device. *IEEE Internet of Things Journal*, 8(6):4830–4840, 2021. doi: 10.1109/JIOT.2020.3031088.

[80] Simon Wong, James She, and Kang Eun Jeon. An Efficient Framework of Energy Status Reporting for BLE Beacon Networks. *IEEE Internet of Things Journal*, 10 (12):10426–10437, 2023. doi: 10.1109/JIOT.2023.3237858.

[81] Inhwan Jung. An IoT-based Smart Parking Management System. *International Journal of Computational Vision and Robotics*, 10(2):122–132, 2020.

[82] Bluetooth Special Interest Group (SIG). Bluetooth Core Specification Version 5.4. *https://www.bluetooth.com/*, 2023.

[83] Ting-Ting Yang and Hsueh-Wen Tseng. Improving Discovery Process toward User Engagement Based on Advertising Extensions in Bluetooth Low Energy Networks. *IEEE Transactions on Mobile Computing*, pages 1–1, 2021. doi: 10.1109/TMC.2021.3054931.

[84] Lalit Kumar Baghel, Gaoyang Shan, and Suman Kumar. Analytical Framework for Data Reception Latency Modelling in BLE 5.x Based Clustered Architecture. *IEEE Communications Letters*, pages 1–1, 2024. doi: 10.1109/LCOMM.2024.3381605.

[85] G. Shan and B.-Hee Roh. Maximized Effective Transmission Rate Model for Advanced Neighbor Discovery Process in Bluetooth Low Energy 5.0. *IEEE Internet of Things Journal*, 9(17):16272–16283, 2022. doi: 10.1109/JIOT.2022.3152513.

[86] Bluetooth Special Interest Group (SIG). Bluetooth Core Specification Version 5.3. *https://www.bluetooth.com/*, 2021.

[87] Gilles Callebaut, Guus Leenders, Jarne Van Mulders, Geoffrey Ottoy, Lieven De Strycker, and Liesbet Van der Perre. The art of designing remote iot devices—technologies and strategies for a long battery life. *Sensors*, 21(3):913, 2021.

[88] Guie Li. Development of Cold Chain Logistics Transportation System based on 5G Network and Internet of Things System. *Microprocessors and Microsystems*, 80: 103565, 2021.

[89] YA Silin. Development of the Information-Measuring System to Maintain the Temperature Balance Inside the Container During Transportation. In *2021 Wave Electronics and its Application in Information and Telecommunication Systems (WECONF)*, pages 1–4. IEEE, 2021.

[90] Muhammad Haikal Satria and Ariep Jaenul1 Adhes Gamayel. Design of Solar Powered Vaccine Backpack. In *4th Forum in Research, Science, and Technology (FIRST-T1-T2-2020)*, pages 590–594. Atlantis Press, 2021.

[91] Mokh Sholihul Hadi, Mochammad Rizal Maulana, Muhammad Alfian Mizar, Ilham Ari Elbaith Zaeni, Arif Nur Afandi, and Mhd Irvan. Self energy management system for battery operated data logger device based on iot. In *2019 International Conference on Electrical, Electronics and Information Engineering (ICEEIE)*, volume 6, pages 133–138. IEEE, 2019.

[92] Sagarkumar S Badhiye, PN Chatur, and BV Wakode. Data Logger System: A Survey. *International Journal of Computer Technology and Electronics Engineering (IJCTEE)*, pages 24–26, 2011.

[93] Silviu Folea, George Mois, Mihai Hulea, Liviu Miclea, and Vio Biscu. Data Logger for Humidity and Temperature Measurement based on a Programmable SoC. In *2014 IEEE International Conference on Automation, Quality and Testing, Robotics*, pages 1–4. IEEE, 2014.

[94] Oka Mahendra, Djohar Syamsi, Ade Ramdan, and Marcella Astrid. Design and Implementation of Data Storage System using USB Flash Drive in a Microcontroller based Data Logger. In *2015 International Conference on Automation, Cognitive*

Science, Optics, Micro Electro-Mechanical System, and Information Technology (ICACOMIT), pages 58–62. IEEE, 2015.

[95] World Health Organization et al. COVID-19 Vaccination: Supply and Logistics Guidance: Interim Guidance, 12 February 2021. Technical report, World Health Organization, 2021.

[96] Swati Chopade, Hari Prabhat Gupta, Rahul Mishra, Aman Oswal, Preti Kumari, and Tanima Dutta. A Sensors based River Water Quality Assessment System using Deep Neural Network. *IEEE Internet of Things Journal*, 2021.

[97] Ye Liu, Yuxuan Liang, Kun Ouyang, Shuming Liu, David Rosenblum, and Yu Zheng. Predicting Urban Water Quality with Ubiquitous Data-A Data-driven Approach. *IEEE Transactions on Big Data*, 2020.

[98] Swati Chopade, Hari Prabhat Gupta, Rahul Mishra, Preti Kumari, and Tanima Dutta. An Energy-Efficient River Water Pollution Monitoring System in Internet of Things. *IEEE Transactions on Green Communications and Networking*, 5(2): 693–702, 2021.

[99] Fowzia Akhter, Hasin R Siddiquei, Md Eshrat E Alahi, Krishanthi Jayasundera, and SC Mukhopadhyay. An IoT-enabled Portable Water Quality Monitoring System with MWCNT/PDMS Multifunctional Sensor for Agricultural Applications. *IEEE Internet of Things Journal*, 2021.

[100] Yuhao Wang, Ivan Wang-Hei Ho, Yang Chen, Yuhong Wang, and Yinghong Lin. Real-time Water Quality Monitoring and Estimation in AIoT for Freshwater Biodiversity Conservation. *IEEE Internet of Things Journal*, 2021.

[101] Oratile Khutsoane, Bassey Isong, Naison Gasela, and Adnan M Abu-Mahfouz. Watergrid-sense: A LoRa-based Sensor Node for Industrial IoT Applications. *IEEE Sensors Journal*, 20(5):2722–2729, 2019.

[102] Hussein Kwasme and Sabit Ekin. RSSI-based Localization using LoRaWAN Technology. *IEEE Access*, 7:99856–99866, 2019.

[103] Pratap Kumar Sahu, Eric Hsiao-Kuang Wu, and Jagruti Sahoo. DuRT: Dual RSSI Trend Based Localization for Wireless Sensor Networks. *IEEE Sensors Journal*, 13 (8):3115–3123, 2013.

[104] Qinghua Luo, Yu Peng, Junbao Li, and Xiyuan Peng. RSSI-based Localization Through Uncertain Data Mapping for Wireless Sensor Networks. *IEEE Sensors Journal*, 16(9):3155–3162, 2016.

[105] Ka-Ho Lam, Chi-Chung Cheung, and Wah-Ching Lee. RSSI-based LoRa Localization Systems for Large-scale Indoor and Outdoor Environments. *IEEE Transactions on Vehicular Technology*, 68(12):11778–11791, 2019.

[106] Rong Peng and Mihail L Sichitiu. Angle of Arrival Localization for Wireless Sensor Networks. In *2006 3rd annual IEEE communications society on sensor and ad hoc communications and networks*, volume 1, pages 374–382. Ieee, 2006.

[107] Tian He, Chengdu Huang, Brian M Blum, John A Stankovic, and Tarek Abdelzaher. Range-free Localization Schemes for Large Scale Sensor Networks. In *Proceedings of the 9th annual international conference on Mobile computing and networking*, pages 81–95, 2003.

[108] Kevin J Krizman, Thomas E Biedka, and Theodore S Rappaport. Wireless Position Location: Fundamentals, Implementation Strategies, and Sources of Error. In *1997 IEEE 47th Vehicular Technology Conference. Technology in Motion*, volume 2, pages 919–923. IEEE, 1997.

[109] Faheem Zafari, Athanasios Gkelias, and Kin K Leung. A Survey of Indoor Localization Systems and Technologies. *IEEE Communications Surveys & Tutorials*, 21(3):2568–2599, 2019.

[110] Yiu-Tong Chan, Wing-Yue Tsui, Hing-Cheung So, and Pak-chung Ching. Time-of-Arrival Based Localization Under NLOS Conditions. *IEEE Transactions on Vehicular Technology*, 55(1):17–24, 2006.

[111] Santiago Mazuelas, Alfonso Bahillo, Ruben M Lorenzo, Patricia Fernandez, Francisco A Lago, Eduardo Garcia, Juan Blas, and Evaristo J Abril. Robust Indoor Positioning Provided by Real-time RSSI Values in Unmodified WLAN Networks. *IEEE Journal of selected topics in signal processing*, 3(5):821–831, 2009.

[112] David Munoz, Frantz Bouchereau, Cesar Vargas, and Rogerio Enriquez. Signal Parameter Estimation for the Localization Problem. In *Position Location Techniques and Applications*, pages 23–29. Elsevier Inc., 2009.

[113] Aditya Kaduskar, Omkar Vengurlekar, and Varunraj Shinde. RSSI Filtering Methods Applied to Localization using Bluetooth Low Energy. *International Journal of Recent Technology and Engineering*, 9, 2020.

[114] Romi Fadillah Rahmat, Mohammad Fadly Syahputra, Maya Silvi Lydia, et al. Real Time Monitoring System for Water Pollution in Lake Toba. In *2016 International Conference on Informatics and Computing (ICIC)*, pages 383–388. IEEE, 2016.

[115] Muhammad Niswar, Sonny Wainalang, Amil A Ilham, Zahir Zainuddin, Yushinta Fujaya, Zaenab Muslimin, Ady Wahyudi Paundu, Shigeru Kashihara, and Doudou Fall. IoT-Based Water Quality Monitoring System for Soft-Shell Crab Farming. In *2018 IEEE International Conference on Internet of Things and Intelligence System (IOTAIS)*, pages 6–9. IEEE, 2018.

[116] Wei Chen, Xiao Hao, Kui Yan, JianRong Lu, Jin Liu, ChenYu He, Feng Zhou, and Xin Xu. The Mobile Water Quality Monitoring System Based on Low-Power

Wide Area Network and Unmanned Surface Vehicle. *Wireless Communications and Mobile Computing*, 2021, 2021.

[117] Hsing-Cheng Chang, Yu-Liang Hsu, San-Shan Hung, Guan-Ru Ou, Jia-Ron Wu, and Chuan Hsu. Autonomous Water Quality Monitoring and Water Surface Cleaning for Unmanned Surface Vehicle. *Sensors*, 21(4):1102, 2021.

[118] Pei Chen. Dairy Cow Health Monitoring System Based on NB-IoT Communication. In *2019 International Conference on Electronic Engineering and Informatics (EEI)*, pages 393–396, 2019. doi: 10.1109/EEI48997.2019.00091.

[119] Muhammad Shoaib Farooq, Osama Omar Sohail, Adnan Abid, and Saim Rasheed. A Survey on the Role of IoT in Agriculture for the Implementation of Smart Livestock Environment. *IEEE Access*, 10:9483–9505, 2022. doi: 10.1109/ACCESS.2022.3142848.

[120] Pinaki S. Chatterjee, Niranjan K. Ray, and Saraju P. Mohanty. LiveCare: An IoT-Based Healthcare Framework for Livestock in Smart Agriculture. *IEEE Transactions on Consumer Electronics*, 67(4):257–265, 2021. doi: 10.1109/TCE.2021.3128236.

[121] H. Bouazza, O. Zerzouri, M. Bouya, A. Charoub, and A. Hadjoudja. A Novel RFID System for Monitoring Livestock Health State. In *2017 International Conference on Engineering and Technology (ICET)*, pages 1–4, 2017. doi: 10.1109/ICEngTechnol.2017.8308159.

[122] S Muthumanickam, B Keertana, L Lavanya, S Madhumitha, and PGK Sathvikaa. Hardware Implementation of Health Monitoring of Domestic Animals Using RFID. In *2021 International Conference on System, Computation, Automation and Networking (ICSCAN)*, pages 1–6, 2021. doi: 10.1109/ICSCAN53069.2021.9526431.

[123] Kunja Bihari Swain, Satyasopan Mahato, Meerina Patro, and Sudeepta Kumar Pattnayak. Cattle Health Monitoring System using Arduino and LabVIEW for Early Detection of Diseases. In *2017 Third International Conference on Sensing, Signal Processing and Security (ICSSS)*, pages 79–82, 2017. doi: 10.1109/SSPS.2017.8071569.

[124] R. Umega and M. A. Raja. Design and Implementation of Livestock Barn Monitoring System. In *2017 International Conference on Innovations in Green Energy and Healthcare Technologies (IGEHT)*, pages 1–6, 2017. doi: 10.1109/IGEHT.2017.8094063.

[125] Michele Magno, Fabien Vultier, Bence Szebedy, Homare Yamahachi, Richard H. R. Hahnloser, and Luca Benini. A Bluetooth-Low-Energy Sensor Node for Acoustic Monitoring of Small Birds. *IEEE Sensors Journal*, 20(1):425–433, 2020. doi: 10.1109/JSEN.2019.2940282.

[126] Jinshan Luo, Atsushi Ito, Akira Sasaki, Madoka Hasegawa, Shiori Ashibe, Yoshikazu Nagao, Yuko Hiramatsu, Kotaro Torii, and Toru Aoki. Sensor Network for Monitoring Livestock Behaviour. In *2020 IEEE SENSORS*, pages 1–4, 2020. doi: 10.1109/SENSORS47125.2020.9278693.

[127] Gaëtanne Hache, Edward D. Lemaire, and Natalie Baddour. Wearable Mobility Monitoring Using a Multimedia Smartphone Platform. *IEEE Transactions on Instrumentation and Measurement*, 60(9):3153–3161, 2011. doi: 10.1109/TIM.2011.2122490.

[128] Emilio Sardini, Mauro Serpelloni, and Viviane Pasqui. Wireless Wearable T-Shirt for Posture Monitoring During Rehabilitation Exercises. *IEEE Transactions on Instrumentation and Measurement*, 64(2):439–448, 2015. doi: 10.1109/TIM.2014.2343411.

[129] Mandeep Singh and Neelu Jain. Performance and Evaluation of Smartphone Based Wireless Blood Pressure Monitoring System Using Bluetooth. *IEEE Sensors Journal*, 16(23):8322–8328, 2016. doi: 10.1109/JSEN.2016.2597289.

[130] Ghassem Mokhtari, Qing Zhang, Ghavameddin Nourbakhsh, Stephen Ball, and Mohanraj Karunanithi. BLUESOUND: A New Resident Identification Sensor—Using Ultrasound Array and BLE Technology for Smart Home Platform. *IEEE Sensors Journal*, 17(5):1503–1512, 2017. doi: 10.1109/JSEN.2017.2647960.

[131] Haydar Ozkan, Orhan Ozhan, Yasemin Karadana, Muhammed Gulcu, Samet Macit, and Fasahath Husain. A Portable Wearable Tele-ECG Monitoring System. *IEEE Transactions on Instrumentation and Measurement*, 69(1):173–182, 2020. doi: 10.1109/TIM.2019.2895484.

[132] Lucile Riaboff, Laurence Shalloo, Alan F Smeaton, Sébastien Couvreur, Aurélien Madouasse, and Mark T Keane. Predicting Livestock Behaviour using Accelerometers: A Systematic Review of Processing Techniques for Ruminant Behaviour Prediction from Raw Accelerometer Data. *Computers and Electronics in Agriculture*, 192:106610, 2022.

[133] Andreina Liendo, Dominique Morche, Roberto Guizzetti, and Franck Rousseau. BLE Parameter Optimization for IoT Applications. In *2018 IEEE International Conference on Communications (ICC)*, pages 1–7, 2018. doi: 10.1109/ICC.2018.8422714.

[134] Dai-Chang Chen, Yang-Lin Zheng, Ya-Shu Chen, and Kai-Xuan Lee. Online Power Management for Latency-Sensitive Bluetooth Low-Energy Beacons. *IEEE Systems Journal*, 14(2):2411–2420, 2020. doi: 10.1109/JSYST.2019.2934771.

[135] Banuleasa Sabin, Munteanu Radu, and Rusu Alexandru. Wearable IoT Power Consumption Optimization Algorithm. In *2020 International Conference and*

Exposition on Electrical And Power Engineering (EPE), pages 429–433, 2020. doi: 10.1109/EPE50722.2020.9305609.

[136] Fuyang Tian, Jun Wang, Benhai Xiong, Linshu Jiang, Zhanhua Song, and Fade Li. Real-Time Behavioral Recognition in Dairy Cows Based on Geomagnetism and Acceleration Information. *IEEE Access*, 9:109497–109509, 2021. doi: 10.1109/ACCESS.2021.3099212.

[137] Long-Shen Liu, Ji-Qin Ni, Ru-Qian Zhao, Ming-Xia Shen, Can-Long He, and Ming-Zhou Lu. Design and Test of a Low-power Acceleration Sensor with Bluetooth Low Energy on Ear Tags for Sow Behaviour Monitoring. *Biosystems Engineering*, 176:162–171, 2018.

[138] Yogi Putra Pratama, Dwi Kurnia Basuki, Sritrusta Sukaridhoto, Alviansyah Arman Yusuf, Heri Yulianus, Faruq Faruq, and Fariz Bramasta Putra. Designing of a Smart Collar for Dairy Cow Behavior Monitoring with Application Monitoring in Microservices and Internet of Things-Based Systems. In *2019 International Electronics Symposium (IES)*, pages 527–533, 2019. doi: 10.1109/ELECSYM.2019.8901676.

[139] Claudia Arcidiacono, M Mancino, SMC Porto, Victor Bloch, and Matti Pastell. IoT Device-based Data Acquisition System with On-board Computation of Variables for Cow Behaviour Recognition. *Computers and Electronics in Agriculture*, 191:106500, 2021.

[140] S. R. Jino Ramson, S. Vishnu, A. Alfred Kirubaraj, Theodoros Anagnostopoulos, and Adnan M. Abu-Mahfouz. A LoRaWAN IoT-Enabled Trash Bin Level Monitoring System. *IEEE Transactions on Industrial Informatics*, 18(2):786–795, 2022. doi: 10.1109/TII.2021.3078556.

[141] Anuj Kumar and Gerhard P. Hancke. A Zigbee-Based Animal Health Monitoring System. *IEEE Sensors Journal*, 15(1):610–617, 2015. doi: 10.1109/JSEN.2014.2349073.

[142] Hui Li and BaoGuo Wang. Design of Dairy Cow's Step and Gesture Detection System Based on Multi-sensor and Lora Network. In *2018 5th International Conference on Systems and Informatics (ICSAI)*, pages 294–298, 2018. doi: 10.1109/ICSAI.2018.8599311.

[143] Achour Brahim, Belkadi Malika, Aoudjit Rachida, Lalam Mustapha, Daoui Mehammed, and Laghrouche Mourad. Dairy Cows Real Time Behavior Monitoring by Energy-efficient Embedded Sensor. In *2020 Second International Conference on Embedded & Distributed Systems (EDiS)*, pages 21–26, 2020. doi: 10.1109/EDiS49545.2020.9296432.